POLITECNICO DI TORINO

Department of Environment, Land and Infrastructure Engineering
Master of Science in Petroleum Engineering

Rate Transient Analysis and Flowing Material Balance for Oil & Gas Reservoir

Supervisor
Prof. Dario Viberti

Co-Supervisor:
Prof. Alberto Guadagnini
Dott. Muhammad Shoaib

Candidate:
Mohamed Amr Mohamed Abdelhamid Aly [S236320]

July 2018

Acknowledgement

"**We raise to degrees whom We please, but over all those endowed with knowledge is the All-Knowing (Allah).**" Quran surah Yusuf 76 (QS 12: 76)

"**You have been given of knowledge nothing except a little.**" Quran surah Al Isra 85 (QS 17: 85)

All praises to ALLAH for the strength he gave to me and his blessings to complete my thesis. My extreme gratitude goes to my supervisor Prof. Dario Viberti for giving me the opportunity to work with him and for his continuous support and guidance through the whole Master of Science program. Over the course of this program I have gained a lot from his knowledge, advice and encouragement. I am also very thankful to the support I have received from my co-supervisor Prof. Alberto Guadagnini, for the time he has dedicated into helping me. Special thanks to Dott. Muhammad Shoaib for his help and the huge efforts he made with me to finish this work.

I would like to acknowledge both KAPPA software platforms, and Schlumberger (SLB) for using the academic license of the rate transient analysis interface (Topaze NL) and (ECLIPSE) respectively in this work.

Finally, I would like to warmly thank my parents and my siblings for their endless support and love. Many thanks to my friends and colleagues who had encouraged me all the time during my studies.

Table of Contents

Index of Figure

Index of Tables

List of Abbreviations

DCA	Decline Curve Analysis
DMB	Dynamic Material Balance
FBHP	Flowing Bottom Hole Pressure
FMB	Flowing Material Balance
MBE	Material Balance Equation
PA	Production Analysis
P_{avg}	Average Reservoir Pressure
PDA	Production Data Analysis
PDG	Permanent Downhole Gauges
PTA	Pressure Transient Analysis
PVT	Pressure Volume Temperature
RTA	Rate Transient Analysis

List of Symbols

$(\boldsymbol{t})_c$	Characteristic time	(second)
$\overline{\boldsymbol{c_g}}$	Gas compressibility at average (static) reservoir pressure	($psia^{-1}$)
$\overline{\boldsymbol{\mu_g}}$	Gas viscosity at average (static) reservoir pressure	(cp)
$\boldsymbol{B_g}$	Gas Formation Volume factor	(SCF/STB)
$\boldsymbol{B_o}$	Oil Formation Volume Factor	(bbl/ STB)
$\boldsymbol{C_A}$	Dietz shape Factor	(-)
$\boldsymbol{G_p}$	Cumulative gas production	(MSCF)
$\boldsymbol{G_{pn}}$	Normalized pseudo cumulative function	(MSCF)
$\boldsymbol{N_p}$	Cumulative oil production	(STB)
$\boldsymbol{N_{pa}}$	Ultimate recovery	(STB)
$\boldsymbol{P_{sc}}$	Pressure at standard conditions	(psia)
$\boldsymbol{P_{th}}$	Tubing head pressure	(psia)
$\boldsymbol{Q_{DA}}$	Dimensionless cumulative production based on area A	(-)
$\boldsymbol{Q_{aD}}$	Dimensionless cumulative production based on r_{wa}^2	(-)
$\boldsymbol{S_{gi}}$	Initial Gas saturation	(-)
$\boldsymbol{T_a}$	New Material Balance Pseudo time function	(second)
$\boldsymbol{T_{sc}}$	Temperature at standard conditions	(R)
$\boldsymbol{V_P}$	Pore Volume	(ft^3)
$\boldsymbol{Z_i}$	Initial gas compressibility factor	(-)

$b_{a,pss}$	Pseudo steady state constant for gas	(psia/MSCF/s)
b_{pss}	Pseudo steady state constant for oil	(psia/STB/s)
c_g	Gas Compressibility	(psia $^{-1}$)
c_{gi}	Initial gas Compressibility	(psia $^{-1}$)
c_o	Oil Compressibility	(psia $^{-1}$)
c_{oi}	Initial Oil compressibility	(psia $^{-1}$)
c_t	Total Compressibility	(psia $^{-1}$)
c_{ti}	Initial total compressibility	(psia $^{-1}$)
$m(p_i)$	Initial reservoir pseudo pressure function	(psia^2/cp)
$\overline{p}$	Reservoir Static (Average) Pressure	(psia)
p_D	Dimensionless Pressure	(-)
p_i	Initial Pressure	(psia)
p_{wD}	Dimensionless wellbore pressure used by Agarwal	(-)
p_{wD}'	Dimensionless wellbore pressure derivative used by Agarwal	(-)
p_{wf}	Bottom hole Flowing Pressure	(psia)
q_{Dd}	Fetkovich Dimensionless rate	(-)
q_g	Gas flow rate at surface conditions	(MSCF/d)
q_o	Oil flow rate at stock tank	(STB/d)
r_D	Dimensionless diameter	(-)
r_e	Drainage radius	(ft)
r_{eD}	Dimensionless outer diameter	(-)
r_w	Wellbore radius	(ft)
r_{wa}	Effective Wellbore radius	(ft)
t_D	Dimensionless time	(-)
t_{DA}	Dimensionless time based on the drainage area	(-)
t_{Dd}	Fetkovich Dimensionless time	(-)
t_c	Material Balance time for oil	(second)
t_{ca}	Material Balance pseudo time function for gas	(second)
t_{cg}	Material Balance time for gas	(second)
t_s	Stabilization time	(second)
μ_g	Gas Viscosity	(cp)

μ_{gi}	Initial gas Viscosity	(cp)
μ_o	Oil Viscosity	(cp)
Δp	Pressure difference between initial and bottom hole flowing pressures	(psia)
B	Formation Volume Factor	(bbl/STB)
D	Nominal decline rate	($second^{-1}$)
F	MBH Function	(-)
G	Initial Gas In-Place	(MSCF)
N	Initial Oil In-Place	(STB)
S	Skin	(-)
T	Reservoir Temperature	(R)
Z	Gas compressibility factor	(-)
h	Net pay thickness	(ft)
k	Effective Permeability	(mD)
$m(\overline{p})_n$	Static (Average) normalized pseudo pressure	(psia)
$m(\overline{p})$	Static (Average) reservoir pseudo pressure function	($psia^2$/cp)
$m(p)_n$	Normalized pseudo pressure	(psia)
$m(p_{wf})$	Bottom hole pseudo pressure function	($psia^2$/cp)
$m(p)$	Gas pseudo-pressure function	($psia^2$/cp)
n	Decline Exponent	(-)
p	Pressure	(psiaa)
q	Flow Rate	(STB/d)
t	Time	(second)
γ	Euler's Constant	(-)
η	Diffusivity constant	(mD/s)
μ	Viscosity	(cp)
ϕ	Porosity	(-)

② Abstract

Rate Transient Analysis and Flowing Material Balance for Oil & Gas Reservoirs

By: Mohamed Amr Aly

Estimation of initial hydrocarbon in place is a critical step for any investment in the oil and gas industry, based on which revenues and further developments are planned and designed. The conventional ways of estimating the hydrocarbon initially in place are Material Balance Equation, Volumetric Methods, and Numerical Simulation Models.

Material Balance Equation and numerical simulation models are based on dynamic data analysis and simulation and therefore require the availability of a significant amount of historical production data (such as produced volumes of oil, gas, and water at the reference thermodynamic conditions) and periodic measurements or estimation of reservoir pressure typically provided by well testing. However, in most of the cases, for reasons related to the market and to the definition of the strategies of an oil company, a preliminary reservoir (or filed) development plan has to be defined within the first or the second year of production life of a reservoir when the amount of available information is limited. Furthermore, the costs of well test operations (i.e.: the time down when the well being shut in and the corresponding loss of production; the time needed to stabilize the bottom hole pressure reservoir) has an impact on the pressure data availability. Therefore, the amount of available production and pressure data reduces the reliability of the conventional material balance method during the first years of production life of a reservoir. The problem is emphasized in unconventional reservoir, or in general, in scenarios characterized by low permeability, high viscosity liquids, etc.

Reservoir Engineers have tools to be coupled and integrated to the Pressure Transient Analysis (Well testing) and other conventional approaches. In this view Production Analysis (PA) or Rate Transient Analysis (RTA) were developed for the interpretation of production data to obtain information about reservoir characteristics, well completion effectiveness and hydrocarbon initially in place. What signifies RTA is that this approach aims to analyze rate as well as pressure. Pressure can be measured during the production by permanent down-hole gauges (PDG) that provide a continuous record of pressure in time. The high cost of PDG installation for each well led to converting wellhead pressure into bottom hole pressure using VLPs for pressure surveillance.

Production Analysis was first introduced by Arps as Decline Curve Analysis (DCA) to empirically estimate the ultimate production recovery. However, Arps Type-curves are only applicable after the transient period i.e. in pseudo-steady-state conditions when the bottom hole pressure is fairly constant. Later in 1980, Fetkovich introduced a type-curve combining the Arps decline curve with the fluid flow behavior in a closed reservoir to provide a technique valid for both the two periods, transient and boundary dominated flow periods. However, this is still only applicable under the condition of constant bottom hole flowing pressure. This was the limitation until the introduction of the material balance time by Blasingame and McCary to transform the variable rate/variable pressure solution into an equivalent constant pressure or constant rate solution.

Flowing Material Balance (FMB) was introduced as a recent approach of Production Analysis in which production data (flow rate and measured or calculated bottom-hole pressure) is used through an iterative approach to estimate the initial hydrocarbon in place. Through the development of these different approaches, reservoir engineers succeed to exploit the production data in an easier way to overcome the limitations of the conventional methods.

The thesis work provides a validation on the production data analysis approaches used to estimate the initial hydrocarbon in place (RTA & FMB) by developing synthetic data on 4 different cases (Dry gas & Dead oil, Single & Multi-well Models) and comparing the results obtained with the numerical simulation models results. The study demonstrates the importance of PVT in Production analysis by importing PVT data represents our models from the PVT tables in Production Analysis software programs to be implemented in the FMB approaches and see how this will affect the obtained results. Analysis of results showed good agreement between the values of Hydrocarbon initially in place estimated through RTA, FMB and the numerical simulation model.

Keywords

Production Analysis, Rate Transient Analysis, Decline Curve Analysis, Flowing Material Balance, Original Hydrocarbon in Place, Reservoir Characterization.

Chapter 1 Introduction

The process of estimating hydrocarbon reserves for a producing reservoir is a continuous process through the life of the reservoir. However, there is always uncertainty in the obtained values from the different methods. This uncertainty is affected by some factors like:

- The type of reservoir,
- The source of Energy (Depletion, Water drive, Gas in solution, Gas Cap),
- Geological and geophysical data and its quality,
- Assumptions adopted in the process,
- Available technology.

There are different approaches for estimating hydrocarbon in place:

Volumetric Method: considers the real extent of the reservoir, the rock pore volume and the fluid content within the pores to provide an estimate of the amount of hydrocarbons-in-place. Then the ultimate recovery could be estimated by applying a recovery factor.

Decline Curve Analysis: uses the production data to be compared by decline curves previously established on empirical equations to calculate the expected ultimate recovery of the reservoir.

Material balance: is a well-established methodology in reservoir engineering for the estimation of Hydrocarbon Originally In-Place (HOIP) and identify drive mechanisms. The methodology is based on production and pressure data only and does not require petrophysical data, etc.

The issue about Conventional Material Balance Equation (MBE) is the need to have a static pressure profile over a long period to be able to roughly estimate the OOIP, OGIP and even to know the drive mechanism and evaluate the volume of the aquifer.

For many complexities related to the reservoir characteristics (e.g. low permeability) or the type of fluid (e.g. heavy oil.), it becomes harder to shut the well to have a reading of the average reservoir static pressure. Hence, the need to have an alternative valid approach could be used to determine the estimate of Hydrocarbon-in-Place without the need to shut the wells to obtain the static pressure or stabilize the reservoir is important and in this thesis work we validate two approaches:

1.1. Rate Transient Analysis

The software Ecrin [Topaze 4.20.05] commercialized by Kappa Engineering was adopted to analyze the production data and validate the results though a comparison with those obtained by the numerical reservoir simulation model [generated using the software Eclipse commercialized by Schlumberger]. The production data were numerically generated for 4 synthetic reservoir models:

- Dry Gas single Well
- Dry Gas Multi Well
- Dead Oil Single Well
- Dead Oil Multi-well

PVT data set for the numerical simulation model was extracted from Topaze database. Data was integrated with Fetkovich, and Blasingame Type-curves to obtain the decline parameters, reservoir extension, permeability and initial hydrocarbon in place.

1.2. Flowing Material Balance

Flowing Material Balance is an analytical approach by which the reservoir engineers could have an initial appropriate estimate of the in-place hydrocarbon volumes without the need to shut in the well to record the static reservoir pressure.

The Flowing Material Balance approach is mainly an iterative approach in which we use the production data (Flowing Bottom Hole Pressure and corresponding flow rates in addition to fluid properties and rock properties) to get an analytical set of equations used in a specific order by assuming a parameter (Initial G or N for instance or P_{avg}) on which the other parameters are dependent and we iterate until we reach an acceptable convergence.

Production data was then tested by FMB approaches for the four models to validate the results obtained by both numerical simulation models and the RTA.

Dead Oil FMB: PVT data (Compressibility and viscosity) were set as constant during the production profile. In addition, a sensitivity analysis was performed to compare the results between case using the compressibility of oil and case using total compressibility in the equation for depletion of the oil.

Dry Gas FMB: The main challenge for developing the FMB for gas was the PVT data and how to correlate PVT data with the corresponding flowing data (Q, Pwf). The other challenge was how to calculate the pseudo function parameters for the gas based on these PVT data.

For Gas, it is necessary to convert the pressure and the time into a pseudo function to consider the change of the gas properties while production.

The results obtained by the two approaches showed a good agreement in terms of the hydrocarbon in place and of the reservoir properties such as permeability..

Chapter 2 State of The Art

Production Data Analysis basically means the use of production date (Flow rate and flowing pressure) to do some analysis aiming to have information about the reservoir characteristics. Production Data Analysis has been developing through time starting from the explicit concept of PA (Production Analysis) to PTA (Pressure Transient Analysis) , RTA (Rate Transient Analysis) and FMB (Flowing Material Balance).

Here we provide a closer focus on RTA starting from the discussion of Decline curve Analysis started by Arps in 1945 and developed by Fetkovich and Blasingame to provide type-curves working for different production scenarios and then the development of these type-curves by (Agarwal, Gardner, Kleinsteiber, & Fussell, 1998).

The introduction of flowing material balance by Blasingame converted the constant flowing pressure production scenario into constant flow rate production conditions. It was the turning point of production data analysis, not only for decline curve analysis but this concept also showed a great effect for the development of Flowing Material Balance concepts (Fekete.com, Material Balance Time Theory).

Flowing Material Balance was first introduced by (McNeil, 1995) and it was an approach to use flowing data to estimate Gas-in-Place without shutting the well-in and overcome the production loss and time down needed to stabilize the reservoir. The main limitation was to keep the flow rate constant. Then the FMB has been extended not only to variable rate dry gas production but also for variable dead oil single well or multi-well production scenarios.

The main point of the two approaches is to confirm how production data could be only used to provide an estimation of hydrocarbon initially in place when the conventional Material balance is not applicable in the first few years.

2.1. Decline Curve Analysis

The concept is mainly estimating the expected ultimate recovery (EUR) by monitoring the performance of the well in the past and extrapolate it in the future based on the assumption that what affects the production in the past will continue to affect it in the future. This is done by building the production performance on a plot using: Flow rate (Dependent Variable) vs. Time or Cumulative Production (Independent Variables). (Fekete.com, Traditional Decline Theory)

These plots are empirical and do not depend on the fluid flow physics in the porous medium. The most common curve used is daily rate vs. month.

The Production Analysis started in 1920 with a pure motive to find the best decline function by which it is possible to predict the revenue of the production in the future on an empirical basis with no technical background in it. Then (Arps , 1945) formulated the constant pressure exponential, hyperbolic and harmonic rate decline. In 1960, Type-curves were first introduced, still assuming constant flowing pressure by Fetkovich. These type-curves have two families one related the transient flowing period and the other for the late boundary-dominated flow. In late 80s and early 90s, (Palacio & Blasingame, 1993) introduces the variable rate/variable pressure type-curves as a log-log plot of productivity index vs. material balance time.

2.1.1. Arps Decline Curve Method

Based on empirical rate-time and associated cumulative-time equation. (DIATI, 2018)

Table 1: Advantages and Disadvantages of Arps Decline Curve Analysis

Advantages	**Limitations**
Simplicity	Fairly constant bottom-hole pressure.
Conservative reserve estimation	Constant well behavior
Applicable to closed reservoir (Exponential Decline)	Constant drainage area
	Transient behavior

The decline curve analysis theory starts with the concept of the nominal decline rate (D). Nominal Decline (D) is defined as the fractional change in rate per unit time which is the negative slope of natural logarithm of the production rate Q vs. time t as shown in Equation 2-1

$$D = -\frac{dln(q)}{dt} = -\frac{dq/dt}{q}$$ **Equation 2-1**

Another way of representing the decline rate is based on rate (q) and the decline exponent constant n.

$$D = Kq^n$$ **Equation 2-2**

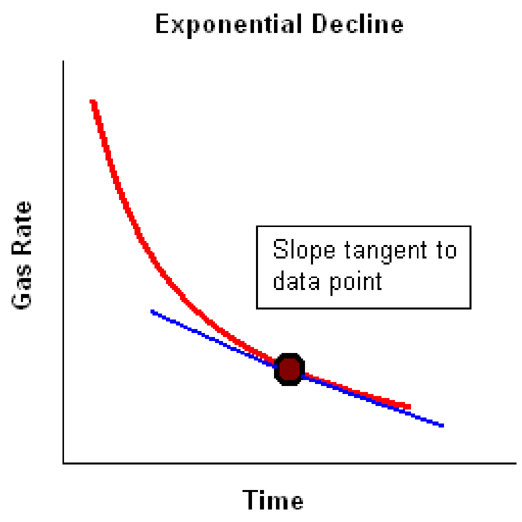

Figure 1: Nominal Decline at a point in time

Production data could follow different behaviors depending on the attitude the nominal decline with rate. These behaviors are characterized by the decline exponent constant (n).

- **Exponential** — n = 0
- **Hyperbolic** — n is a value between 0 and 1
- **Harmonic** — n = 1

Arps' typecurve analysis was basically used for boundary dominated flow with fairly constant bottom hole flowing pressure. We first define the n power, initial nominal decline rate, abandonment time t_a and then the ultimate recovery N_{pa}.

2.1.2. Fetkovich typecurve Analysis Theory

(Fetkovich, 1980) explained that Arps are not valid for early time production data (Transient) and therefore he used the analytical equation for the transient flow to generate type-curves for transient flow that are combined with the type-curves of the Arps. Using the concepts of well testing with the empirical equations Arps used in his type-curves.

He used in his study a model of well centered producing well in a circular reservoir with constant flowing bottom-hole pressure with the same standard assumptions used in describing the reservoir in well testing. (Fekete.com, Fetkovich Theory)

He used the (Van Everdingen & Hurst, 1949) solution to solve the problem in developing the equation for the transient period and proving that boundary dominated flow period solution described by Arps had a theoretical background.

He defined a new term of dimensionless rate and dimensionless time by which he succeeded to make the new type-curves that has two parts.

$$q_{Dd} = q_D \left[\ln\left(\frac{r_e}{r_{wa}}\right) - \frac{1}{2}\right] \qquad \textbf{Equation 2-3}$$

$$t_{Dd} = \frac{t_D}{\frac{1}{2}\left[\ln\left(\frac{r_e}{r_{wa}}\right)^2 - \frac{1}{2}\right]\left[\ln\left(\frac{r_e}{r_{wa}}\right) - \frac{1}{2}\right]} \qquad \textbf{Equation 2-4}$$

The left part of Fetkovich type-curves describes the transient dominated flow. This part is different from q_D vs t_D type-curves where transient flow was represented only with one cure. Instead, in Fetkovich type-curves the transient flow was represented by a stem of curves representing the different reservoir sizes r_e/r_w. From this part we can define the reservoir characteristics (Permeability, skin and well effective radius r_{wa}). (Fetkovich, 1980)

The right part of Fetkovich type-curves describes the boundary dominated flow in which Fetkovich succeeded to combine his solution with Arps empirical equation using the new dimensionless rate and dimensionless time he defined and showed that depending less on the reservoir size, dimensionless rate is exponentially depending on dimensionless time. $q_{Dd} = e^{-t_{Dd}}$

This is exactly the same exponential equation of Arps for exponential decline regime where b=0. Then he extended this solution to cover the hyperbolic decline and include all possible decline types that could happen in the boundary dominated flow.

A match will decide the type of decline defined here by (b) which is equal to (n) in Arps decline curves. In addition, the match will provide with the values of r_e (Drainage radius), kh, Di and qi and therefore the reservoir pore volume can be calculated. With knowledge of PVT and reservoir characteristics we could define the Initial hydrocarbon in place.

2.1.3. Blasingame Typecurve Analysis Theory

(Fekete.com, Blasingame Theory) The previous techniques introduced by Arps and Fetkovich do not account for variations in bottom-hole flowing pressure and also the change in the PVT properties of gas with the change of pressure caused by production (Depletion).

(Fetkovich, 1980) believed that the exponent "b" could vary between 0 and 1 and that can be correlated with fluid properties and recovery mechanism. As a proof; single phase oil flow would align the exponential decline curve where b=0 (Exponential). However, Single phase gas flow would exhibit b>0 because of the change in gas properties with production.

(Palacio & Blasingame, 1993) used the concept introduced by Fraim and Wattenbarger of pseudo time that accounts for the change of gas fluid properties. Therefore, boundary dominated gas flow against a constant back pressure would exhibit the same behavior that an oil reservoir would (Exponential Decline b=0).

(Palacio & Blasingame, 1993) introduced a function that would change the variable-pressure/variable-rates solution into an equivalent constant pressure or constant rate solutions. They reported that using a pressure-normalized flow rate when the bottom hole pressure varied significantly is not a remedy of the problem, refereeing to variable rate/variable pressure situation. They introduced two time functions, t_{cr} the constant rate time function and t_{cp} for constant pressure. Plotting the pressure normalized rate vs. t_{cr} on a log-log scale will result in a negative unit slope line for boundary dominated flow.

Later, (Palacio & Blasingame, 1993) introduced a superposition time function that accounts for the variable rate/variable pressure production conditions to appear as constant rate production regime and what used to match the exponential decline on Fetkovich would match the harmonic decline on Blasingame type-curves. This time function is called Material Balance time.

Using Material Balance time by Blasingame allowed depletion at a constant pressure to appear as it was depletion at constant flow rate. In fact, (Palacio & Blasingame, 1993) have shown that boundary dominated flow with both declining pressure and rates appear as pseudo-steady state depletion at a constant rate provided that the pressure and rate decline monotonically. This would follow the harmonic decline instead of exponential and hyperbolic decline curves.

The significance was readily evident by considering the inverse of the flowing pressure plotted against time, pseudo-steady state depletion at constant flow rate follows a harmonic decline trend.

(Fekete.com, Blasingame Theory) Blasingame, McCary and Placio developed type-curves which follow the analytical transient stems as Fetkovich type-curves but with harmonic decline stem. In addition to overcome the noise of production data and smoothen it to match the type-curves, they introduced other two functions: Rate Integral and Rate Integral Derivative.

Material Balance Time Theory

(Fekete.com) defined the material balance time as the time needed to produce this cumulative production amount with the instantaneous flow rate value. Figure 2 shows how variable rate/variable pressure production scenarios can be transformed into a constant rate production scenario. (Fekete.com, Material Balance Time Theory)

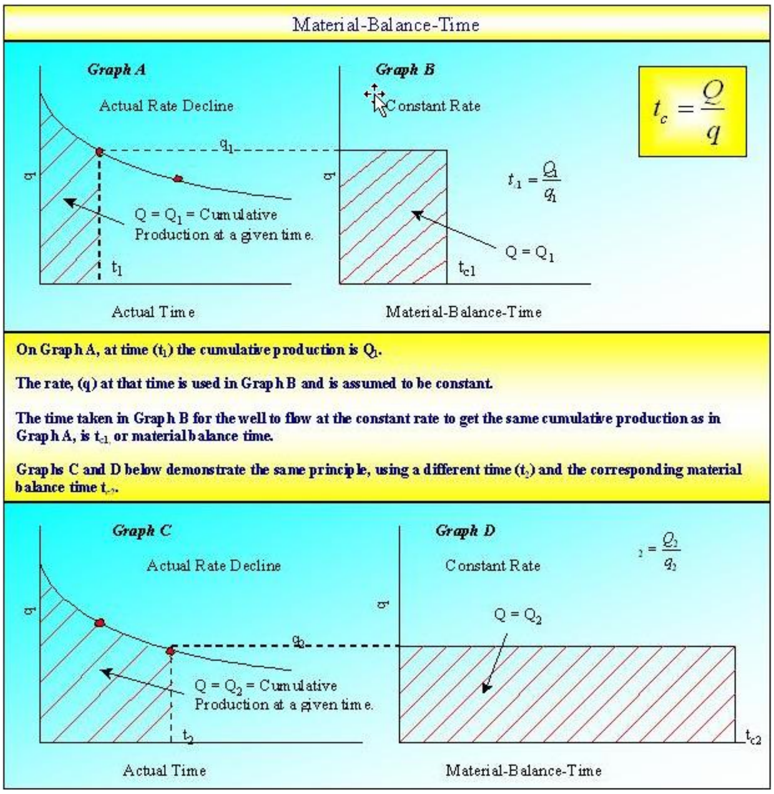

Figure 2: How material balance time is used to change the variable rate scenario into constant rate scenario (Fekete.com, Material Balance Time Theory)

Material Balance time for Oil:

$$t_c = \frac{N_p}{q_o} \qquad \textbf{Equation 2-5}$$

Material Balance for Gas:

$$t_{cg} = \frac{G_p}{q_g} \qquad \textbf{Equation 2-6}$$

The introduction of material balance time to gas production is different because of the effect of gas properties change with production. Hence, the concept of oil material balance time is limitedly used to gas production scenarios. The precise formulation of gas material balance time is defined as material balance pseudo time (Fekete.com, Material Balance Time Theory):

$$t_{ca} = \frac{(\mu_g c_g)_i}{q_g} \int_0^t \frac{q_g}{\mu_g c_g} dt \qquad \textbf{Equation 2-7}$$

Which in some cases is defined in terms of total compressibility to account for other fluids compressibilities and the compressibility of rocks:

$$t_{ca} = \frac{(\mu_g c_t)_i}{q_g} \int_0^t \frac{q_g}{\overline{\mu_g c_t}} dt$$ **Equation 2-8**

2.1.4. Agarwal Type-curves Theory Analysis

(Agarwal, Gardner, Kleinsteiber, & Fussell, 1998) used the concept developed by Fetkovich, Palacio and Blasingame of equalizing the constant rate and constant pressure solutions to introduce the decline type-curves to analyze production data. The dimensionless variables used by Agarwal and Gardner were built on the conventional well testing definition instead the ones Fetkovich presented and used by Blasingame. (Fekete.com, Agarwal-Gardner Theory)

In addition, they included derivative plots (Primary derivative and inverse semi log derivative) used to illustrate some features between transient and PSS flow in decline analysis. Moreover, they presented their decline type-curves in additional formats: the rate vs. cumulative, and cumulative vs. time analysis type-curves. (Fekete.com, Agarwal-Gardner Theory)

Dimensionless variables used by Agarwal: The dimensionless variables used in type-curves for pressure transient analysis are dimensionless pressure P_{wD} and its derivative with respect to dimensionless time $\frac{dP_{wD}}{dt_D}$ and with respect to log of dimensionless time $\frac{dP_{wD}}{dlnt_D}$. To make a type-curve appear like a decline curve we should use the reciprocal of P_{wD} to produce a graph of $\frac{1}{Pw_D}$ and $\frac{\frac{1}{dP_{wD}}}{dlnt_D}$ plotted against dimensionless time. (Agarwal, Gardner, Kleinsteiber, & Fussell, 1998)

Production Decline Type-curves are represented in three types:

- Rate – Time
- Rate – Cumulative production
- Cumulative production – time.

2.1.4.1. Rate-Time Type-curves

(Agarwal, Gardner, Kleinsteiber, & Fussell, 1998) The dimensionless time representing the x-axis on the log-log plot could be represented in two different ways:

1) Based on the drainage area A: used to distinguish features during transient and PSS flow periods

Table 2: Comparison between Transient and Pseudo Steady State Conditions in Rate-Time Type-curves, Based on Drainage Area A

	Transient Flow	Pseudo-Steady State Flow
$1/P_{wD}$	Is a function of r_e/r_{wa}	A negative unit slope line
P_{wD}'	A negative unit slope line	Constant value of 2π (Zero Slope)
$1/\ dP_{wD}/dlnt_D$ $(1/dlnP_{wD}')$	Constant value of 2.0 (constant slope)	A negative unit slope line

2) Based on the effective wellbore radius squared r_{wa}^2: used to estimate reservoir parameters like permeability and skin

Table 3: Comparison between Transient and Pseudo Steady State Conditions in Rate-Time Type-curves, Based on Effective Well Radius r_{wa}^2

	Transient Flow	Pseudo-Steady State Flow
$1/P_{wD}$	Single curve for all r_e/r_w values	Different negative unit slope lines for each r_e/r_w.
P_{wD}'	Negative unit slope line	Different zero slope with different constant values representing the different r_e/r_w values.
$1/\ dP_{wD}/dlnt_D$ $(1/dlnP_{wD}')$	Zero slope with a constant value of 2.0 line except for $t_D<100$	Different negative unit slope lines for each r_e/r_w.

2.1.4.2. Rate- Cumulative Production Type-curves

a) Based on the drainage area A

Table 4: Comparison between Transient and Pseudo Steady State Conditions in Rate-Cumulative Production Type-curves, Based on Drainage Area A

	Transient Flow	Pseudo-Steady State Flow
$1/P_{wD}$ (log-log graph)	Curves are obtained for different r_e/r_w values.	All curves merge into a single value of $Q_{DA} = \frac{1}{2\pi} = 0.159$
$1/P_{wD}$ (Cartesian graph)	Curves are obtained for different r_e/r_w values.	These curves become linear and converge at $Q_{DA} = \frac{1}{2\pi} = 0.159$

(Agarwal, Gardner, Kleinsteiber, & Fussell, 1998) The significance of that feature that an approximate estimation of the Initial Hydrocarbon in Place would fit the production data at the anchor point $Q_{DA} = \frac{1}{2\pi} = 0.159$. Optimistic estimation would undershoot the anchor point and a pessimistic estimate will overshoot the anchor point.

b) Based on the effective wellbore radius squared r_{wa}^2

Table 5: Comparison between Transient and Pseudo Steady State Conditions in Rate-Cumulative Production Type-curves, Based on Effective Well Radius r_{wa}^2

	Transient Flow	Pseudo-Steady State Flow
$1/P_{wD}$	One curve with a negative slope for all r_e/r_{wa} values	Different seemingly vertical lines for different values of r_e/r_{wa}
P_{wD}'	One negative unit slope curve	Positive different positive unit slope curves for different values of r_e/r_{wa}

(Agarwal, Gardner, Kleinsteiber, & Fussell, 1998) The feature of this graph is that $1/P_{wD}$ and the derivative forms an envelope with a vertical tangent corresponding to the Initial Hydrocarbon in Place.

2.1.4.3. Cumulative Production- Time Type-curves

Based on the effective wellbore radius squared r_{wa}^2

Table 6: Comparison between Transient and Pseudo Steady State Conditions in Cumulative Production-Time Type-curves, Based on Effective Well Radius r_{wa}^2

	Transient Flow	Pseudo-Steady State Flow
Q_{aD} Vs. t_D (Log-Lg graph)	Single Curve is obtained for all r_e/r_{wa} values with a unit slope except for t_D<100	The curves stabilize and become flat at different times according to the value of r_e/r_{wa}

(Agarwal, Gardner, Kleinsteiber, & Fussell, 1998) These type-curves allow us to use production data with the absence of transient data and would be a useful tool to characterize some reservoir parameters (Permeability, skin and reserves).

2.2. Flowing Material Balance

When Flowing Material was first introduced for gas production in pseudo steady state conditions where the pressure decline at any point in the reservoir at the same rate and therefore, $\Delta p_{wf} = \Delta p_{avg}$ and then by plotting $\frac{P_{wf}}{Z}$ vs G_p we will get a line. Knowing Pi we can draw a line from $\frac{P_i}{Z}$ parallel to $\frac{P_{wf}}{Z}$ that intersect the x-axis in G. This was the main concept introduced by (McNeil, 1995) as the Flowing Material Concept.

This approach was verified in some case studies, and the results of Initial Gas in Place were not far from the values obtained by conventional Material Balance or numerical simulation models. (Fekete.com, Flowing Material Balance Theory)

2.2.1. (Mattar & McNeil, The "Flowing" Gas Maerial Balance , 1998; McNeil, 1995)

- **Conditions**: Dry Gas reservoirs with constant flow rate in a PSS flow regime.[Single or Multi-well]
- **Approach**: Using the concept of at a PSS regime the pressure drop at any point in the reservoir is the same at any time step. Therefore the pressure drop at the well is the same at the boundary. Drawing $\frac{P_{wf}}{Z}$ or $\frac{P_{th}}{Z}$ vs. time or total production and get a straight line with a negative slope. Then defining the Pi or the initial tubing pressure, respectively, and draw a parallel line. The x-intercept gives the initial Gas in Place.

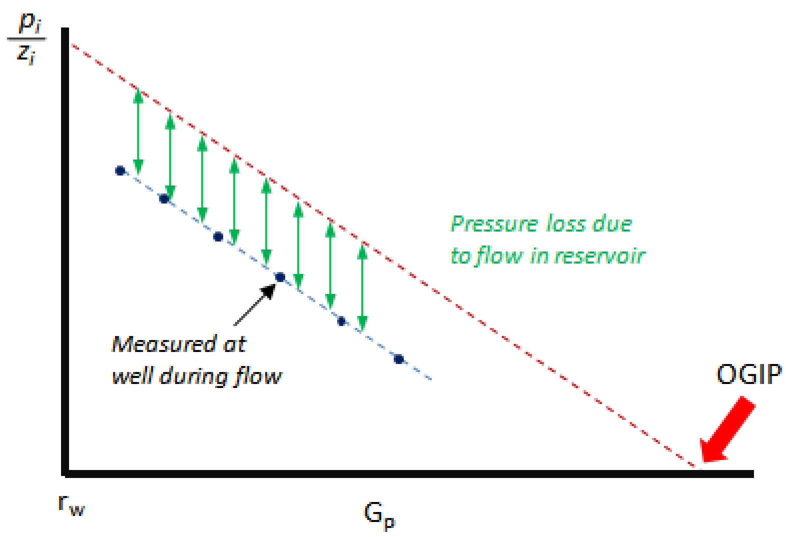

Figure 3: Pi/zi plot as Parallel to Pwf/Z line in Pseudo Steady State Conditions. Flowing Material Balance Approach. (Fekete.Com)

- Case Studies:
  - (Choudhury & Gomes, 2000), Bangladesh: the study was developed on Bakhrabad field
    - → Medium permeability (50-700 md)
    - → 4 Sand Formations with 8 wells.

The field had been through different stages of development and at the time of the study there were 4 wells producing from the major sand formation J-Sand.

<u>Application steps</u>:

- They divided J-Sand formation into 4 drainage volumes and each is allocated to a producing well.
- For FMB, the following pressure data was plotted for each well individually to calculate the reserve of the drainage volume assigned to it.
- The total gas in place in J-formation was calculated by summation of the reserves estimated for each drainage area.
- Flowing well bore pressure values have been calculated from flowing well head pressure data using Beggs and Brill method.
- Pressure surveys could not be conducted in the J-sand formation due to critical supply condition.

- For confirming the assumption of the 4 drainage volumes J-sand formation FMB was plotted as (average P/z vs. total production) as shown in Table 7
- The study showed comprehensive results compared with static material balance and numerical simulation models.

No liquid build up in the well bore was present and gas wells were producing under PSS conditions. This was a direct implementation of the method through which it showed near values of the Gas in place when it was compared with the conventional MBE approach as shown in Table 8.

Table 7: (Choudhury & Gomes, 2000) Gas in Place Estimates and the status of J sand

J sand	OGIP			Recovery %	Remaining Reserves (BCF)	Cum. Prod (BCF)	Reserves (BCF) (FBHP)
	SBHP	FWHP	FBHP				
Bk1	155.46	155.00	155.00	62.38%	19.3	96.7	116
Bk6	85.14	89.00	85.00	59.00%	9.8	50.2	60
Bk7	115.22	121.5	118.50	55.52%	18.2	65.8	84
Bk8	99.54	104.0	102.00	57.94%	12.9	59.1	72
Total J	455.36	469.5	460.50	59.00%	60.2	271.8	332

Table 8: (Choudhury & Gomes, 2000) Comparison of Gas in Place estimates by different methods

Sand	Welldrill	IKM	Petrobangla	Mobil	Simulation	Present Study (FBHP)
J	585	597	665.0	666	427	460.50
G	370	318	245.5	244	233	216.00
DL	200	148	176.0	175	168	144.50
DU	167	180	180.3	187	174	150.00
B	231	145	166.6	167	202	151.00
Total BK	1553	1388	1433.4	1439	1204	1122.00

- (Guzman, Arevalo, & Espinola, 2014) provided a case study of implementing FMB for estimating on two Dry Gas reservoirs in Mexico.
  - → A (22 producing well, 4 with downhole sensors).
  - → B (7 producing wells, 2 with downhole sensors).

For some wells it was possible to have information about static and dynamic pressure profiles.

Table 9: (Guzman, Arevalo, & Espinola, 2014) Summary of OGIP (MMSCF) Calculation by Different Studies

Study	Volumetric	Decline Curve Analysis	Conventional Material Balance	Reservoir Numerical Simulation	Flowing Gas Maerial Balance	Difference FDMB vs Numerical Simulation
Reservoir 1 Field A	552	424.6	701	510	499	2.2%
Reservoir 1 Field B	97	69	81	86	93	8%

However, for the ones that lack information, data was modeled through tubing head pressure and a multiphase flow simulator.

The large difference between conventional and flowing material balance for field A in Table 9 was due to the lack of shut-in pressure.

Results in Figure 9 showed error that did not exceed 10% that could be acceptable in case of the need of estimating the initial Gas in place with no shut-in pressure.

2.2.2. (Mattar & Anderson, Dynamic Material Balance(Oil or Gas-In-Place Without Shut-In), 2005)

- **Conditions**: For under saturated oil reservoir and Dry Gas reservoir both constant or variable flow rate scenarios. Boundary Dominated flow should be existing.
- **Approach**: this method uses the flowing data at any point to convert the measure flowing pressure to the average pressure that exists at the reservoir at this time. Then, using the calculated average pressure and the corresponding cumulative production we can calculate the original volume in place by the conventional material balance method.
  a) **FMB [Constant Rate, Gas]**: The use of the previously explained method of (McNeil, 1995) and (Mattar & McNeil, 1998)
  b) **FMB [Constant rate, Oil]**: Using the Pseudo Steady State equation with the depletion equation of under-saturated oil reservoir we reach this equation:

$$P_i - P_{wf} = \frac{q_o t}{C_o N} + \frac{141.2\, q_o B_o \mu_o}{kh}[\ln\left(\frac{r_e}{r_w}\right) - \frac{3}{4}] \quad \textbf{Equation 2-9}$$

This can be written as: $$P_i - P_{wf} = \frac{q_o t}{C_o N} + b_{pss}\, q_o \quad \textbf{Equation 2-10}$$

Where b_{pss} (The Pseudo-Steady State Constant), (the reciprocal of productivity index):

$$b_{pss} = \frac{141.2\, q_o B_o \mu_o}{kh} [\ln\left(\frac{r_e}{r_w}\right) - \frac{3}{4}] \qquad \textbf{Equation 2-11}$$

This is constant and was first presented by (Palacio & Blasingame, 1993) It can be obtained by rearranging the equation into:

$$\frac{(P_i - P_{wf})}{q} = \frac{q_o t}{c_o N q_o} + b_{pss} = \frac{N_p}{C_o N q_o} + b_{pss} \qquad \textbf{Equation 2-12}$$

A Cartesian plot of $\frac{(P_i - P_{wf})}{q_o}$ vs. $\frac{N_p}{q_o}$ will yield a straight line with an intercept of $b_{pss.}$

Then Average Pressure could be obtained by:

$$\bar{P} = P_{wf} + b_{pss} * q_o \qquad \textbf{Equation 2-13}$$

c) **Dynamic Material Balance [Variable rate, Oil]:** (Agarwal, Farim and Palacio) have proved that replacing the flow time by the material balance time makes the previous procedure of (b_{pss}) could be still applicable for variable production rate Equation 2-5 and the same method with the same steps used for the constant rate scenario could be used. (Fekete.com, Flowing Material Balance Theory)

d) **Dynamic Material Balance [Variable rate, Gas]:** two important steps should be considered; Converting the pressure into pseudo-pressure to consider the viscosity and Z factor dependence on pressure in addition to replacing the flow time with the material balance pseudo-time for gas (t_{ca}) to consider the gas properties change with pressure.

Where Pseudo-Pressure is:

$$m(p) = 2 \int \frac{P}{\mu_g\, Z}\, dp \qquad \textbf{Equation 2-14}$$

Using the same manner and starting with the material balance equation (depletion equation) with the Pseudotime function we reach:

$$m(p_i) - m(\bar{p}) = \frac{2 p_i q_g\, t_{ca}}{G Z_i} \qquad \textbf{Equation 2-15}$$

Where:

$$t_{ca} = \int \frac{dt}{\overline{\mu_g}\; \overline{c_g}} \qquad \textbf{Equation 2-16}$$

From the Pseudosteady state flow equation for gas:

$$m(\bar{p}) = m\left(p_{wf}\right) + q_g\, b_{a,pss} \qquad \textbf{Equation 2-17}$$

Where

$$b_{a,pss} = \frac{1.417 \times 10^6\, T}{kh} [\ln\left(\frac{r_e}{r_w}\right) - \frac{3}{4}] \qquad \textbf{Equation 2-18}$$

$b_{a,pss}$ can be obtained by merging the two equations and get:

$$\Delta m(p) = \frac{24 * 2348 * T\, q_g\, t_{ca}}{\pi\, \phi\, \mu_{gi}\, c_{gi}\, {r_e}^2\, h} + \frac{1.417 * 10^6\, T\, q}{kh} [\ln\left(\frac{r_e}{r_w}\right) - \frac{3}{4}]$$ **Equation 2-19**

Then average pseudo pressure can be calculated through Equation 2-17 that would be converted to average pressure to plot the gas P/z plot vs G_p

(Mattar & Anderson, 2005)) provided the steps of the "Dynamic Material Balance" for gas production a variable flow rate are:

1. Convert initial pressure and the flowing pressures to pseudo pressures, $m(p_i)$, $m(p_{wf})$
2. Assume an initial value for G to calculate the average reservoir pressure values corresponding to the cumulative production.
3. Calculate Pseudotime function t_{ca} based on the gas properties estimated at the average pressure values.
4. Plot $\frac{\Delta m(p)}{q_g}$ vs. pseudo material balance time t_{ca} and the intercept gives $b_{a,pss}$.
5. Calculate the average pseudo-pressure
6. Convert the average pseudo-pressure to average reservoir pressure
7. Calculate P/z values and plot them against G_p just like conventional MBE and get the intercept, G
8. Iterate until reaching a good convergence for the G value.

**Note: When Equation 2-15 was compared with other literature it showed that the dominator misses the gas viscosity and compressibility

$$m(p_i) - m(\bar{p}) = \frac{2p_i q\, t_{ca}}{GZ_i}$$ **Equation 2-20**

In our thesis work we will call the Dynamic Material Balance for a variable gas rate production as the Gas Flowing Material Balance Approach to generalize the concept and to be easier compared with the other approaches implemented.

2.2.3. Agarwal-Gardner Normalized rate

It's similar to the dynamic material balance approach and it is called Normalized Rate/Normalized cumulative analysis. (Fekete.com, Agarwal-Gardner Theory)

- **Conditions**: It is applicable for both oil and gas for constant and variable flow rate scenarios.
- **Approach**: to get the average reservoir pressure representing the time step of the flowing data and then applying the conventional material balance approach. We plot the normalized rate against the normalized cumulative. A straight line is set for the best fit of the points, and the x-intercept gives G. The equation for the straight line for the Agarwal-Gardner analysis is:

$$\frac{q_g}{\Delta m(p)} = \frac{-1}{b_{a,pss}} \frac{2\, q_g\, t_{ca} P_i}{\left(c_{ti}\, \mu_{gi}\, Z_i\right)\left(m(p_i) - m(p_{wf})\right)} + \frac{1}{b_{a,pss}} \quad \textbf{Equation 2-21}$$

Where, $$Q_m = \frac{G(m(p_i) - m(\bar{p}))}{\left(m(p_i) - m(p_{wf})\right)} = \frac{2\, q_g\, t_{ca}\, P_i}{\left(c_{ti}\, \mu_{gi}\, Z_i\right)\left(m(p_i) - m(p_{wf})\right)} \quad \textbf{Equation 2-22}$$

$$Normalized\ Cum. = \frac{G(m(p_i) - m(\bar{p}))}{\left(m(p_i) - m(p_{wf})\right)} \quad \textbf{Equation 2-23}$$

$$Normalized\ Rate = \frac{q_g}{m(p_i) - m(p_{wf})} \quad \textbf{Equation 2-24}$$

Using the conventional Material Balance equation to calculate the average reservoir pressure:

$$\frac{\bar{P}}{Z} = \frac{P_i}{Zi}\left(1 - \frac{G_p}{G}\right) \quad \textbf{Equation 2-25}$$

The steps of generating the Agarwal-Gardner analysis for gas production with a variable flow rate are:

1. Convert initial pressure and the flowing pressures to pseudo pressures, $m(p_i)$, $m(p_{wf})$
2. Assume an initial value for G to calculate the average reservoir pressure values corresponding to the cumulative production using lookup tables of P_{avg}/Z values from the MBE.
3. Convert average reservoir pressure to pseudo-pressure.
4. Using Equation 2-22, plot a graph of normalized rate versus normalized cumulative.
5. Draw a straight line through the best fit of the data points. (The intercept on the x-axis gives original gas-in-place.)
6. Using this new value of original gas-in-place, repeat steps 2-6 until the original gas-in-place converges.

The only drawback of this method is that the resulting plot is not intuitive as that for the P/Z plot and the normalized cumulative term becomes a true representative of cumulative gas production only when the material balance line intercept the cumulative gas production line and nowhere else.

❖ **Case Study**: (Ismadi, Kabir, & Hasan, 2012) provided a case study that compares the two approaches (Dynamic Material Balance of Gas by (Mattar & Anderson, 2005) and Agarwal – Gardner Analysis in estimating the original gas initially in place. The difference between the two methods was in calculating the average reservoir pressure by which the conventional material balance is applied. The DMB by (Mattar & Anderson, 2005) showed more iterative steps and values of Initial Gas in place were not similar to the ones calculated by the actual static pressure data with conventional MBE as shown in Figure 4: (Ismadi, Kabir, & Hasan, 2012) Comparison of the two FMB approaches [Gas FMB vs. Agarwal] for homogenous system. The reason is that any variations happen in the flowing data is reflected in $b_{a,pss}$ and then in calculating the average reservoir pressure. However, Agarwal's method includes a combined approach of static material balance with his normalized rate/normalized cumulative in calculating average reservoir pressure and then G.

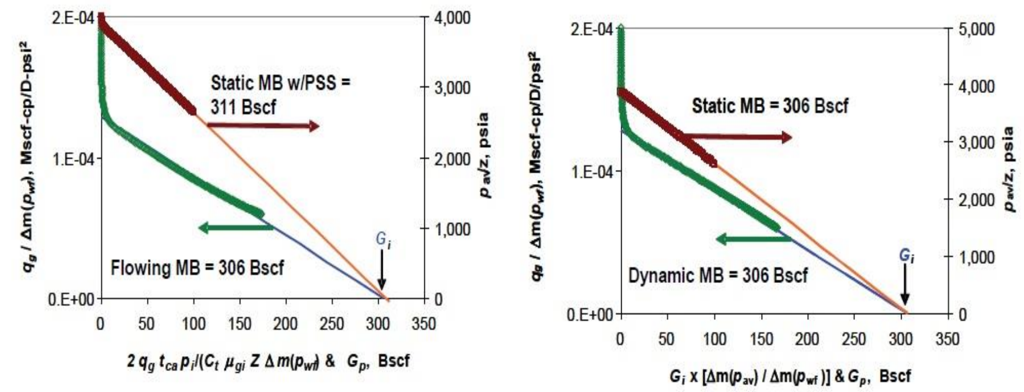

Figure 4: (Ismadi, Kabir, & Hasan, 2012) Comparison of the two FMB approaches [Gas FMB vs. Agarwal] for homogenous system.

2.2.4. Flowing Material Balance using a new Pseudotime function

This approach was presented by (Mohammed & Enty, 2013) in their paper of Analysis of Gas Production Using Flowing Material Balance Method where:

- Provided a derivation for a new pseudotime material balance function through which he proved the theoretical background of the material balance time and it is not just intuitive as it has been considered for years.

- They also provided a flow equation based on this new pseudotime function that represents the flow rate normalized pseudo cumulative that has been first introduced by (Callard & Schenewerk, 1995), but not used for this approach.

- Provided a simpler approach to calculate Gas-In-Place after defining PSS regime using type-curves.

- Provided a method to validate computed initial gas in place calculated by any method.

Between The Material Pseudotime and The new Pseudotime Functions

Material Balance Pseudotime (t_{ca}) has gained a widespread acceptance as it has the ability to handle the variable pressure or variable rate scenarios and it also considers the variations of gas properties (Viscosity and compressibility) with the average reservoir pressure change.

Although it's suitable to handle long term boundary dominated flow and it's rigorous for real gas, it's dependent on time step size and it's not suitable for shut in periods and requires the knowledge of average reservoir pressure or indirectly Gas-in-place.

It has first introduced by Palacio and Blasingame (1993) and used by Agarwal (1999) and Mattar and Anderson (2005) included in the gas flow equations applied for Flowing Material Balance approaches.

The New Pseudotime Function (T_a) is not sensitive to the time step size and offers a simpler approach to handle the viscosity-compressibility variations as viscosity-compressibility ratio is a function of the cumulative production. Viscosity-Compressibility variation showed a sensitive impact on the flowing material balance field data that have been plotted. It appeared as a fluctuation in the late-time boundary dominated flow data that caused a change in the slop of the straight line.

It is defined as:

$$T_a = \frac{1}{q_g} \int_0^{G_p} \frac{(\mu_g c_t)_i}{\overline{\mu_g} \overline{c_t}} \, dG_p \qquad \textbf{Equation 2-26}$$

(Mohammed & Enty, 2013) provided a simple approach to include the new material balance pseudo time in the general flow equation for variable rate or variable pressure scenarios. They started from the general expression for $d\overline{P}$ is given by (Farim and Wattenbarger 1987):

$$d\overline{P} = \frac{-q_g B_g}{V_P S_{gi} \overline{c_t}} \, dt \qquad \textbf{Equation 2-27}$$

Where the relation between gas cumulative production and gas flow rate is given by:

$$q_g = \frac{dG_p}{dt} \qquad \textbf{Equation 2-28}$$

Combining Equation 2-27 and Equation 2-28 yields:

$$d\bar{P} = -\frac{B_g}{V_P S_{gi}\overline{C_t}} dG_p$$ **Equation 2-29**

Knowing that formation volume factor can be expressed as:

$$B_g = \frac{\bar{Z}T\,P_{sc}}{\bar{P}T_{sc}}$$ **Equation 2-30**

Therefore, by substitution in Equation 2-29 we have:

$$d\bar{P} = -\frac{\bar{Z}T}{P}\left(\frac{P_{sc}}{T_{sc}}\right)\left[\frac{1}{V_P S_{gi}\overline{C_t}}\right] dG_P$$ **Equation 2-31**

Here, we introduce the normalized pseudopressure given by (Meunier, Kabir, & Wittmann, 1987) and (Palacio & Blasingame, 1993):

$$m(\bar{P})_n = \frac{(\mu_g Z)_i}{P_i}\int_0^P \frac{\bar{P}}{\bar{\mu}\bar{Z}} d\bar{P}$$ **Equation 2-32**

This is differentiated to give:

$$dm(\bar{P})_n = \frac{(\mu_g Z)_i}{P_i}\frac{\bar{P}}{\bar{\mu}\bar{Z}} d\bar{P}$$ **Equation 2-33**

Now we substitute Equation 2-31 into Equation 2-33 and we get:

$$-dm(\bar{P})_n = \left[\frac{T}{V_P S_{gi}\left({}^{P_i}/_{Z_i}\right)}\left(\frac{P_{sc}}{T_{sc}}\right)\right]\frac{\mu_{gi}}{\overline{\mu_g}\overline{C_t}}\, dG_p$$ **Equation 2-34**

Initial Gas in Place is expressed as:

$$G = \frac{V_P S_{gi}\left({}^{P_i}/_{Z_i}\right)}{T}\left(\frac{T_{sc}}{P_{sc}}\right)$$ **Equation 2-35**

We combine Equation 2-34 & Equation 2-35to have:

$$-dm(\bar{P})_n = \left[\frac{\mu_{gi}}{G}\right]\frac{1}{\overline{\mu_g}\overline{C_t}}\, dG_p$$ **Equation 2-36**

We can now integrate Equation 2-36 from the initial normalized pseudopressure, which corresponds to zero cumulative, to any given average reservoir pressure, which corresponds to a cumulative production of G_P. In other words, we are integrating from initial time (i.e., t=0) to any given time, t, to reach:

$$-\int_{m(P_i)_n}^{m(\bar{P})_n} dm(\bar{P})_n = \frac{1}{GC_{ti}}\int_0^{G_p}\frac{(\mu_{gi}C_{ti})}{\overline{\mu_g}\overline{C_t}}\, dG_p$$ **Equation 2-37**

Which then becomes:

$$m(P_i)_n - m(\bar{P})_n = \frac{1}{GC_{ti}}\int_0^{G_p}\frac{(\mu_{gi}C_{ti})}{\overline{\mu_g}\overline{C_t}}\, dG_p$$ **Equation 2-38**

Here, we introduce the pseudocumulative function given by (Callard & Schenewerk, 1995)

$$G_{pn} = \int_0^{G_p} \frac{\left(\mu_{gi} C_{ti}\right)}{\overline{\mu_g}\overline{C_t}}\, dG_p$$ **Equation 2-39**

Therefore, $$m(\bar{P})_n = m(P_i)_n - \frac{1}{GC_{ti}} G_{pn}$$ **Equation 2-40**

This equation is similar now to the liquid material balance given by (Dake):

$$\bar{P} = P_i - \frac{1}{NC_t} N_p$$ **Equation 2-41**

Using normalized pseudo pressure instead of actual pressure and pseudocumulative instead of actual cumulative linearizes the single phase gas flow equation and this allows us to solve single phase problems with the liquid solution.

Including gas flow equation during Pseudosteady state (PSS) flow regime is given by (Palacio & Blasingame, 1993):

$$m(\bar{P})_n - m\left(P_{wf}\right) = q_g b_{a,pss}$$ **Equation 2-42**

Then we combine Equation 2-38 and Equation 2-42 to have:

$$\frac{m(P_i)_n - m\left(P_{wf}\right)_n}{q_g} = \left[\frac{1}{GC_{ti}} \int_0^{G_p} \frac{1}{q_g} \frac{\left(\mu_{gi} C_{ti}\right)}{\overline{\mu_g}\overline{C_t}}\, dG_p\right] + b_{a,pss}$$ **Equation 2-43**

And the expression in the bracket on the right hand side (RHS) of Equation 2-46 becomes our basis for defining the new material balance Pseudotime function T_a in Equation 2-26

$$\frac{m(P_i)_n - m\left(P_{wf}\right)_n}{q_g} = \frac{1}{GC_{ti}} T_a + b_{a,pss}$$ **Equation 2-44**

Equation 2-44 shows that both the material balance pseudotime function and the new function have sound theoretical proof and they are equivalent.

$$\frac{m(P_i)_n - m\left(P_{wf}\right)_n}{q_g} = \frac{1}{GC_{ti}} \frac{G_{pn}}{q_g} + b_{a,pss}$$ **Equation 2-45**

By Plotting Equation 2-45 we get the x-intercept as G*C_{ti}

$$\frac{q_g}{\Delta m(p)_n} = -\frac{1}{b_{a,pss}\, GC_{ti}} \frac{G_{pn}}{\Delta m(p)_n} + \frac{1}{b_{a,pss}}$$ **Equation 2-46**

(Mohammed & Enty, 2013) Stated the steps for the FMB approach using the new material balance pseudo function using the normalized pseudo cumulative function:

1. Make a polynomial plot of viscosity-compressibility ratio against actual cumulative production at least to the third degree and set the intercept to 1. In our study for more accurate we developed it to the fifth order.
2. Integrate the resulting polynomial equation with respect to the actual cumulative production.
3. Substitute each actual cumulative production data point into the integral expression to obtain the corresponding pseudocumulative.
4. Make an approximate plot using G_p instead of G_{pn} in the previous equation. If data did not follow one straight line and two segments are observed (i.e., early and late time

PSS periods), extrapolate the early time PSS Period to the x-axis and solve for G. This yields the correct G at one time. However, if the early time PSS line is absent, any known method can be used to solve for G. This is explained in Table 10.

5. Once we have a value of G. Use the material balance equation to compute the average reservoir pressure profile, and, subsequently, the viscosity compressibility values.
6. Compute for pseudocumulative from steps 1, 2, 3.
7. Plot the pressure normalized pseudo cumulative function vs. pressure normalized flow rate on linear axes.

Table 10: Flowing Material Balance Approach introduced by (Mohammed & Enty, 2013)

Rate and Pressure scenario	y-axis	x-axis	Linearization (Pss flow regime)	Computation of Gc_{ti} on x-intercept
General (Rigorous)	$\frac{q_g}{\Delta m(p)_n}$	$\frac{G_{pn}}{\Delta m(p)_n}$	(almost) complete (one straight line)	Extrapolation to GC_{ti}
General Approximation	$\frac{q_g}{\Delta m(p)_n}$	$\frac{G_p}{\Delta m(p)_n}$	Partial (two straight lines are observed)	1. Early Straight line extrapolation to Gc_{ti} 2. Late straight line overestimates the Gc_{ti}

Therefore, we will test 3 different approaches for dry gas starting from (Mattar & Anderson, 2005)approach; (Agarwal, Gardner, Kleinsteiber, & Fussell, 1998) normalized rate and the new pseudotime function approach introduced by (Mohammed & Enty, 2013). For the dead oil model we will use the approach presented by (Mattar & Anderson, 2005) and comparing the results obtained using oil compressibility once and total compressibility once.

Chapter 3 Methodology

Studying the two proposed approaches needs to have production data and our study mainly based on synthetic data developed by Eclipse Simulator. Having the production data enables us to start analyzing them by Topaze (RTA Interface of Ecrin v4.20.05) by first model matching and then RTA. The last step is to build Flowing Material Balance approaches to obtain the Hydrocarbon in place estimation using flowing data.

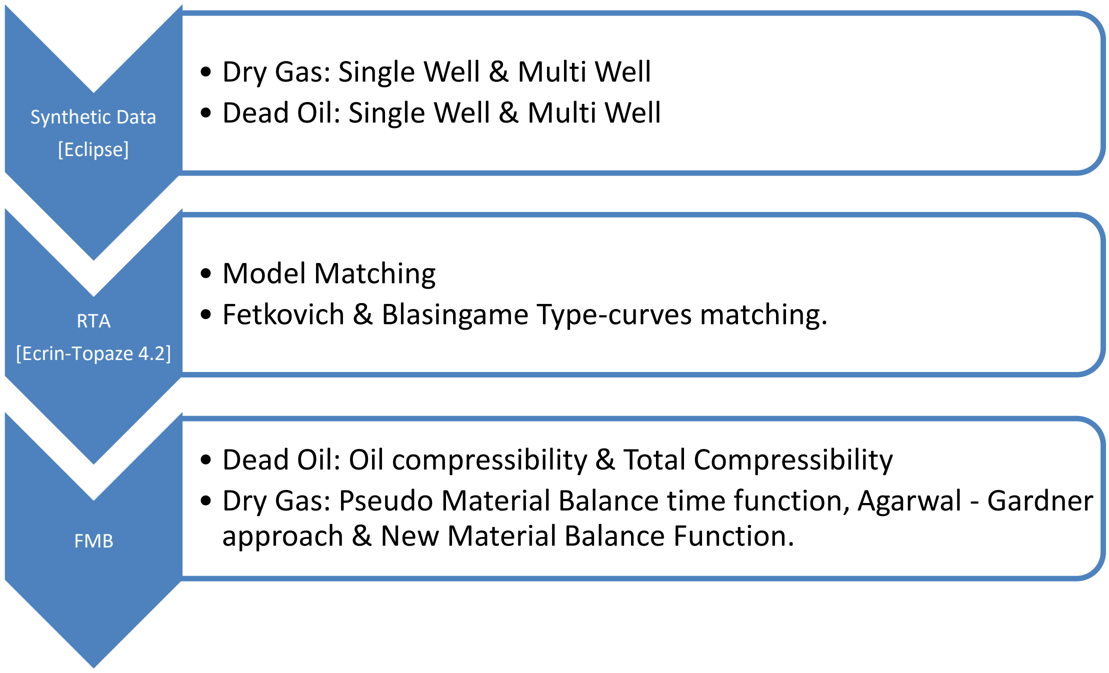

Figure 5: Steps of Methodology done in this study

3.1. Synthetic Data by Eclipse

3.1.1. Dead Oil Single Well

Model Description

Table 11 includes

PVT and densities data are synthetic data used from Eclipse database. Relative permeability and capillary pressure curves are imported from Eclipse Data Base as shown in Figure 6. The well is symmetrically centered in the reservoir described in Table 11.

Production starts on 15/05/2018 with an exponential fine time steps to match the pressure distribution in the transient period in Topaze.

Table 11: Dead Oil Singe Well Model Description

Two Phase Model: Oil & Water	
Reservoir Dimensions	2000 m * 2000 m * 50 m
Grids	100 * 100 * 20
Reservoir Pressure	4500 psi
Rock Compressibility	4e-6 psi^{-1}
Oil Compressibility @ Pi	1.26E-05 psi^{-1}
Oil Viscosity @ Pi	1.8 cp
Oil FVF (Bo)	1.2 bbl/STB
Reservoir Top Depth	8000 ft
OWC Depth	8200 ft
Swi	25%
Production control condition	Constant Pwf @ 900 psi
Well Diameter	0.6667 ft
Porosity	20%
Permeability (Kx, Ky, Kz)	(200,200,50) mD
Net Pay h	50 m

```
PROPS
-- Densities in lb/ft3
--       Oil      Water    Gas
--       --       --       --
DENSITY
         49       63       0.01 /

-- PVT data for dead oil
--       P        Bo       Vis
--       --       --       --
PVDO
         300      1.25     1.0
         800      1.20     1.1
         6000     1.15     2.0 /

-- PVT data for water
-- P     Bw       Cw       Vis      Viscosibility
-- --    --       --       --       -------------
PVTW
   4500 1.02      3e-06    0.8      0.0 /

-- Rock compressibility
--       P        Cr
--       --       --
ROCK
         4500     4e-06 /

-- Water and oil rel perms and capillary pressu
-- Sw    Krw      Kro      Pc
-- --    --       --       --
SWOF
   0.25 0.0       0.9      4.0
   0.5  0.2       0.3      0.8
   0.7  0.4       0.1      0.2
   0.8  0.55      0.0      0.1 /
```

Figure 6: Dead Oil Single Well Eclipse Model PVT data

3.1.2. Dead Oil Multi Well

For Multi-well we have the same model. The main difference is the number and the location of the wells. In this model we have 4 wells, symmetrically located. The grid numbers of each well are shown in Figure 7.

```
WELSPECS
   W1            G1     25     25         8082   OIL/
   W2            G1     75     25         8082   OIL/
   W3            G1     25     75         8082   OIL/
   W4            G1     75     75         8082   OIL/
/
```

Figure 7: Dead Oil Single Multi Well Model, Well Locations

3.1.3. Dry Gas Single Well

Model Description

PVT and densities data are synthetic data used from Ecrin database. Figure 8 shows the PVT data window in Ecrin software interface.

The well is symmetrically centered in the reservoir described in Table 12.

Production starts 01/06/2018 with fine linear time step.

Table 12: Dry Gas Single Well Model Description

Two Phase Model: Gas & Water	
Reservoir Dimensions	2000 m * 2000 m * 24.5 m
Grids	100 * 100 * 20
Reservoir Pressure	4500 psi
Reservoir Temperature	212 F
Rock Compressibility	4e-6
Reservoir Top Depth	8000 ft
OWC Depth	8200 ft
Swi	22%
Production control condition	Constant Pwf @ 3000 psi
rw	0.6667 ft
Porosity	20%
Permeability (Kx, Ky, Kz)	(50*50*20) mD
Net Pay h	24.5 m

- Exporting PVT data (Viscosity, Density, Z factor, Gas FVF, Compressibility). As shown in the figure below, reservoir pressure is set as 4500 psia and reservoir temperature as 212 F. By importing the PVT we could obtain the PVT as a function of pressure at any point. Therefore we could create PVT table for the Eclipse model from the imported data. Data imported and used for Eclipse are shown in Figure 9.

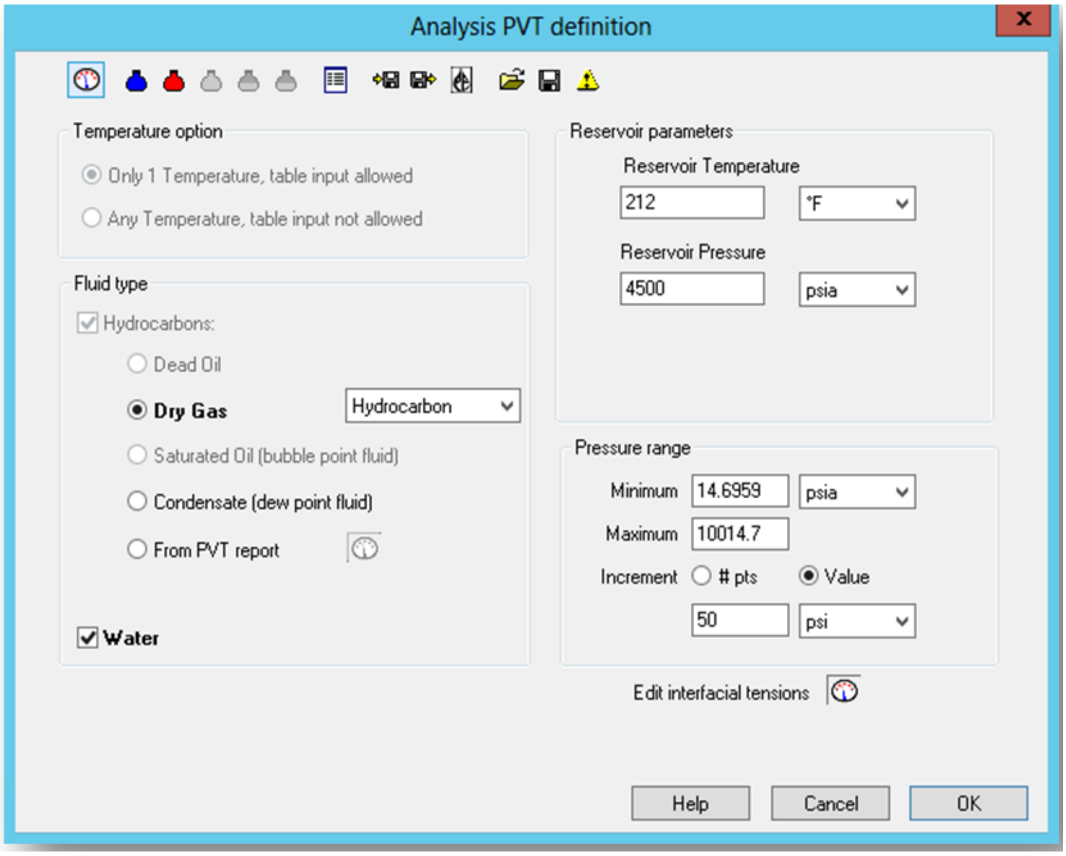

Figure 8: Importing PVT data from Ecrin. Topaze database representing our model parameters of Pressure and temperature

```
PROPS
-- Densities in lb/ft3
--       Oil      Water    Gas
--       --       --       --
DENSITY
         49       63       0.0537/

-- PVT data for DRY GAS
--       P        Bg Vis
--       --       --       --

PVDG

         -- Pg         Bg          mu_g
         14.6959 229.7542297     0.0135411
         256.028 12.92607302     0.013702
         497.36  6.527853963     0.0139589
         738.691 4.317292965     0.0142871
         980.023 3.201745325     0.0146804
         1221.35 2.532911843     0.0151359
         1462.69 2.090276046     0.0156511
         1704.02 1.77813179      0.0162224
         1945.35 1.548140695     0.0168452
         2186.68 1.373155833     0.0175134
         2428.01 1.236694568     0.0182203
         2669.35 1.128135352     0.0189585
         2910.68 1.040318789     0.0197206
         3152.01 0.968242208     0.0205
         3393.34 0.908317008     0.0212904
         3634.67 0.857914515     0.0220866
         3876    0.815070347     0.0228842
         4117.34 0.77830098      0.0236794
         4358.67 0.746466607     0.0244694
         4600    0.718680321     0.0252519
/
```

Figure 9: Dry Gas Single Well Eclipse Model PVT data

For the relative permeability and capillary pressure curves, data is imported from Eclipse Database where the **SGWFN** keyword is used for the two phase model (Water and gas) and columns represent respectively (Gas saturations, Gas relative permeability values representing the saturation values, water relative permeability values representing these saturations and capillary pressure values at these saturations). (Ltd., 2014, p. 2104)

```
SGWFN
        .0000 .0000 1.0000 .0000
        .0400 .0000 0.9000 .2000
        .1000 .0220 0.8000 .5000
        .2000 .1000 0.5000 1.0000
        .3000 .2400     1*     1*
        .5000 .4200     1*     1*
        .6000 .5000 0.1125 3.0000
        .7000 .8125 0.0000 3.5000
        .7800 1.0000 0.0000 3.9000
/
```

Figure 10: Dry Gas Single Well Eclipse Model capillary pressure data

3.1.4. Dry Gas Multi Well

Model Description

For the multi-well model, we reduced the permeability from 50 to 30 to reduce the production rate and have a longer profile of production with changing the bottom hole flowing pressure to 2000 psi instead of 3000 psi.

The same PVT data imported from Ecrin-Topaze, and the relative permeability and capillary pressure curves used for the single well model are used here.

The model consists of 4 wells symmetrically distributed in the reservoir as shown in Figure 11.

```
WELSPECS
   W1          G1       25      25         8082
   W2          G1       75      25         8082
   W3          G1       25      75         8082
   W4          G1       75      75         8082
/
```

Figure 11: Dry Gas Multi Well Model, Well Locations

3.2. Rate Transient Analysis [Ecrin v4.20.05- Topaze Interface]

After running the model on Eclipse we get the .RSM file with the production data and we input the production flowing data (Pwf, Qo) in Ecrin for each model. After this we build the model. For the single well model, we used the analytical approach and for the multi well we used the numerical model to compare the results of the two approaches.

3.2.1. Dead Oil Single Well

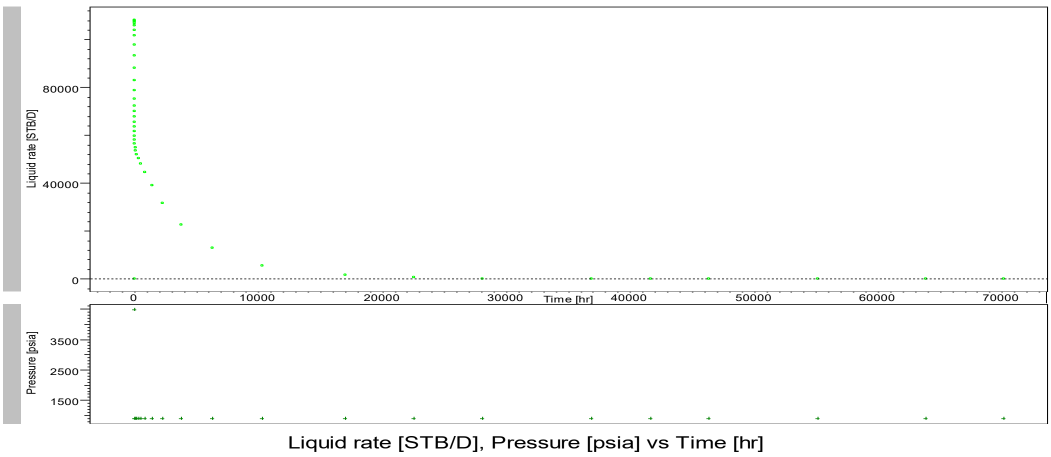

Figure 12: Dead Oil Single Well, Production rate and bottom hole flowing pressure vs. time

Figure 13 shows PVT as described in the Eclipse Model. The PVT data are considered constant for the production profile.

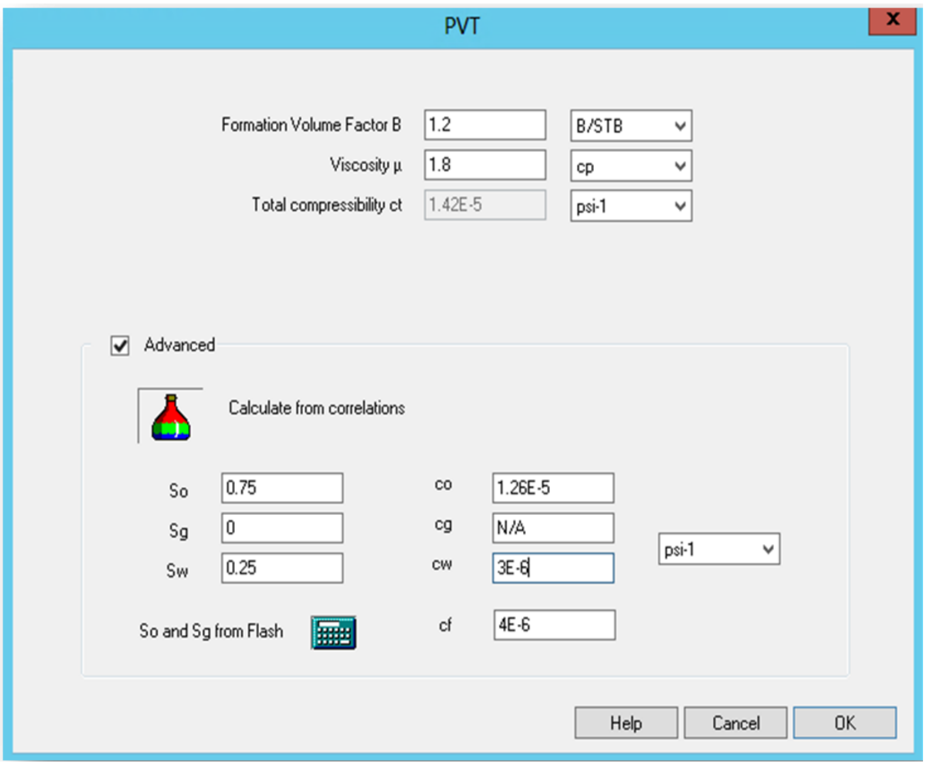

Figure 13: Dead Oil Single Well PVT data input in Ecrin. Topaze

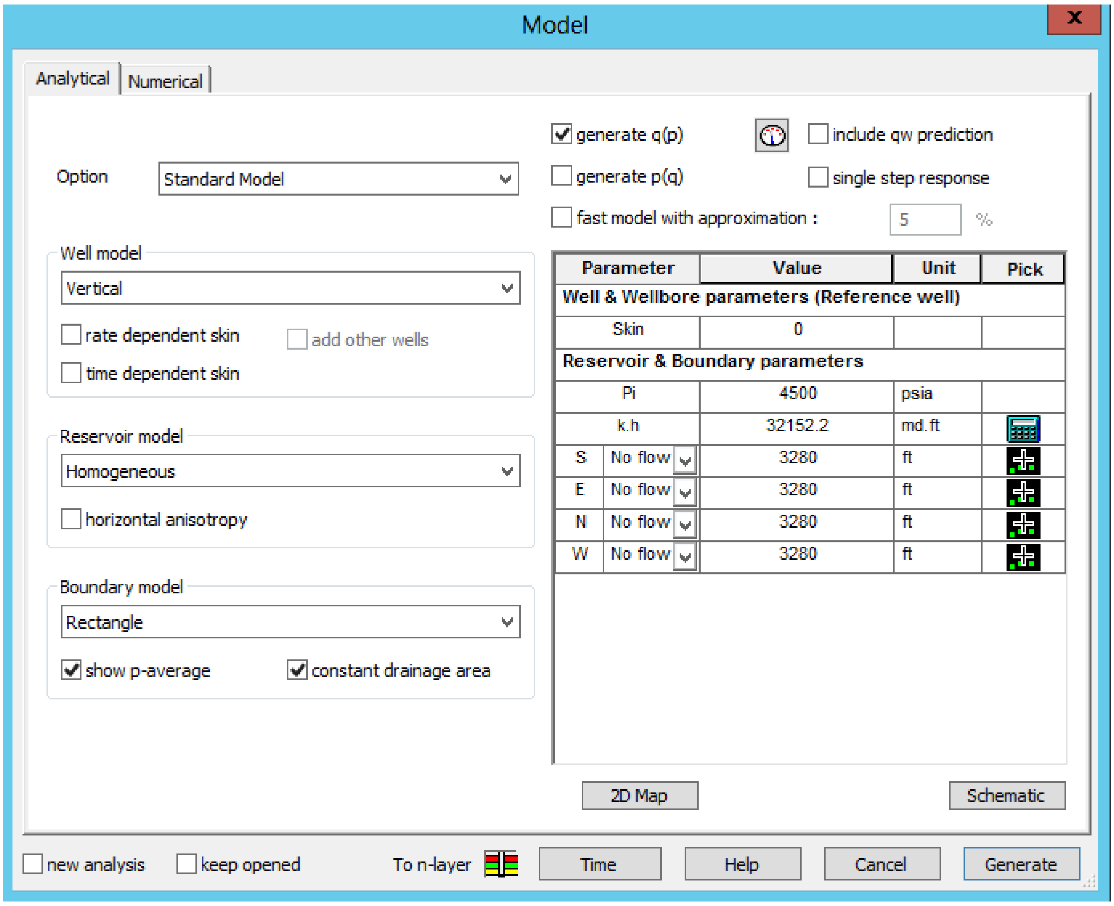

Figure 14: Dead Oil Single Well Analytical Model Description

The model is adjusted analytically as shown in Figure 14 by setting the boundaries as no flow boundaries and adjusting the net pay thickness to match the model created by Eclipse.

3.2.2. Dead Oil Multi Well

Figure 15 shows the production cumulative after inputting the production data in Topaze.

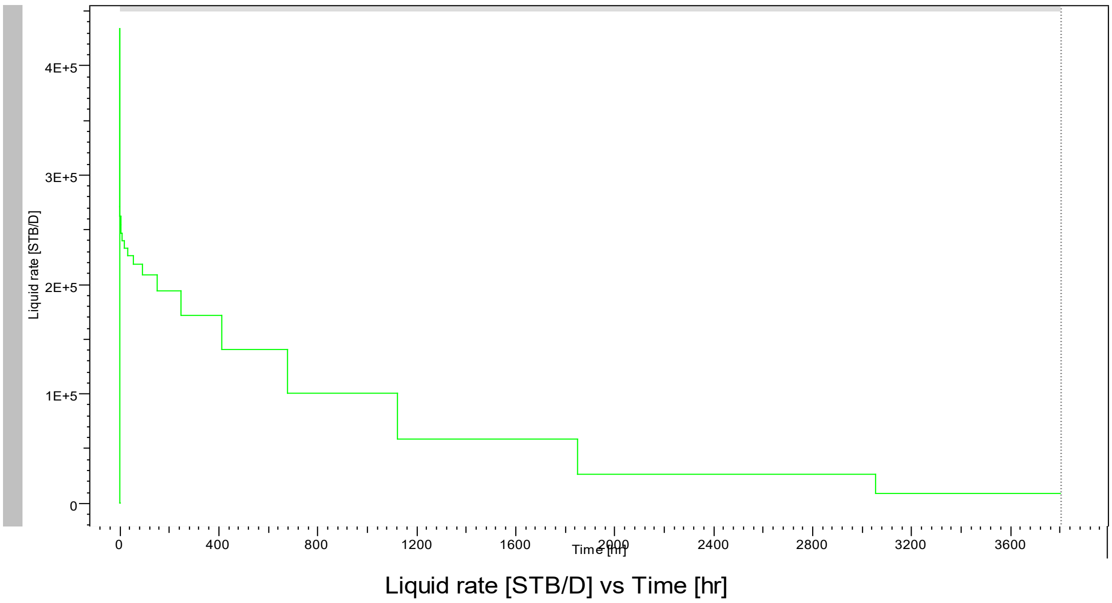

Figure 15: Dead Oil multi-well cumulative production vs. time

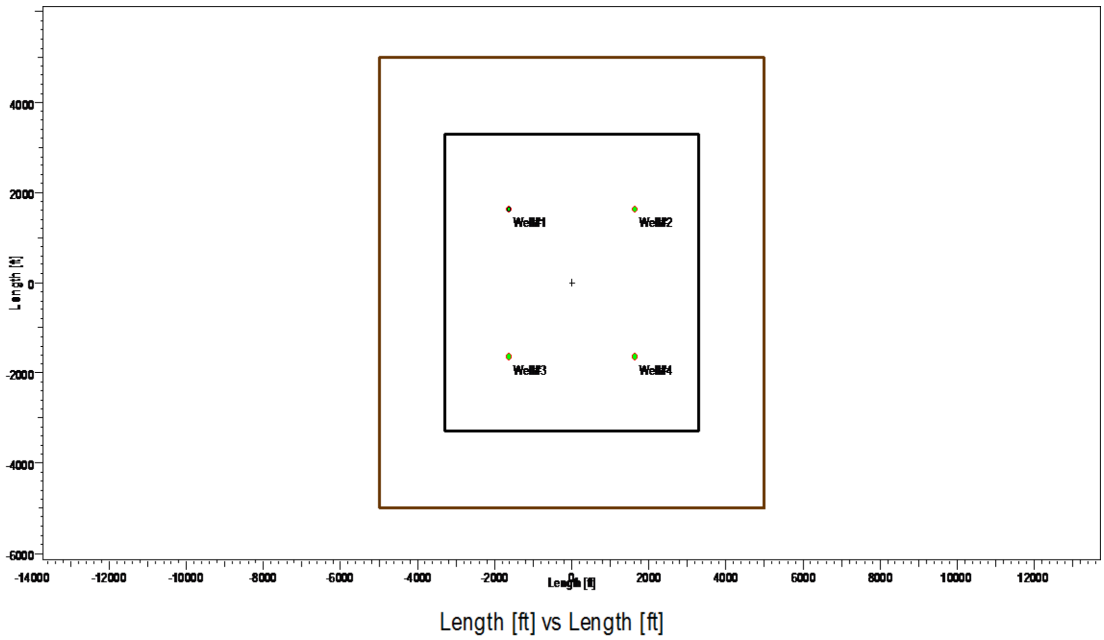

Figure 16: Dead Oil Multi-well Model. Well location.

The multiwall model is solved numerically by drawing the boundaries of the reservoir and locating the wells as shown in Figure 16. Then, by selecting the "add other wells" option in the model window, the model considers the pressure disturbance created by the other wells in the same map defined and therefore, no need to set the boundaries like we did in the single well.

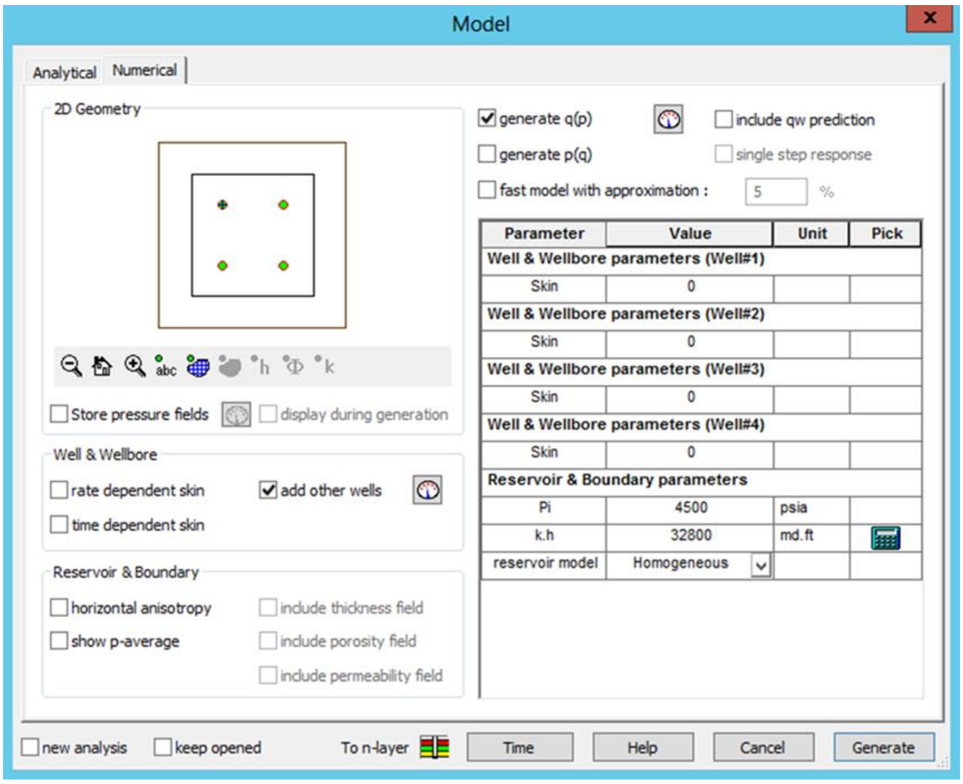

Figure 17: Dead Oil Multi-well Numerical Model description.

3.2.3. Dry Gas Single Well

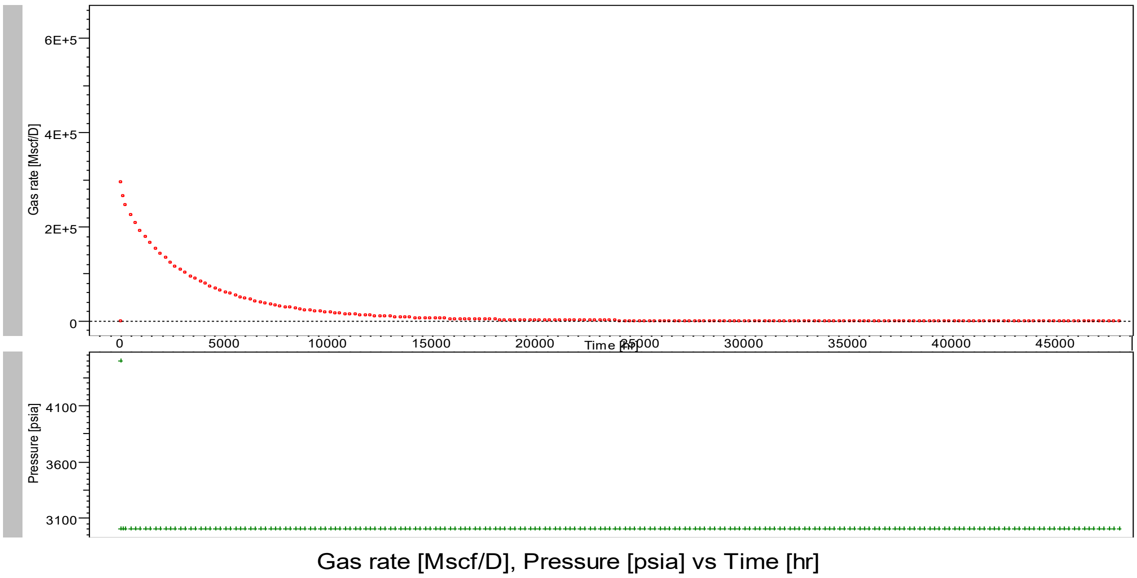

Figure 18: Dry Gas Single Well production and Bottom Hole Pressure Vs. Time

After inputting the production data for the dingle well model as shown in Figure 18, we need to define the PVT data as shown in Figure 8. And before extraction the data, we define the model. For single well model the solution of analytical or numerical model are equivalent. However, it is easier for single well to set the model analytically by defining the boundaries and and their locations from the well as shown in Figure 19.

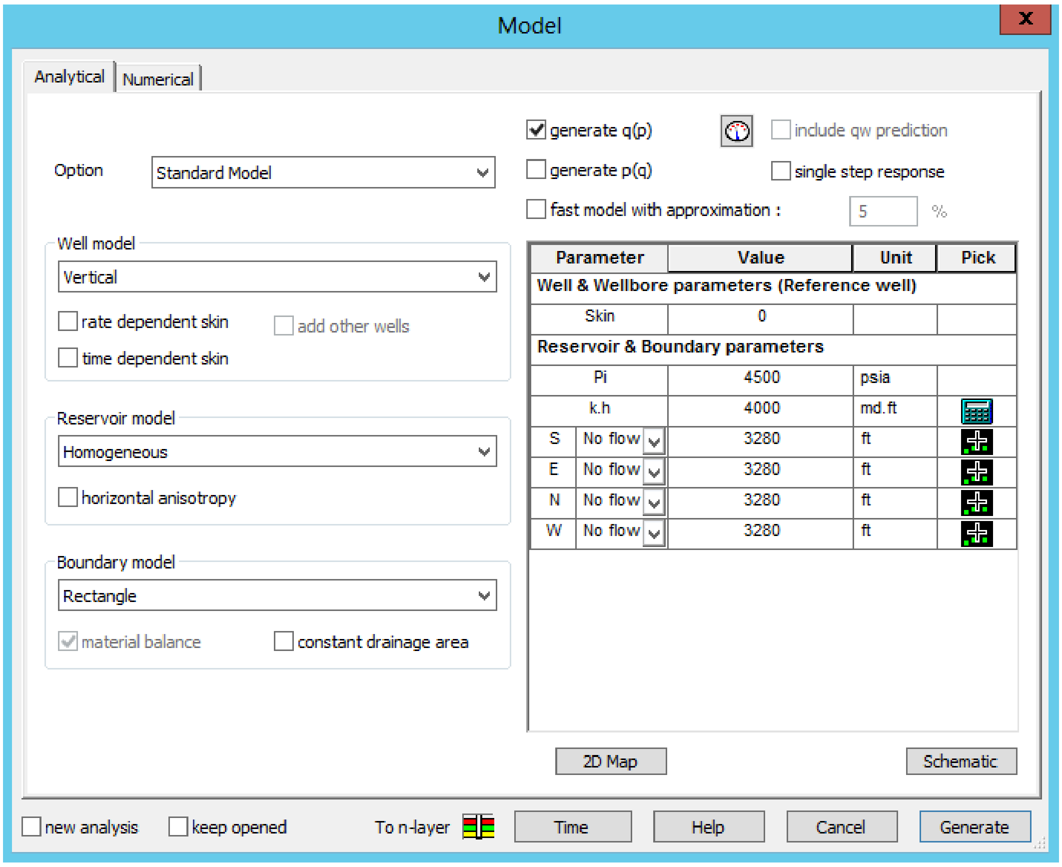

Figure 19: Dry Gas Single Well Analytical Model Description

3.2.4. Dry Gas Multi Well

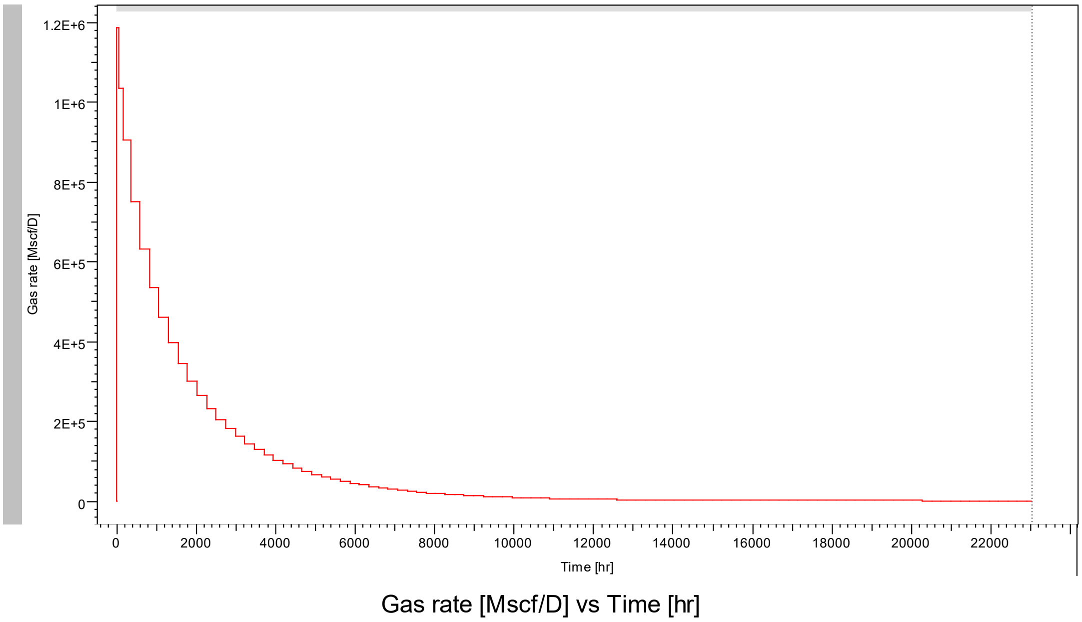

Figure 20: Dry Gas Multi-Well Cumulative production vs. time.

For multi-well model, after inputting the production data of each well, the cumulative gas production of the reservoir could be obtained as a function of pressure as shown in figure 20.

As mentioned in the case of multi-well dead oil by locating the wells and the boundaries of the reservoir on the map as in Figure 21.

One important note for all the models is we assume no wellbore skin for all the models as in Figure 22.

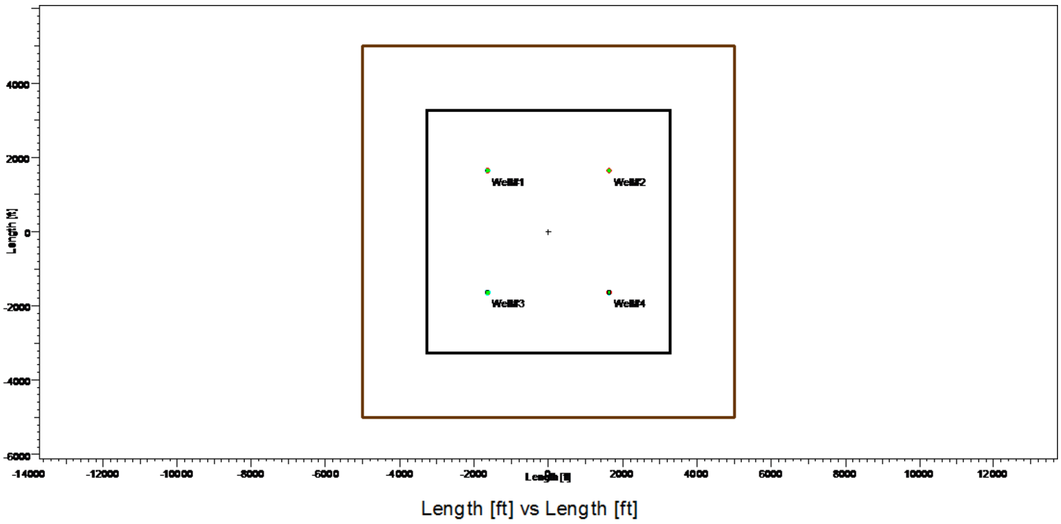

Figure 21: Dry Gas Multi well Model. Well Locations.

The model in multiwell case is set numerically.

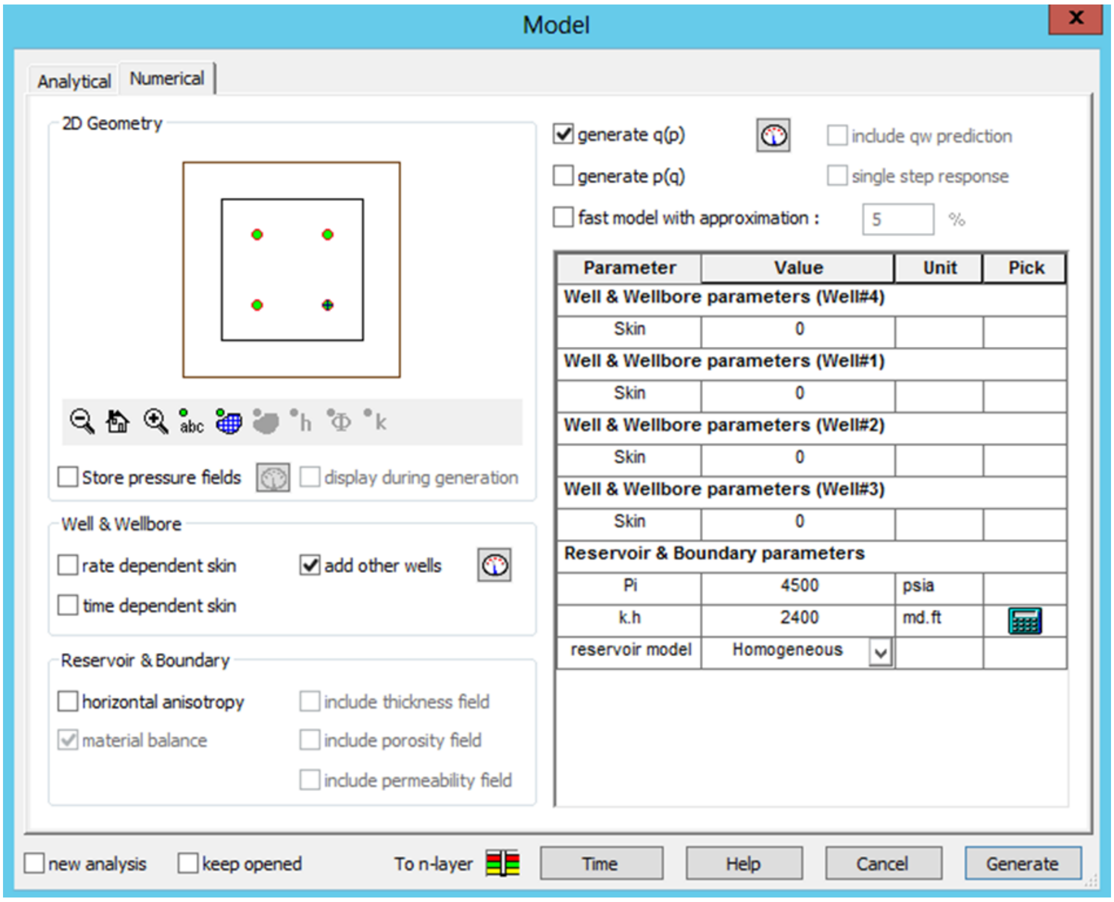

Figure 22: Dry Gas Multi-well Numerical model Description

3.3. Flowing Material Balance

3.3.1. Dead Oil

To establish the FMB for dead oil we use the approach introduced by (Mattar & Anderson, 2005). This Approach is valid for constant/variable flow rate conditions in which he replaced the production time with the material balance time previously introduced by (Palacio & Blasingame, 1993). The approach aims to estimate the original oil in place using the fluid flow equation in pseudo steady state conditions and combining it with the depletion equation for dead oil reservoirs.

Starting from liquid flow equation in Porous medium in Pseudo-Steady State Conditions, See Appendix A:

$$p_{wf} = \bar{p} - \frac{q_o\, \mu_o}{4\, \pi k h} \left[\ln\, 2.25\, \frac{A}{C_A r_w^2}\right] \qquad \textbf{Equation 3-1}$$

Setting Dietz factor for a single well symmetrically located in a rectangular drainage area as 30.9

Using the Material Balance equation for dead oil reservoir above bubble point (Depletion Equation):

$$p_i - \bar{p} = \frac{q_o t}{c_o A h \phi} \qquad \textbf{Equation 3-2}$$

$$p_i - \bar{p} = \frac{q_o t}{N c_o} \qquad \textbf{Equation 3-3}$$

By combining the two equations we reach

$$P_i - P_{wf} = \frac{q_o t}{c_o N} + \frac{141.2\, q_o B_o \mu_o}{kh}\left[\ln\, 2.25\, \frac{A}{C_A r_w^2}\right] \qquad \textbf{Equation 3-4}$$

This can be written as:

$$P_i - P_{wf} = \frac{q_o t}{c_o N} + b_{pss}\, q_o \qquad \textbf{Equation 3-5}$$

Where b_{pss} (The Pseudo-Steady State Constant), (the reciprocal of productivity index):

$$b_{pss} = \frac{141.2\, B_o \mu_o}{kh}\left[\ln\, 2.25\, \frac{A}{C_A r_w^2}\right] \qquad \textbf{Equation 3-6}$$

This is constant and was first presented by Blasingame. It can be obtained by rearranging the equation into:

$$\frac{(P_i - P_{wf})}{q_o} = \frac{q_o t}{c_o N q_o} + b_{pss} = \frac{N_p}{c_o N q_o} + b_{pss} \qquad \textbf{Equation 3-7}$$

This equation is only valid for constant flow rate, however by replacing the production time with Material Balance time Equation 2-5

$$\frac{(P_i - P_{wf})}{q_o} = \frac{q_o t_c}{c_o N q_o} + b_{pss} = \frac{t_c}{c_o N} + b_{pss} \qquad \textbf{Equation 3-8}$$

A Cartesian plot of $\frac{(P_i - P_{wf})}{q_o}$ vs. t_c will yield a straight line with an intercept of $b_{pss.}$ Then Average Pressure could be obtained by:

$$\bar{P} = P_{wf} + b_{pss} * q_o \quad \textbf{Equation 3-9}$$

A Cartesian plot of $(p_i - \bar{p})$ vs. $\frac{N_p}{C_o}$ will yield a straight line with a slope equal to $\frac{1}{N}$.

Anderson 2005 used the compressibility of the oil c_o. However, further developments of the flowing material balance showed the same approach but using the total compressibility c_t instead of the oil compressibility. In this study we developed the oil in place using the two approaches to study the effect of the compressibility on the total oil in place.

Note that in the Flowing Material Balance for oil, the fluid properties over the production life (Production period) are assumed to be constant.

For single well, the production data is analyzed and fully representing the whole reservoir. Therefore, N represents the Initial Oil in place of whole reservoir.

For Multi well, the production data is obtained from four different wells. Therefore, the N from the analysis of one set of production data represents the approximate drainage area of this well. In the development of multi-well approach, we assumed that the production of the 4 wells started at the same, wells are symmetrically distributed in the reservoir boundary and boundary is constant, hence pressure disturbance is uniform.

3.3.2. Dry Gas

In reality, the production data is obtained from the daily flow rate at the surface and Permanent Down Hole Gauges (PDG) in front of the perforation just to have a valid correct representing bottom-hole pressure for the representing production flow rate. The use of Downhole Gauges helped reservoir engineers to establish the way for Rate Transient Analysis and deep analysis of production data. However, the use of permanent downhole Gauges are not widely used because of its cost. Other ways of obtaining the bottom-hole pressure from the well head pressure have showed their applicability as well using correlations and pressure loss equations to estimate Pwf.

The development of the Flowing material balance for gas reservoir does not only require the production flowing data, but also the representing PVT data for each production data to account for the change of the gas properties change with the continuous production. That is why (Mattar & Anderson, 2005) introduced another function called the material balance pseudo time to account for gas properties change with time. Equation 2-8

$$t_{ca} = \frac{(\mu_g c_t)_i}{q_g} \int_0^t \frac{q_g}{\mu_g c_t} dt \quad \textbf{Equation 2-8}$$

To overcome this point, we have used the PVT data imported from Ecrin database related to the reservoir and gas properties (Pi, T, Gas Gravity and Gas composition) to build polynomial equations representing each property as a function of pressure, therefore we could have a representing set of PVT for the production data at each time step.

The another difference between FMB gas and FMB oil is the use of the pseudo pressure function instead of the pressure when it comes to gas, hence, the building of polynomial equations between pressure and pseudo pressure function to be easily able to have values of m(p) at different P values and vice versa.

The estimation of the fluid properties at the representing time step or the production points needs to have the average pressure value. However, the method introduced aims to overcome the main obstacle of conventional material balance which is obtaining the average reservoir pressure by shutting the well in. Therefore we build an iterative method based on initial assumption of the G value from which we can further obtain the average reservoir pressure at the different cumulative production using the conventional gas material balance equation and then we calculate the gas properties to be able to estimate the gas pseudo material balance function to implement the FMB for gas and obtain the initial Gas in place. We iterate until we reach a final value of G that represents the Gas initial in place for the reservoir.

Generating PVT data represents the production data at each time step

To convert the Pressure values into pseudo pressure function m (p), from the Ecrin PVT Import option we have a P & m (p) values representing our reservoir. Therefore, we build a polynomial equation to be able to get m (p) at any value of P.

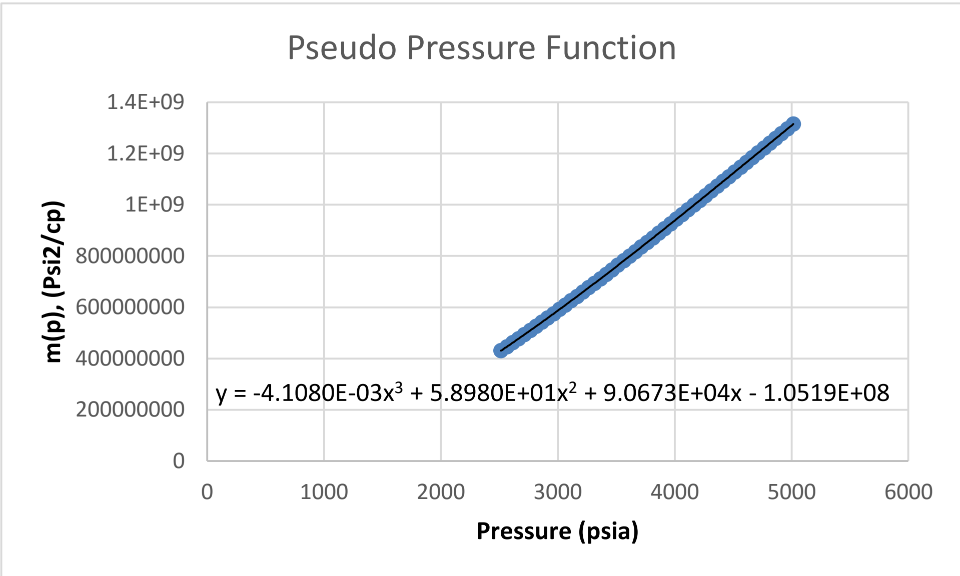

Figure 23: Pseudo Pressure Function polynomial equation as a funcation of pressure

We chose only the range of pressure we are interested in to have the best fit and we developed a polynomial equation from the third order for better approximation.

After obtaining $m(\bar{p})$ from the FMB plot, we need to convert it to average pressure to build the conventional Material Balance equation for Gas. We us the polynomial equation developed in Figure 24.

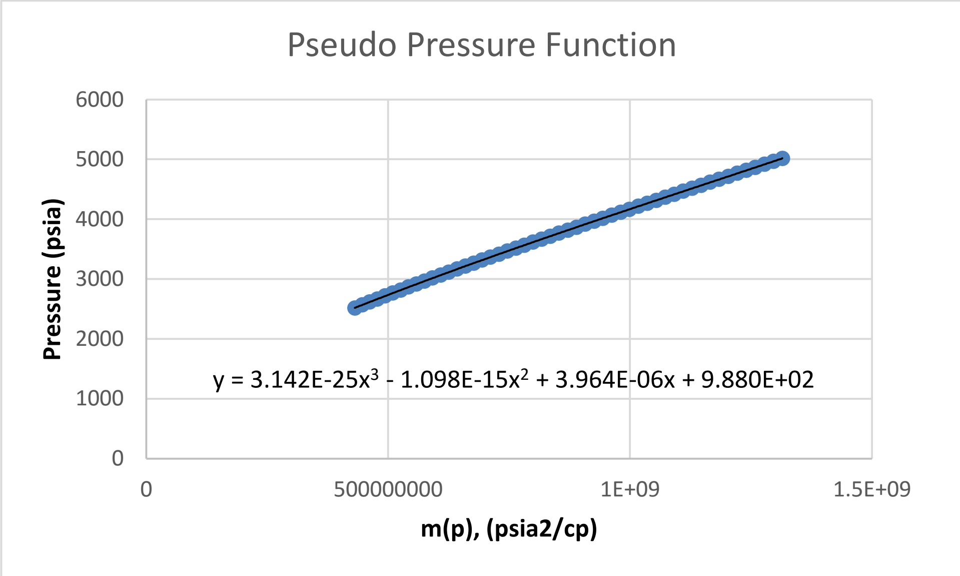

Figure 24: Average Reservoir Pressure polynomial equation as a function of gas pseudo pressure.

From Step (2) in the Gas FMB procedure, we obtain P/Z values at different Gp values. However, we need to obtain the average pressure to calculate the gas properties at this value. Therefore, again from the PVT data imported from Ecrin Database representing our reservoir. We get P/z values and then build a function of P from these P/z values as shown in Figure 25. We chose on the range of pressure in our interest for better fitting the polynomial equation (2500: 4600 Pisa).

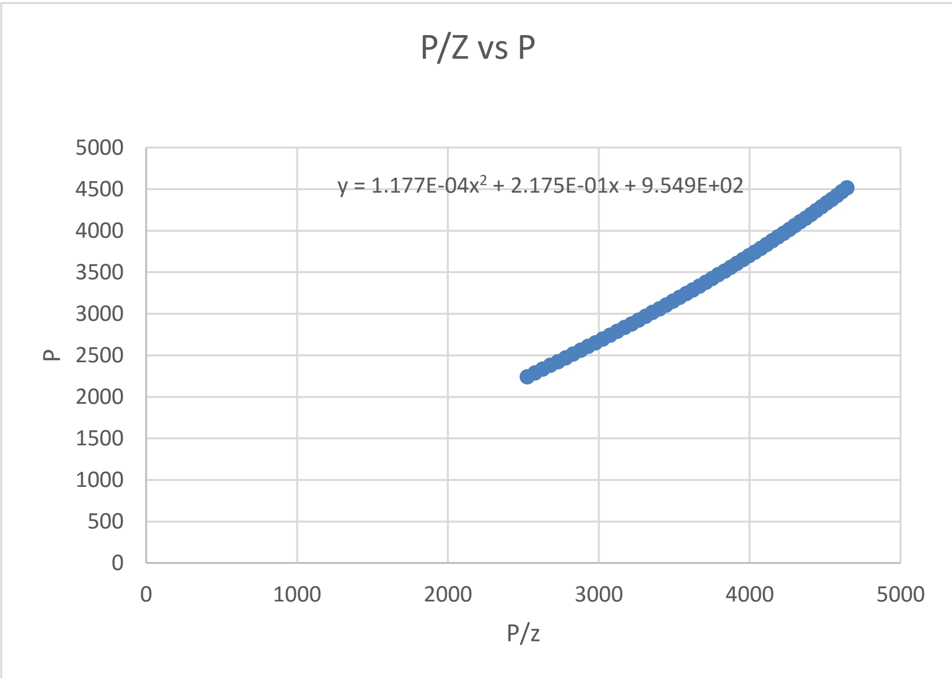

Figure 25: Average Reservoir Pressure Polynomial Equation as a Function of P/Z.

To calculate the gas compressibility at different average pressure values that would be necessary even for the New material balance function calculations, we plot the imported daya from Ecrin (Compressibility values as a function of pressure and from the fit equation on Figure 26 we could obtain the values of gas compressibilites at each value of average pressure. Total compressibility is then calculated assuming constant saturation values through the production profiles and assuming constant rock compressibility as well.

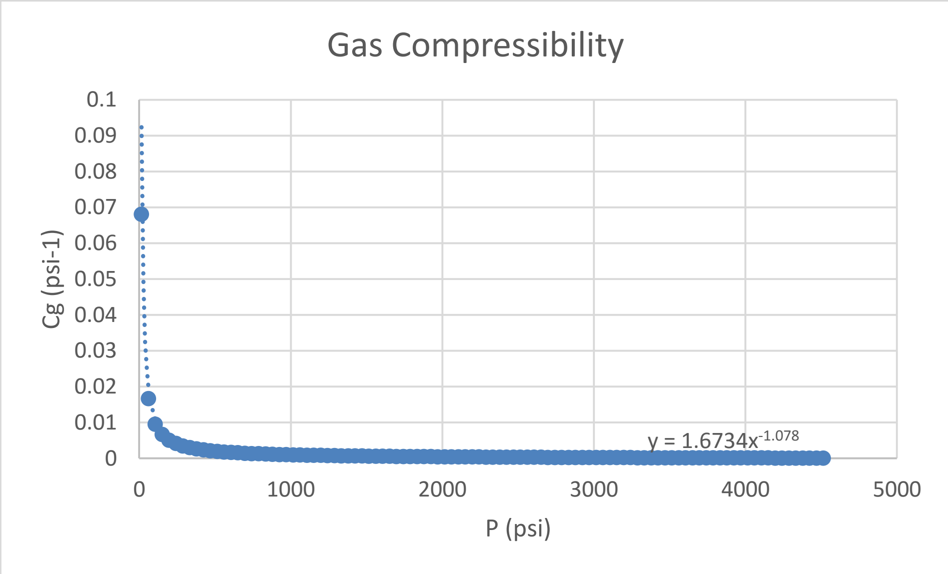

Figure 26: Gas Copressibility as a function of Pressure.

To build the conventional P/Z graph we need to have values for the Z compressibility factor at each time step. We plot the imported data from Ecrin (Z vs average pressure and use the generated polynomial equation on Figure 27.

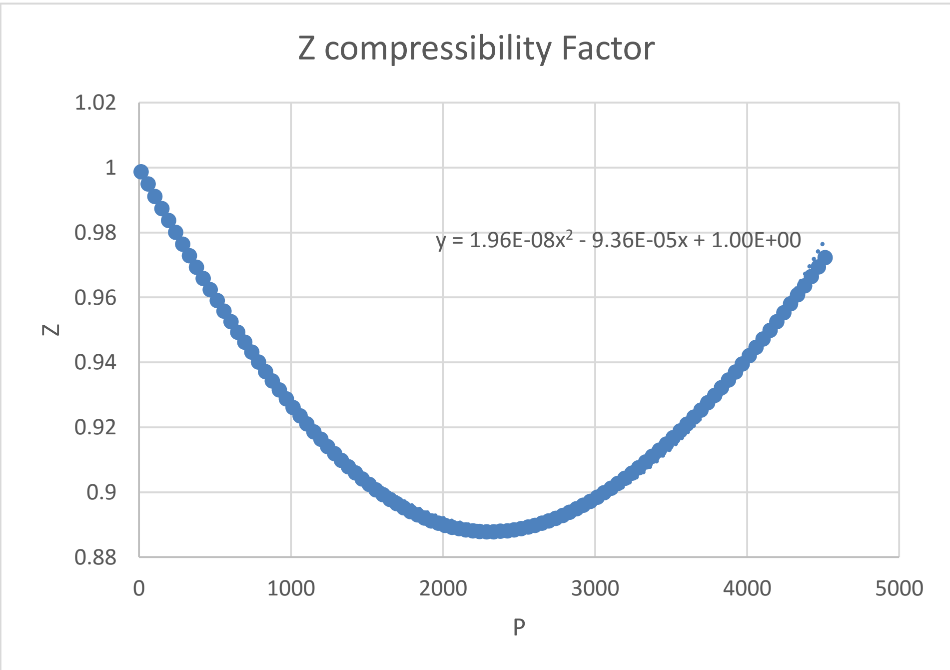

Figure 27: Gas Compressibility factor as a function of pressure.

For the gas viscosity, the same technique is also developed and the polynomial equation representing the range we are interested in on Figure 28 is used for generating the gas viscosity values at different average pressure values.

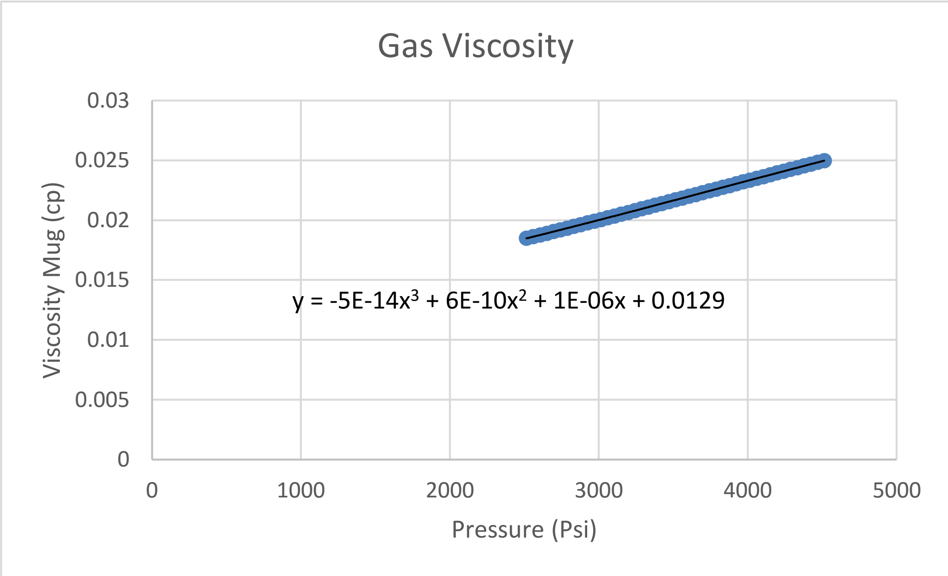

Figure 28: Gas viscosity as a function of pressure.

3.3.2.1. Gas Flowing Material Balance

The method used is based on driving the FMB equation from the fluid flow equation and combining it with the conventional material balance equation as proposed by (Mattar & Anderson, 2005).

The first approach introduced by (McNeil, 1995) needs to have valid PVT data representing the production points because it is mainly P_{wf}/Z plotting vs G_p. Therefore, the approach we used to assume an initial G and with the help of the correlation built using PVT database on Ecrin will not be an appropriate method and might gibe high error.

Starting from the gas flow equation in a porous medium in pseudo steady conditions in Appendix A

$$m(p_{wf}) = m(\bar{p}) - \frac{q_g\, T}{2\pi\, k\, h}\left(\frac{P_{sc}}{T_{sc}}\right)\left[\ln\, 2.25\, \frac{A}{C_A r_w^2}\right] \qquad \textbf{Equation 3-10}$$

Setting Dietz factor for a single well symmetrically located in a rectangular drainage area as 30.9 Using the material balance equation for gas introduced (Mattar & Anderson, 2005)*

$$m(p_i) - m(\bar{p}) = \frac{2p_i q_g\, t_{ca}}{G Z_i C_{ti} \mu_{gi}} \qquad \textbf{Equation 3-11}$$

Equation 3-11 mentioned in literature without the term ($C\mu_i$) in the dominator. However, the same equation was found in other literatures (Morad & Clarkson, 2006) indicating to the missing term.

Combining the two equations we reach:

$$m(p_i) - m(p_{wf}) = \frac{2p_i q_g\, t_{ca}}{G Z_i C_{ti} \mu_{gi}} + \frac{q_g\, T}{2\pi\, k\, h}\left(\frac{P_{sc}}{T_{sc}}\right)\left[\ln\, 2.25\, \frac{A}{C_A r_w^2}\right] \qquad \textbf{Equation 3-12}$$

$$\frac{m(p_i) - m(p_{wf})}{q_g} = \frac{2p_i\, t_{ca}}{G Z_i C_{ti} \mu_i} + b_{a,pss} \qquad \textbf{Equation 3-13}$$

$$m(\bar{p}) = m(p_{wf}) + q_g\, b_{a,pss} \qquad \textbf{Equation 3-14}$$

Where,

$$b_{a,pss} = \frac{T}{2\pi\, k\, h}\left(\frac{P_{sc}}{T_{sc}}\right)\left[\ln\, 2.25\, \frac{A}{C_A r_w^2}\right] \qquad \textbf{Equation 3-15}$$

From b_{pss}, we can have an estimation of the gas effective permeability k if we know h.

By plotting $\frac{m(p_i)-m(p_{wf})}{q_g}$ vs t_{ca} we get $b_{a,pss}$ as intercept. Then we get $m(\bar{p})$. Which is converted to Pavg to build the conventional P/z plot.

t_{ca}, here is developed from the explicit Pseudo material balance function. Equation 2-8

Comparison between the two methods is developed to see the effect on calculating the permeability and the gas in place.

Gas FMB Steps in the thesis work:

1) Assume an initial value of G. This depends on the production profile. Assume that total Gp=30% of G.
2) Use Conventional Material Balance (P/Z) Equation for Gas to obtain the average reservoir pressure at each time step.
3) Calculate the gas properties at this P_{avg} (Viscosity & Gas compressibility)
4) Calculate the material balance time function t_{ca}.
5) Convert all pressures in pseudo pressure function (Pwf & Pavg).
6) Plot $\frac{m(p_i)-m(p_{wf})}{q_g}$ $vs\ t_{ca}$ to obtain $b_{a,pss}$ as an intercept
7) Get $m(\bar{p}) = m(p_{wf}) + q_g b_{a,pss}$
8) Convert $m(\bar{p})$ into P avg and build the P_{avg}/Z graph o obtain Gi.
9) Repeat until we reach the real value of G.

3.3.2.2. Agarwal Gardner Method

By Plotting the normalize flow rate vs the normalized cumulative to have the initial gas in place as the intercept of x-axis. Equation 2-23 & Equation 2-24.

3.3.2.3. New Pseudo Material Balance time function

This approach needs to convert the pseudo pressure function into normalized pseudo pressure function.

$$dm(\bar{P})_n = \frac{(\mu_g Z)_i}{P_i} \frac{\bar{P}}{\bar{\mu}\bar{Z}} d\bar{P}$$ **Equation 3-16**

Then plotting $\frac{q_g}{m(P_i)_n - m(P_{wf})_n}$ vs $\frac{q_g}{G_{pn}}$ we obtain G as intercept. See Flowing Material Balance using a new Pseudotime function

$$T_a = \frac{1}{q_g} \int_0^{G_p} \frac{(\mu_g c_t)_i}{\overline{\mu_g c_t}} dG_p$$ **Equation 3-17**

$$G_{pn} = \int_0^{G_p} \frac{(\mu_{gi} C_{ti})}{\overline{\mu_g} \overline{C_t}} dG_p$$ **Equation 3-18**

$$T_a = \frac{G_{pn}}{q_g}$$ **Equation 3-19**

T_a, is defined as the new pseudo material balance function. The calculating of $G_{pn}$is done by fitting the polynomial equation of the $\frac{(\mu_{gi} C_{ti})}{\overline{\mu_g} \overline{C_t}}$ term at different pressures as a function of the cumulative production as shown in Figure 29.

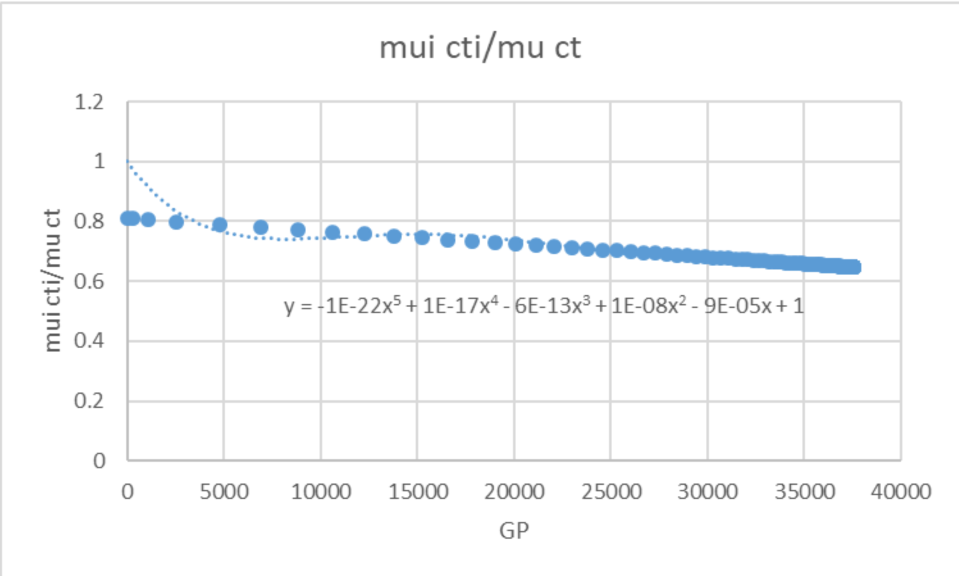

Figure 29: Viscosity compressibility ratio as a function of cumulative production.

The steps were followed as explained in the Flowing Material Balance using a new Pseudotime function section (P. 20 & 21).

The comparison between the three methods of FMB introduced here is performed with a close comparison on the effect on the different calculation approaches of pseudo material balance function and the pseudo normalized cumulative function.

Chapter 4 Results & Discussion

The main purpose of the study is to estimate the Initial Hydrocarbon in place for the different models by validating two approaches; Rate Transient Analysis & Flowing Material Balance to prove that Production Data could be used to estimate the hydrocarbon in place without the need to shut the well in and implementing the conventional methods. These approaches aim to show how close the results obtained from these approaches to the most valid one (Numerical simulation model).

RTA provides us with information about the boundaries of the reservoir and when stabilization occurs. This helps us to make sure that we are in pseudo steady state conditions as the flowing Material balance is valid when the production reaches the pseudo steady conditions when all boundaries are touched and depletion starts to occur. One important note is here we are working on single phase production in explicit depletion conditions (No water drive, no gas in solution or gas cap expansion).

The results we have from this study are:

- Numerical simulation model HOIP estimation.
- Rate Transient Analysis (RTA):
    - Ecrin, Topaze Model Match
    - Fetkovich Type-curves Match
    - Blasingame Type-curves Match
- Flowing Material Balance (FMB):
    - Dead Oil: using Material balance time
        - Using total compressibility
        - Using oil compressibility
    - Dry Gas:
        - Using Pseudo Material Balance Function
        - Using Normalized Rate – Normalized Cumulative Approach
        - Using Normalized Pseudo Cumulative Function

Comparing these results will tell us how far we are from the exact value and what the error percentage for each case is.

4.1. Dead Oil Single Well

4.1.1. Numerical Simulation Model

The Original Oil in Place value obtained from the numerical simulation model was around 162 MMSTB.

The data developed by Eclipse needed different runs until model of Ecrin is matched. The main issue was the matching of the transient period. Therefore, a very fine exponentially increasing time steps were used.

4.1.2. Rate Transient Analysis Model

Model Matching

From the figure shown below, we found that the production data has matched the model built using Ecrin 4.20.05, Topaze. The model gave initial oil in place equal to 157 MMSTB.

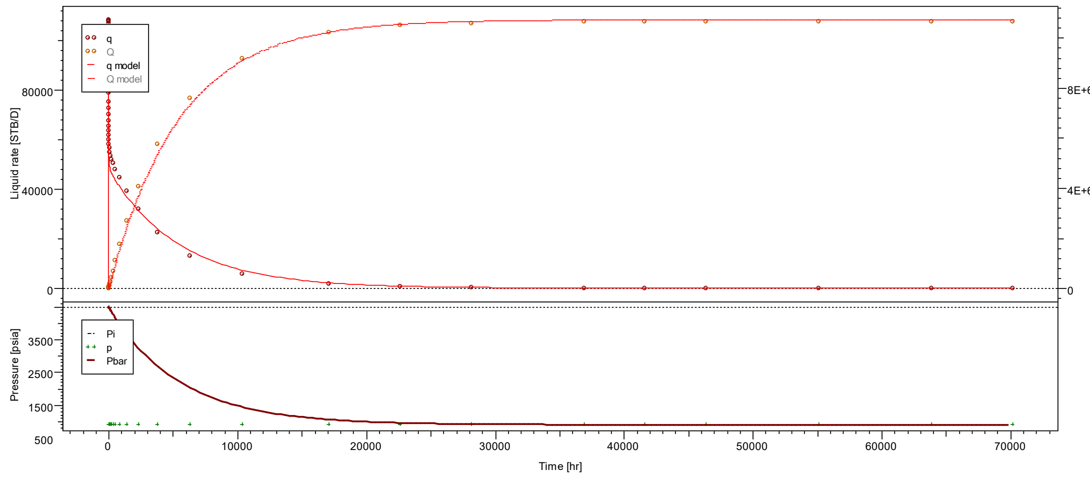

Production history plot (Liquid rate [STB/D], Pressure [psia] vs Time [hr])

Figure 30: Dead Oil Single Well Production History Match. Rate, Cumulative production, flowing pressure and model reservoir average pressure vs. Time.

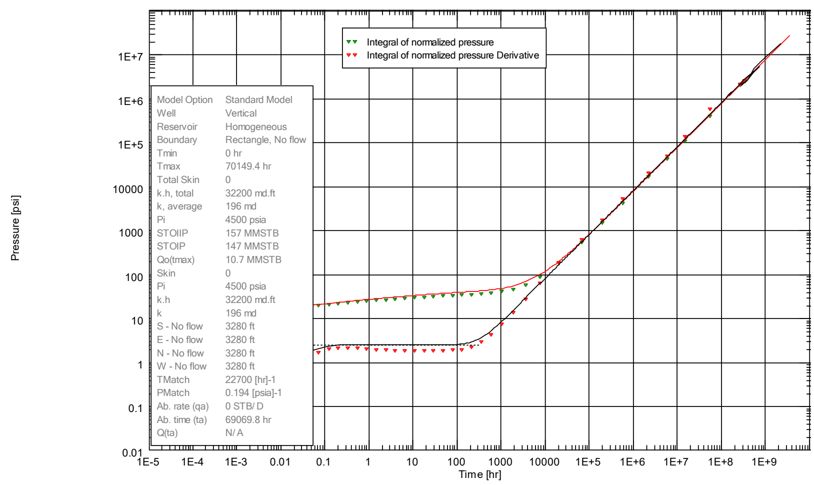

Loglog plot: Int[(pi-p)*q_ref/q]/te and d[Int[(pi-p)*q_ref/q]/te]/dln(te) [psi] vs te/2 [hr]

Figure 31: Dead Oil Single Well Log-Log Plot Match

This graph shows that the late part of the data is already in the pseudo steady state conditions that we are in interest of. The log-log plot of the integral of the normalized pressure and its derivative also confirms the same results obtained from the model.

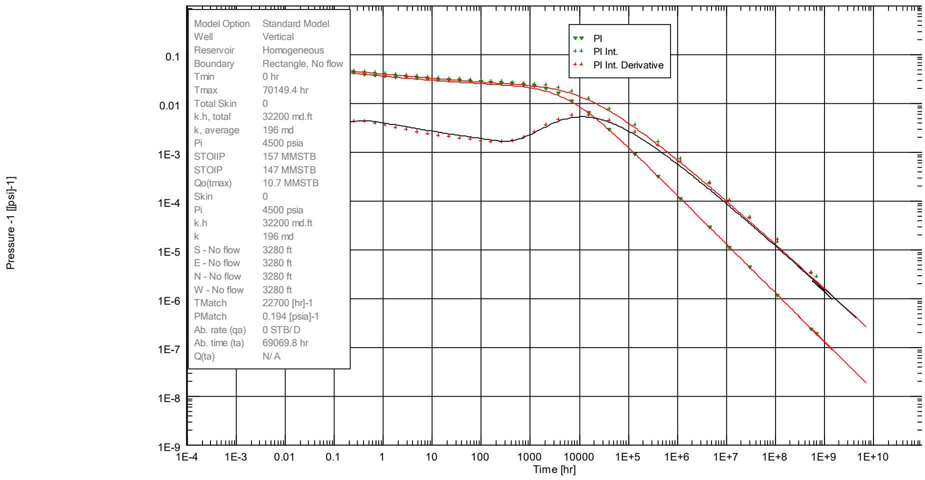

Blasingame plot: q/q_ref/(pi-p), Int[q/q_ref/(pi-p)]/te and d[Int[q/q_ref/(pi-p)]/te]/dInte [[psi]-1] vs te [hr]

Figure 32: Dead Oil Single Well Model Blasingame Plot Match.

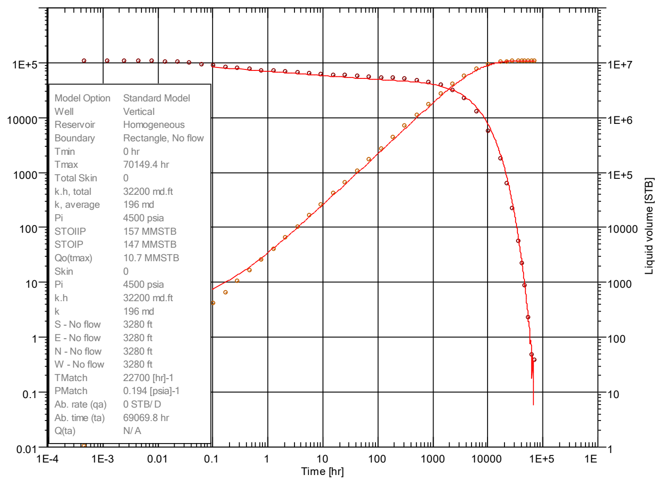

Fetkovich plot: q [STB/D], Q [STB] vs dt [hr]

Figure 33: Dead Oil Single Well Model Fetkovich Plot Match.

From the Fetkovich Plot of the model we can confirm that Pseudo Steady State conditions already reached after around 2000 hr of the production.

The model shows around 3.00% of error between the numerical simulation model and the RTA model.

Fetkovich Type-curves Match

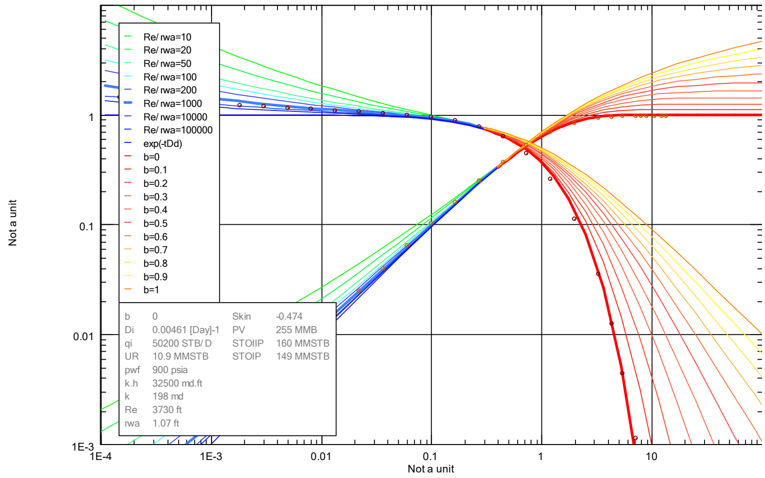

Fetkovich type curve plot: qDd and QDd vs tDd

Figure 34: Dead Oil Single Well Fetkovich Type-curves Match

From the match of the production data with Fetkovich Type-curves, we obtain OOIP as around 160 MMSTB with permeability 198 mD. Comparing these results with the numerical simulation model**;**

Table 13: Comparison between results obtained by Fetkovich Type-curves match and Numerical Simulation Model.

Models	OOIP (MMSTB)	Permeability (md)
Numerical Simulation	162	200
Fetkovich Type-curves	160	198

Comparing the results with the numerical simulation values, we obtain an error ~ 1.25 %.

Blasingame Type-curves Match

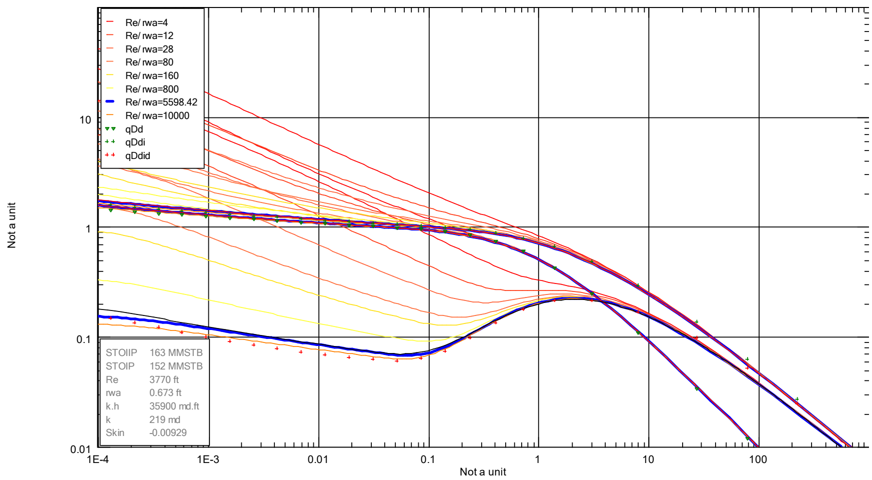

Blasingame type curve plot: qDd, qDdi and qDdid vs tDd

Figure 35: Dead Oil Single Well Blasingame Type-curves Match.

The match of the production data with Blasingame's Type-curves showed OOIP as ~163 MMSTB with an over estimation of permeability as 219 mD (Which still in the same order of magnitude).

4.1.3. Flowing Material Balance

For Dead Oil, the most critical issue is to have a valid PVT data representing the production data of your reservoir. As we have mentioned that for Dead Oil FMB the PVT data is considered constant over the production profile. Therefore, the oil compressibility, oil viscosity and oil formation volume factor are considered constants.

Table 14: Dead Oil Single Well PVT Data used in RTA & FMB

Pi (psia)	4500
viscosity (cp)	1.8
co psia-1	1.26E-05
ct psia-1	1.42E-05
Bo	1.2

Our area is represented by a rectangle (2000m*2000m) with a net pay thickness of 50 m. Therefore with setting a well in the center we get a Dietz Shape factor as 30.9. This is important in calculating the reservoir permeability from the Pseudo Steady State Constant (bpss).

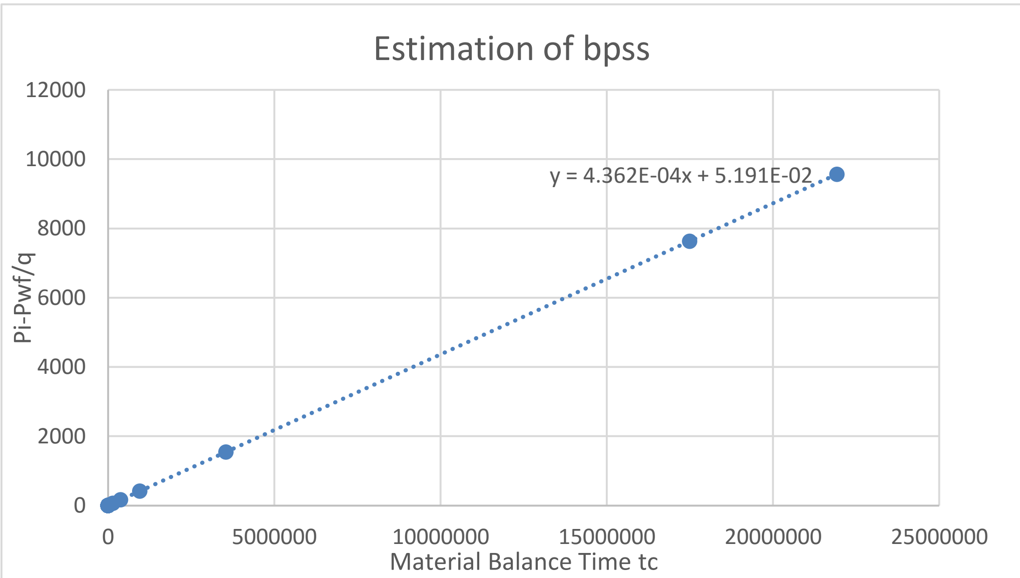

Figure 36: Dead Oil Single Well FMB, b_{pss} is obtained as the Y-intercept of the straight line

From the graph we get:

Table 15: Dead Oil Single Well, reservoir permeability using FMB approach.

b_{pss}	5.19E-02	psia/STB/D
Kh	3.94E+04	mD.ft
k	240	mD

We notice that the value of the permeability from the Flowing material balance approach is over estimated by around 20%

From b_{Pss} we get P_{avg} to plot $\frac{Pi-\bar{P}}{q}$ vs $\frac{Np}{c}$ to get the Original Oil in place as $\frac{1}{slope}$. The first values representing the transient period where they do not follow the straight line.

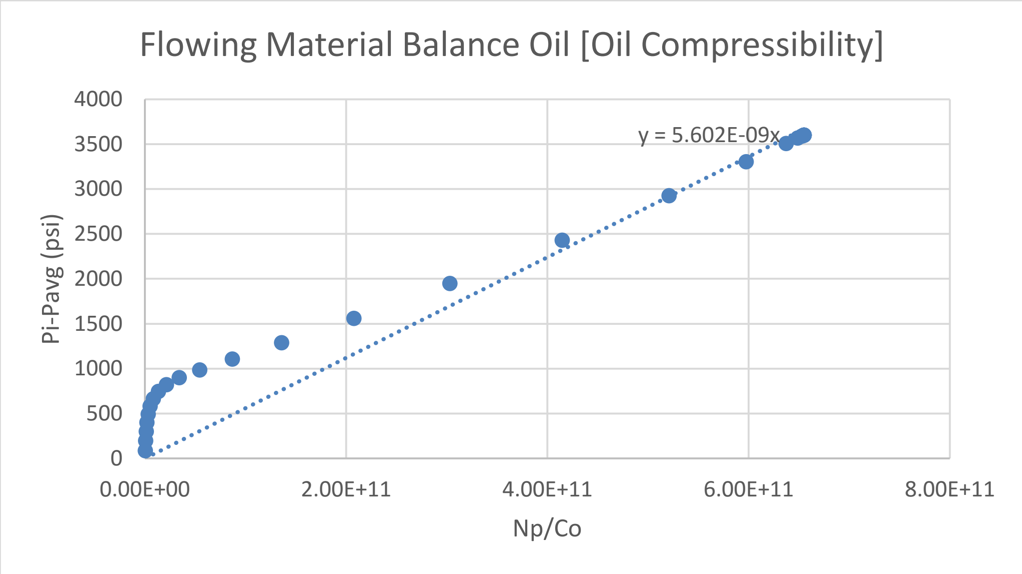

Figure 37: Dead Oil Single Well Flowing Material Balance using Oil Compressibility

From Figure 37, we get the slope as 1/N which gives N equal to 178.5 MMSTB

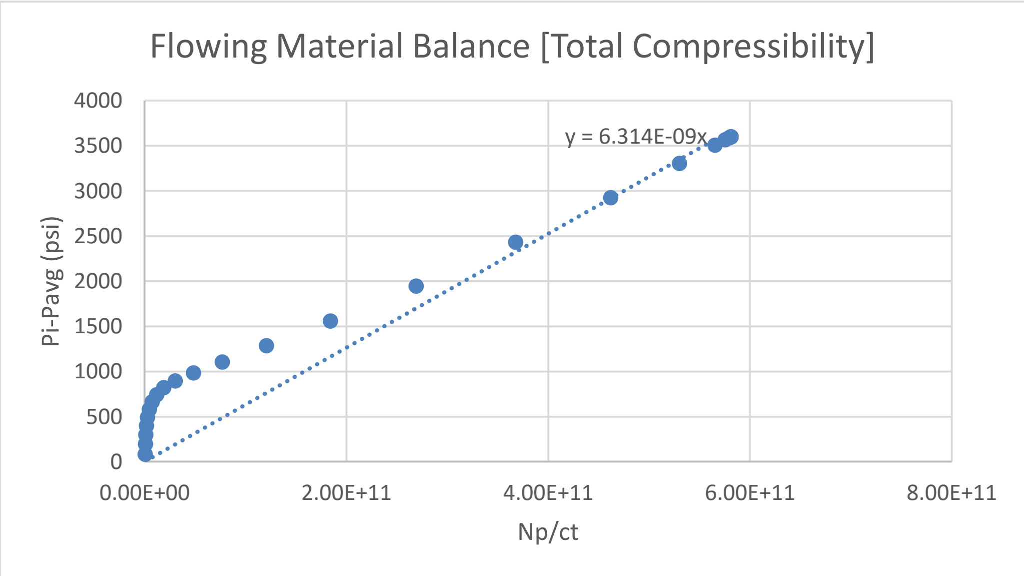

Figure 38: Dead Oil Single Well Flowing Material Balance using total Compressibility.

Figure 38 shows theat the slope increased when using the total compressibility which in return gives N as 158.5 MMSTB. This value is more reliable comparing with the numerical simulation model.

Table 16: Dead Oil Single Well OOIP comparison between the different approaches.

	Numerical Simulation Model	RTA Model	Blasingame type-curve plot	Fetkovich type-curve plot	FMB Total C
OOIP	162 MMSTB	157 MMSTB	163 MMSTB	160 MMSTB	158.5
K	200 mD	198 mD	219 mD	196 mD	240

Therefore, we see that the approach introduced by (Mattar & Anderson, 2005) that using total compressibility instead of the oil compressibility gives better estimation of the oil in place.

4.2. Dead Oil Multi Well

4.2.1. Numerical Simulation Model

The same model with the same parameters have been used for the multi-well case. Therefore, the same value of OOIP from the numerical simulation model was obtained as ~ 162 MMSTB.

The same time steps used for the single model was also implemented in this case to match the cumulative production cure in Topaze in the transient period.

4.2.2. Rate Transient Analysis

Model Matching

The model built using Topaze for the 4 wells matched the production data and gave the same result provided by the single well as ~ 157 MMSTB.

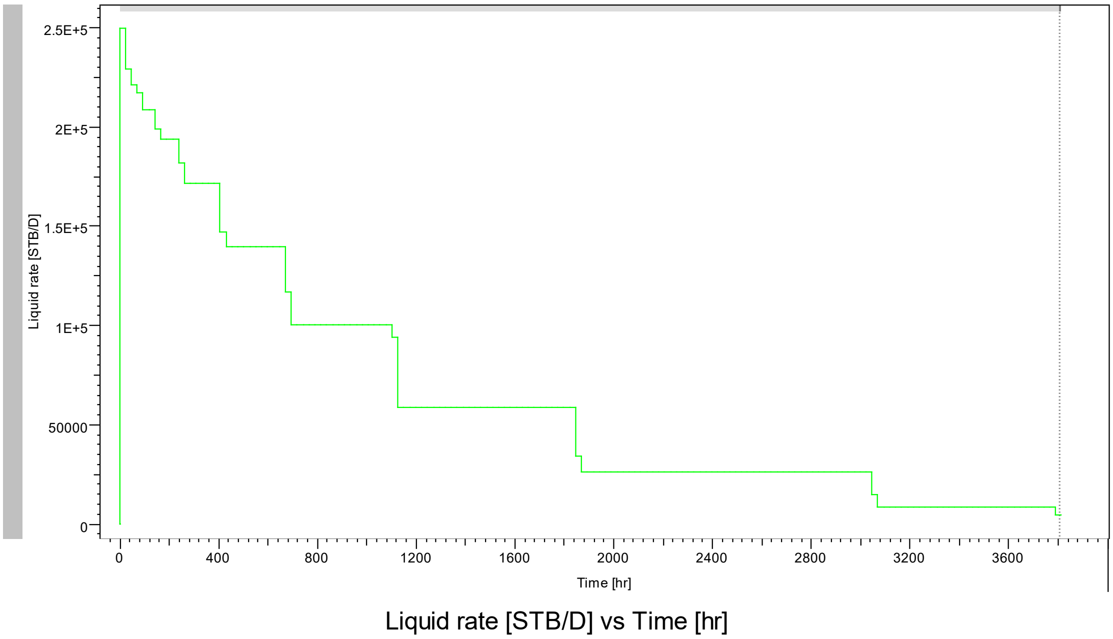

Figure 39: Dead Oil Multi Well Cumulative Production vs. time.

Well #1

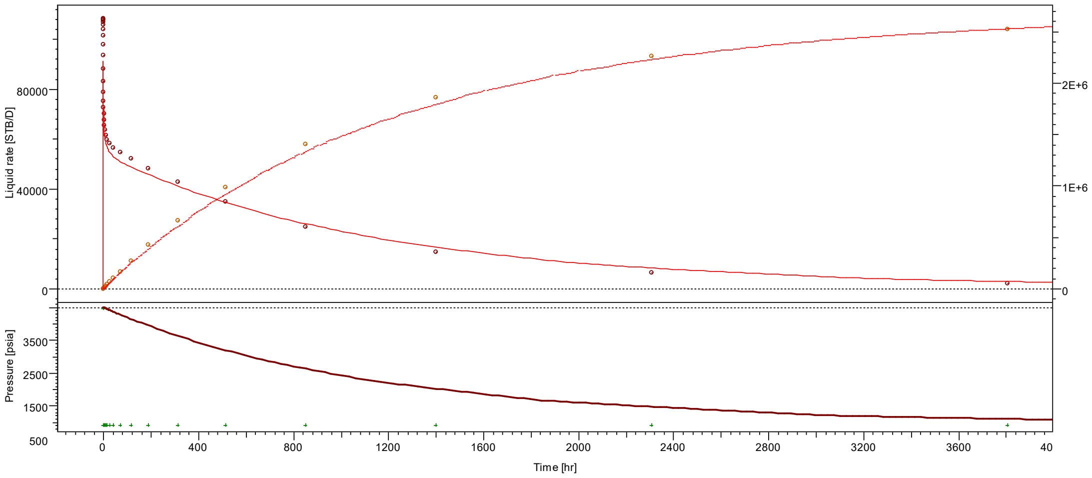

Production history plot (Liquid rate [STB/D], Pressure [psia] vs Time [hr])

Figure 40: Dead Oil Multi-well Well #1 History Match. Rate, Cumulative production, flowing pressure and model reservoir average pressure vs. Time.

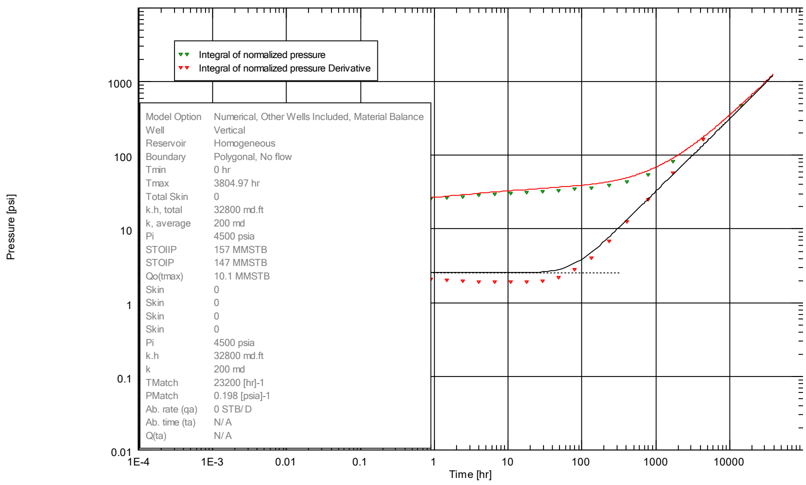

Loglog plot: Int[(pi-p)*q_ref/q]/te and d[Int[(pi-p)*q_ref/q]/te]/dln(te) [psi] vs te/2 [hr]

Figure 41: Dead Oil Multi-well Well #1 Log-Log Plot Match

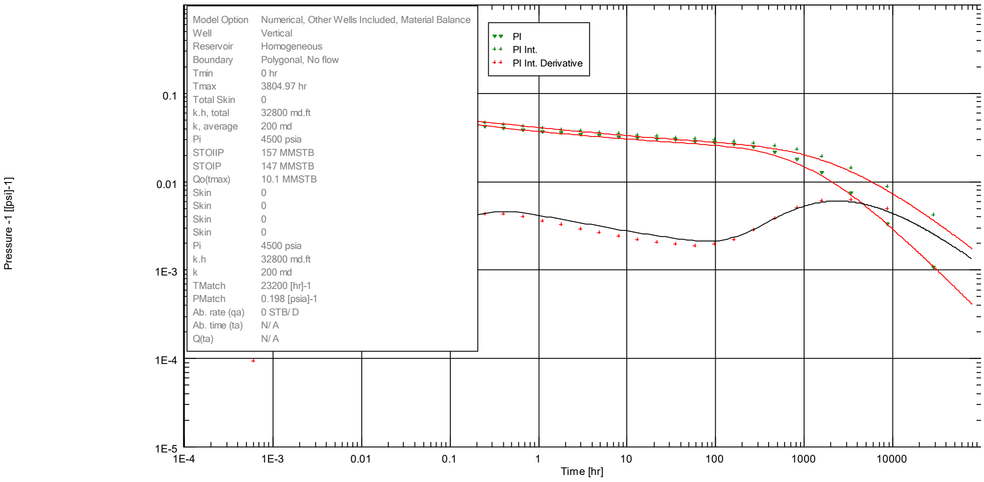

Blasingame plot: q/q_ref/(pi-p), Int[q/q_ref/(pi-p)]/te and d[Int[q/q_ref/(pi-p)]/te]/dlnte [[psi]-1] vs te [hr]

Figure 42: Dead Oil Multi-well Well #1 Model Blasingame Plot Match.

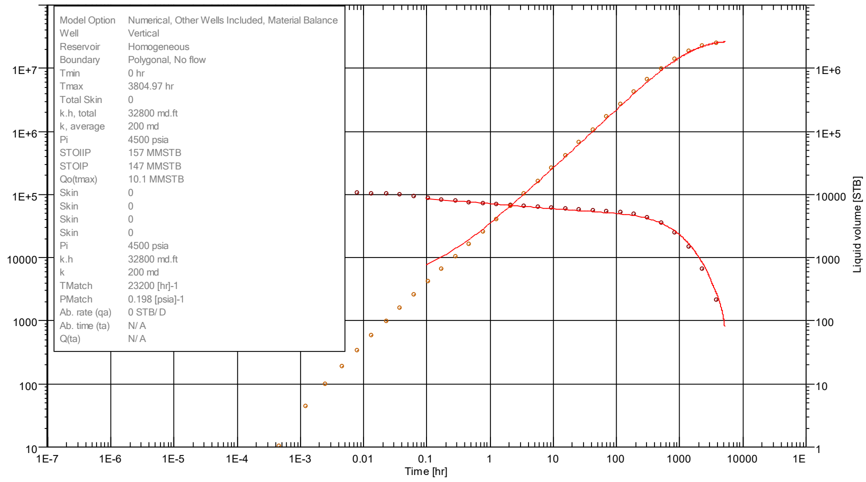

Fetkovich plot: q [STB/D], Q [STB] vs dt [hr]

Figure 43: Dead Oil Multi-well Well #1 Model Fetkovich Plot Match.

From both the Log-Log Plot and Fetkovich plot match of the model we confirm that the late period of production for the well is already in the pseudo steady state conditions.

In our study we focus only on how the production data could be analyzed to provide estimation on the hydrocarbon in place, therefore skin is set equal to zero.

The Match of the model plots (Log-Log, Blasingame, Fetkovich) with the production data confirms the validation of the model built with the production data of each well and also the estimation of the OOIP.

Fetkovich Type-curves Match

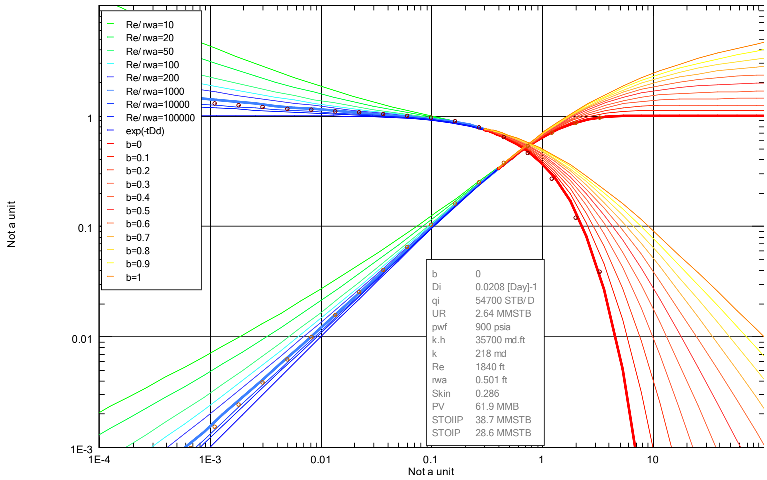

Fetkovich type curve plot: qDd and QDd vs tDd

Figure 44: Dead Oil Multi-well Well #1 Fetkovich Type-curves Match.

From Fetkovich Type-curves match we obtain the OOIP in the drainage area of each well. For well #1 we obtain ~ 38.7 MMSTB

Blasingame Type-curves

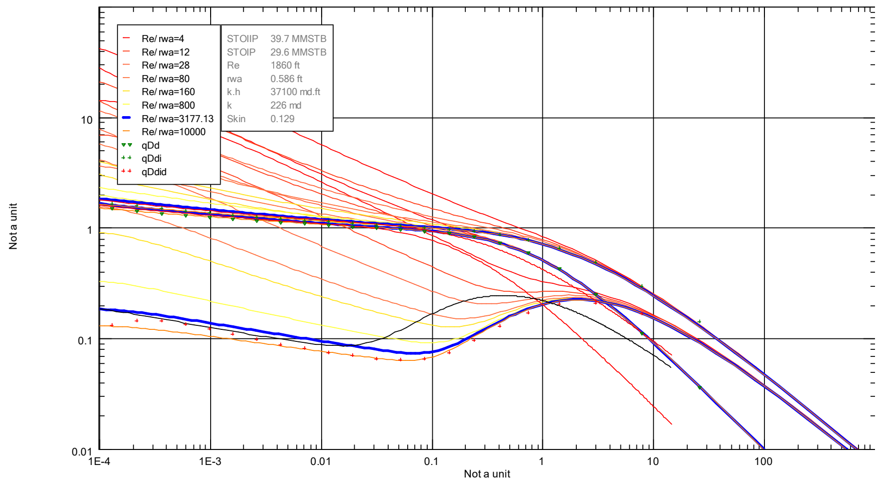

Blasingame type curve plot: qDd, qDdi and qDdid vs tDd

Figure 45: Dead Oil Multi-well Well #1 Blasingame Type-curves Match.

The match of the Blasingame type-curve gives an estimation of the OOIP stored in the drainage area covered by each well. For Well #1, it gives ~ 39.7 MMSTB

4.2.3. Flowing Material Balance

The same approach used for single well is implemented for the production data of each well separately to give an estimation of the OOIP covered by the drainage area of each well.

The PVT data for the single well with the same assumption of constant PVT over the production period are considered.

Table 17: Dead Oil Multi-well Well #1 Well PVT Data used in RTA & FMB

Pi (psia)	4500
viscosity (cp)	1.8
co psia-1	1.26E-05
ct psia-1	1.42E-05
Bo	1.2

The only difference in this analytical approach is the Dietz Shape factor regarding the multiwall case as in the single well it was only a symmetrically centered well in a rectangular area. However, here we have 4 wells; considering the new Dietz Shape factor 17.7 for each well.

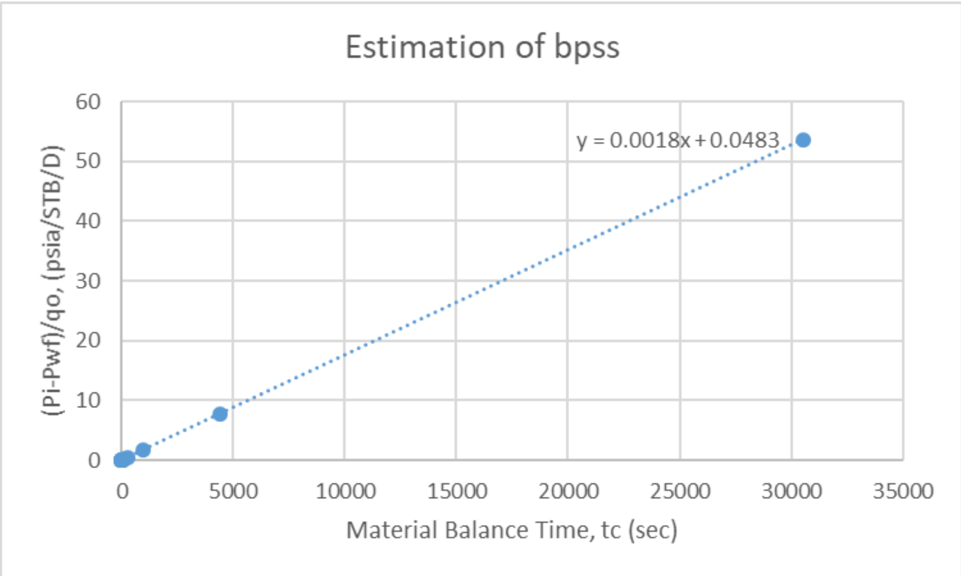

Figure 46: Dead Oil Multi-well Well #1 FMB, bpss is obtained as the Y-intercept of the straight line

Table 18: Dead Oil Multi-well Well #1, reservoir permeability using FMB approach.

b_{pss}	0.0483	psia/STB/D
Kh	44123.43	mD.ft
k	269.0	mD

The permeability estimated by the flowing material balance is over estimated and this might be because of the neglecting of the skin effect.

From b_{Pss} we get P_{avg} to plot $\frac{Pi-\bar{P}}{q}$ vs $\frac{Np}{c}$ to get the Original Oil in place as $\frac{1}{slope}$. The first values representing the transient period where they do not follow the straight line.

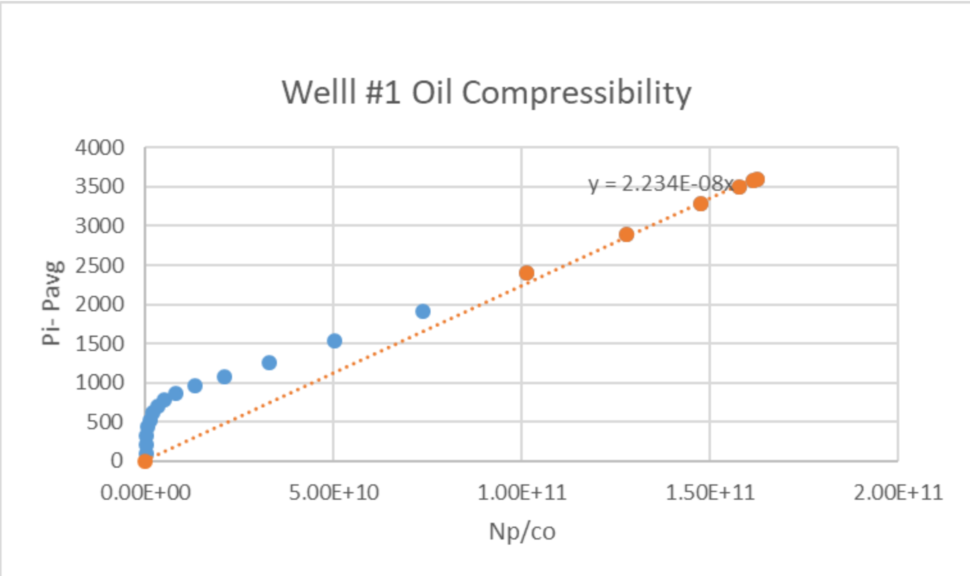

Figure 47: Dead Oil Multi-well Well #1 Flowing Material Balance using Oil Compressibility

N1= 44.8 MMSTB

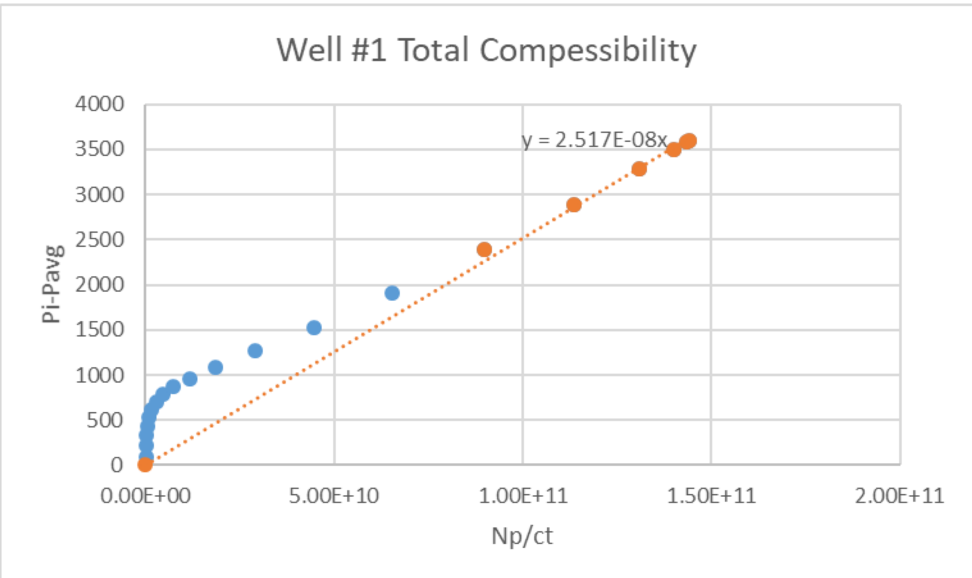

Figure 48: Dead Oil Multi-well Well #1 Flowing Material Balance using Total Compressibility.

N1= 39.7 MMSTB

Again the early data representing the transient period do not follow the straight line of the Pseudo Steady Sate.

Table 19: Dead Oil Multi-well OOIP comparison between the different approaches.

Again, the using of the total compressibility instead of the oil compressibility gives more reliable and closer results to the ones obtained from the RTA. However, the usage of oil compressibility in the multiwall model overestimates the oil in place which is opposite to what happened with the single well model. See Appendix B for Well #2, #3, and #4 graphs.

Approach	Well #1	Well #2	Well #3	Well #4	OOIP MMSTB
Numerical Simulation Model					162
RTA Model					157
Blasingame Type-curve	39.7	39.2	39.2	40.7	158.8
Fetkovich Type-curve	38.7	39.2	39.2	39.2	155.7
FMB total compressibility	39.7	40.0	40.0	40.2	159.9

From the results we see that the flowing material balance approach gives the best results comparing the numerical simulation model estimation and proves its validation as a production data analysis approach for estimating the Oil Originally in place without the need to implement the conventional methods.

4.3. Dry Gas Single Well

4.3.1. Numerical Simulation Model

Some difference applied to the dry gas model from the dead oil model. These difference were applied to be able to match the production data with the Ecrin Topaze model.

a) Changing in the dimension of the reservoir by changing the reservoir thickness from 50 m to ~ 24.4 m (164 ft to 80 ft)
b) Changing the reservoir permeability from 200mD to 50 md for the single well (and 30 mD for the multi well model).
c) Changing the time steps from exponentially increasing time steps into linear time steps.

The first two changes were to be able to reduce the total cumulative gas production limit provided with the model. The production cumulative was out of the range of the model. Therefore, we wanted to reduce the production rate so that the total cumulative could be reduced and matches the model built on Ecrin Topaze.

The time steps change was due to the convergence problem on Eclipse as the linear fine time steps showed a good convergence with no errors.

The Numerical simulation model Original Gas in Place value is ~ 131 BSCF.

4.3.2. Rate Transient Analysis Model

Model Matching

The match of the analytical model on Ecrin, Topaze showed that the reservoir has ~135 BSCF. For single well model, the analytical or the numerical model Ecri. Topaze will give the same values. However, for multiwall model it is better to use the numerical model.

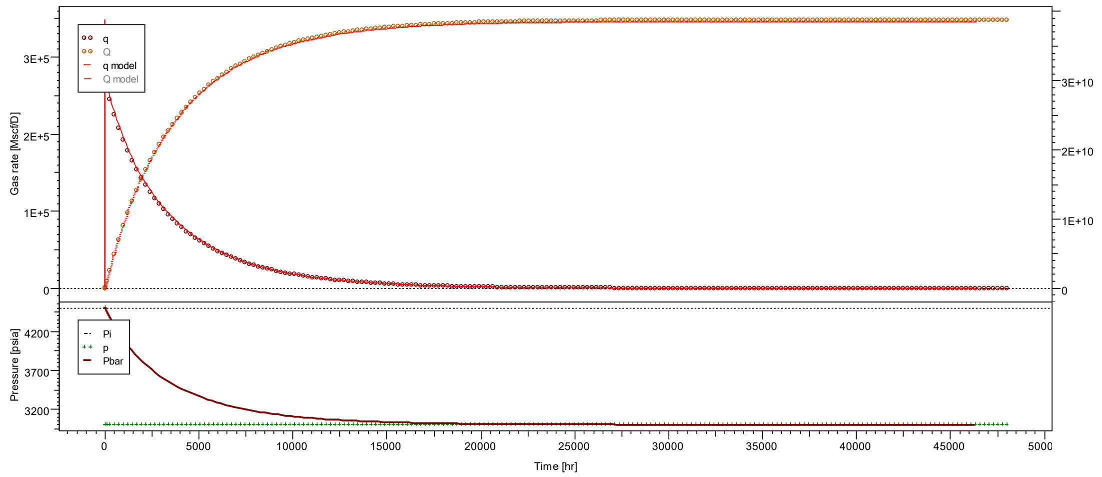

Production history plot (Gas rate [Mscf/D], Pressure [psia] vs Time [hr])

Figure 49: Dry Gas Single Well Well #4 History Match. Rate, Cumulative production, flowing pressure and model reservoir average pressure vs. Time.

Again from the log-log plot we confirm that the reservoir has reached the pseudo steady state conditions when the integral and the integral derivative merge in a straight line with a unit slope. This is also easily confirmed from the Fetkovich plot. And that is what we need to confirm to be able to continue our further analysis using the flowing material balance as well.

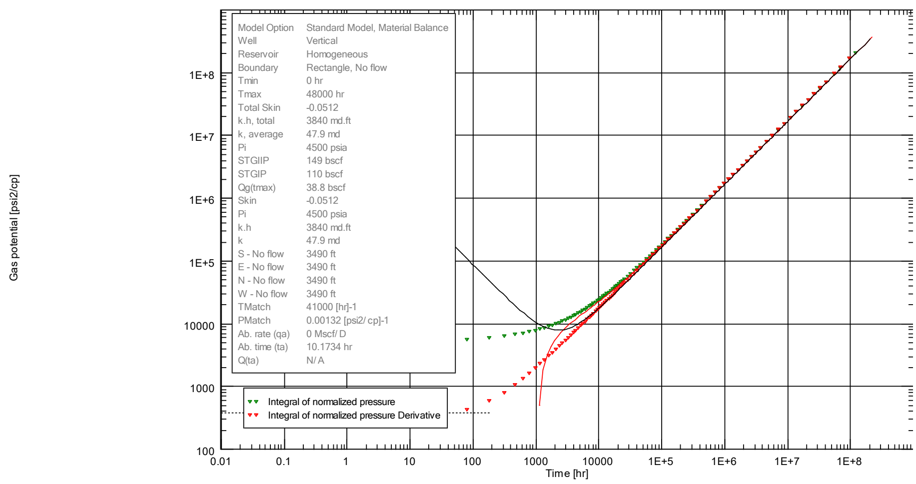

Loglog plot: Int[(m(pi)-m(p))*q_ref/q]/te and d[Int[(m(pi)-m(p))*q_ref/q]/te]/dln(te) [psi2/cp] vs te/2 [hr]

Figure 50: Dry Gas Single Well Log-Log Plot Match.

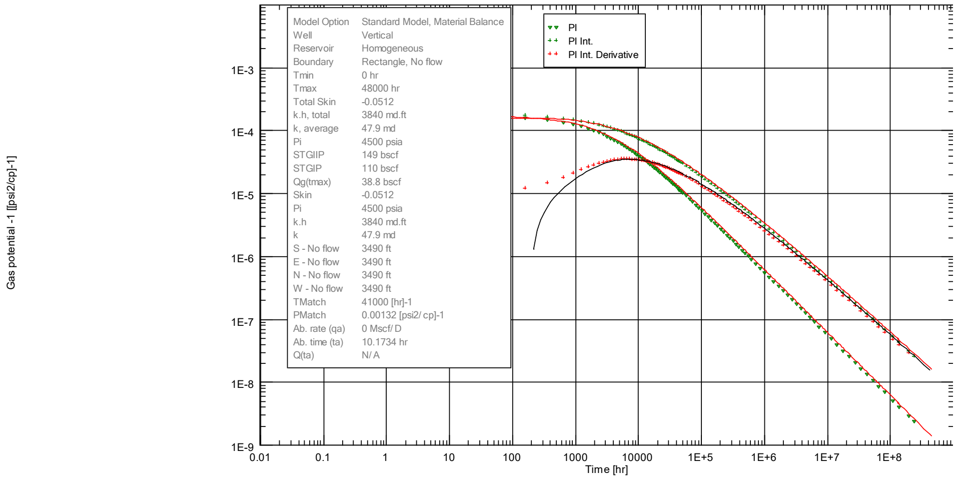

Blasingame plot: q/q_ref/(m(pi)-m(p)), Int[q/q_ref/(m(pi)-m(p))]/te and d[Int[q/q_ref/(m(pi)-m(p))]/te]/dlnte [[psi2/cp]-1] vs te [hr]

Figure 51: Dry Gas Single Well Model Blasingame Plot Match.

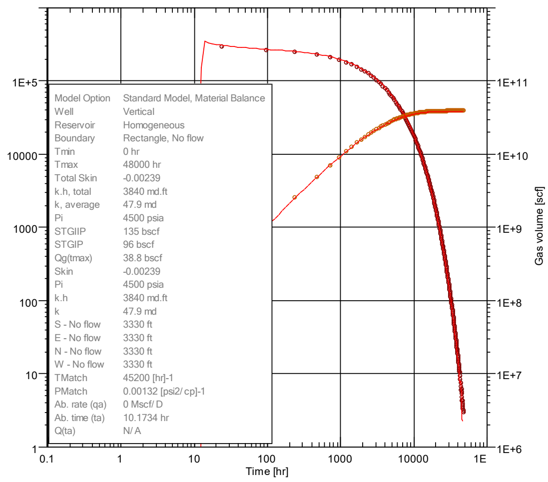

Fetkovich plot: q [Mscf/D], Q [scf] vs dt [hr]

Figure 52: Dry Gas Single Well Model Fetkovich Plot Match.

Fetkovich Type-curves Match

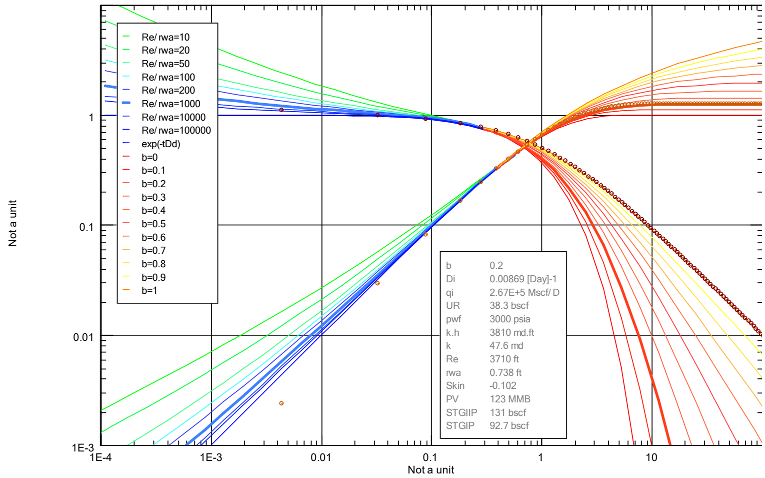

Fetkovich type curve plot: qDd and QDd vs tDd

Figure 53: Dry Gas Single Well Fetkovich Type-curves Match.

The match of the production data on Fetkovich Type-curves showed an estimation of OGIP as ~ 131 BSCF.

Blaingame Type-curves

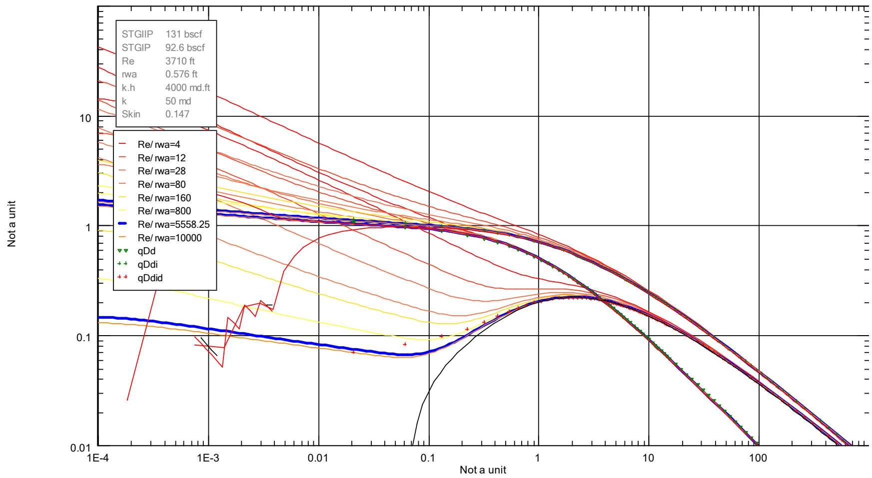

Figure 54: Dry Gas Single Well Blasingame Type-curves Match.

Also the match of the production data on Blasingame Type-curves gave the same result as ~ 131 BSCF which confirms the validation of the RTA as an approach for dry gas reservoir to give an estimation of the OGIP.

4.3.3. Flowing Material Balance

As we mentioned in the Methodology chapter that in our study we tried to provide the different approaches stated in the literature with a comparison on the results of these methods.

The main issue of the gas FMB is the change of gas properties with the production or with pressure decline therefore the development of material balance time for gas has not only solved the problem of the constant/variable flow rate but also it consider the gas properties change in its function to be the material balance pseudo function for gas.

For gas Flowing material balance we have used 3 approaches that agree on the same concept of assuming an initial value of G that would be used in the conventional gas material balance to evaluate the static (reservoir average) pressure at the corresponding P_{wf} and therefore correlate the PVT data at these static pressure values. However, they only differ in the final step of estimating the OGIP.

Gas Flowing Material Balance

By calculating the pseudo material balance function, tca and plotting $\frac{m(p_i)-m(p_{wf})}{q_{sc}}$ vs t_{ca} to calculate the b_{pss}.

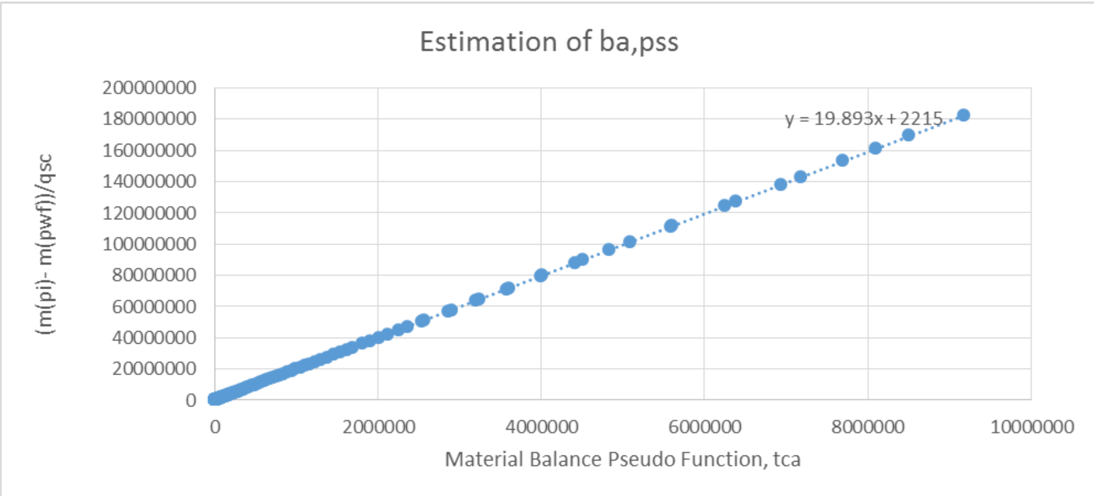

Table 20: Dry Gas Single Well reservoir permeability using FMB approach.

Figure 55: Dry Gas Single Well FMB, b_{pss} is obtained as the Y-intercept of the straight line

$b_{a,pss}$	2215	
kh	3402	md.ft
k	43	md

After getting $b_{a,pss}$ we calculate the m(Pavg) that would be transformed in Pavg to plot the conventional P/z plot.

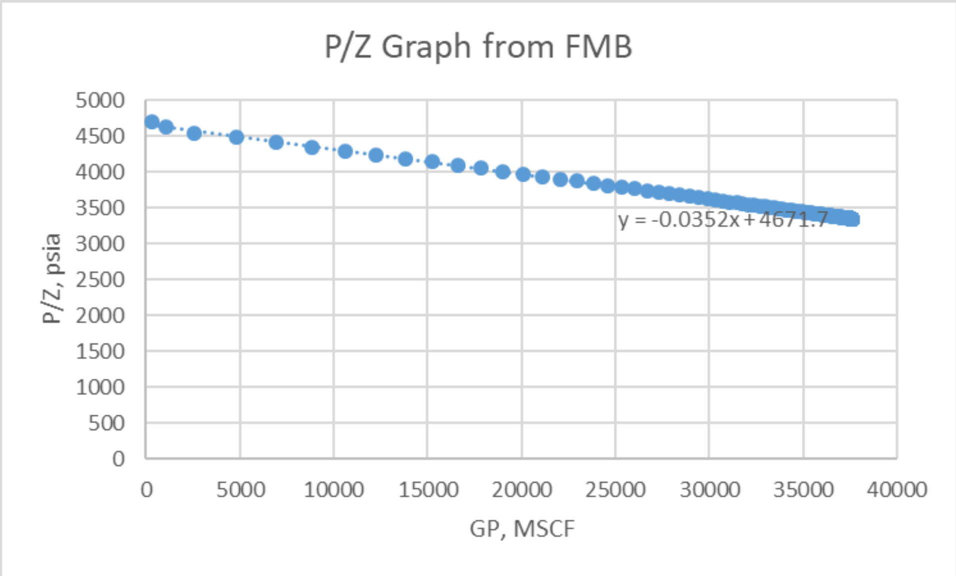

Figure 56: Dry Gas Single Well, Gas Flowing Material Balance, P/z Plot.

By solving this equation we get G ~ 131 BSCF.

Agarwal – Gardner Method

By plotting the normalized cumulative vs. the normalized rate we get the OGIP as an x-intercept when the normalized rate is equal to zero. See Agarwal Type-curves Theory Analysis. By solving the equation in Figure 57 we obtain G ~ 132.7 BSCF.

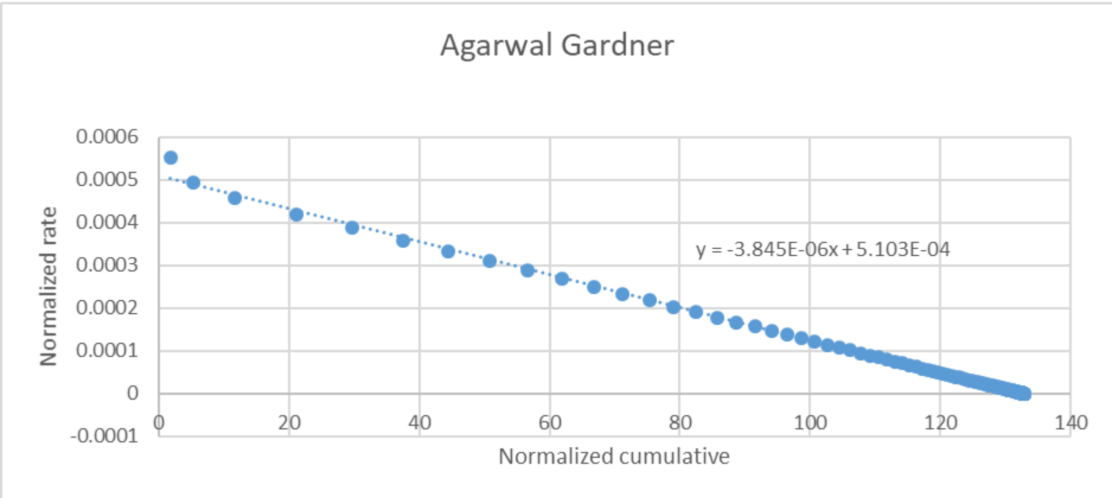

Figure 57: Dry Gas Single Well, Agarwal Gardner Approach.

The new Material Balance function

This method requires a valid PVT as it highly overestimated the OGIP. The main aim of this approach was to overcome the dominant effect of gas properties change with time by introducing a new pseudo material balance function that is insensitive of the time step, but is a function of the cumulative production.

$$T_a = \frac{1}{q_g} \int_0^{G_p} \frac{(\mu_g c_t)_i}{\overline{\mu_g} \overline{c_t}} \, dG_p$$

By Plotting this equation we get the x-intercept as $G*C_{ti}$

$$\frac{q_g}{\Delta m(p)_n} = -\frac{1}{b_{a,pss}\, G C_{ti}} \frac{G_{pn}}{\Delta m(p)_n} + \frac{1}{b_{a,pss}}$$

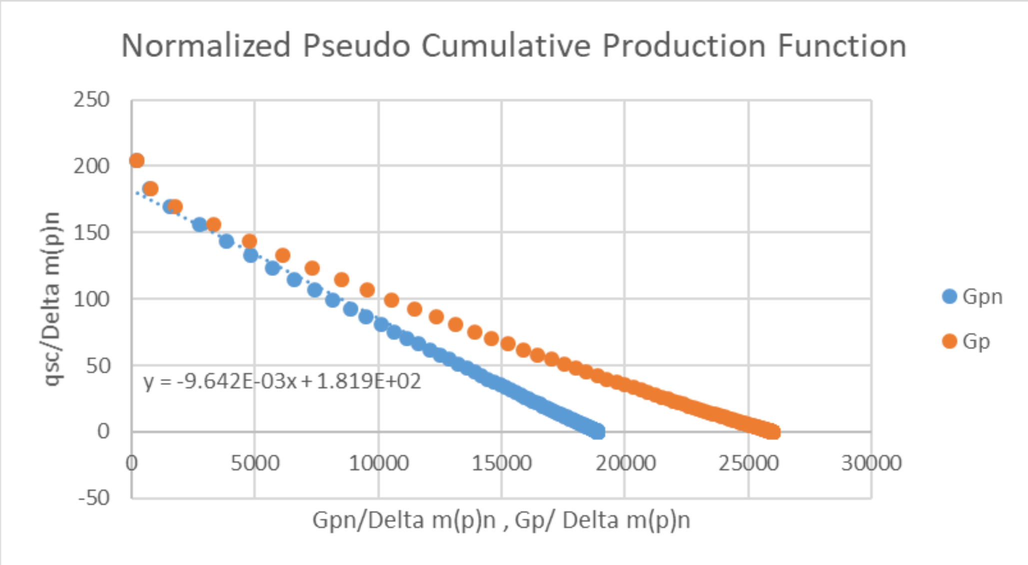

Figure 58: Dry Gas Single Well, Using The New Pseudo Material Balance Function.

G ~ 150 BSCF

(Mohammed & Enty, 2013) stated that for early dominated pseudo state flow the plot of Gp or G_{pn} overlab showing the same behavior. However, for late dominated pseudo steady state, the behavior changes due do the effect of viscosity-compressibility change as a function of production and the cumulative production plot shows another line overestimating the Original Gas in place. The use of Gpn function should give a one straight line that gives G*Cti at the intercept. The usage of cumulative production plot is just helpful for giving an initial estimation of G that would be used for iteration.

For our study using this approach we get an overestimated G ~ 150 BSCF. The over estimation is due to the not perfectly representing PVT data. As the PVT data in this model are all correlated using polynomial equations set from the PVT tables imported from Ecrin.

Table 21: Dry Gas Single Well OGIP comparison between the different approaches.

Approach	Numerical Simulation Model	Rate Transient Analysis			Flowing Material balance		
		Model Match	Fetkovich Type-curves	Blasingame Type-curves	Gas FMB	Agarwal Gardner	New Material Balance function
G (BSCF)	131	135	131	131	131	132.7	150

From these results, we see that RTA and FMB show comparable results of OGIP. The only overestimation is due to the lack of valid PVT data representing the production profile.

4.4. Dry Gas Multi Well

4.4.1. Numerical Simulation Model

The same OGIP for the single well mode as we only changed the permeability from 50mD to 30 mD. G ~ 131 BSCF

4.4.2. Rate Transient Analysis Model

The numerical model built for the multi-well case gave the exact same value of OGIP however; it does not perfectly match the cumulative production. The cumulative production starts to deviate when the reservoir reaches the pseudo steady state conditions.

The Model gas a value of G ~ 131 BSCF.

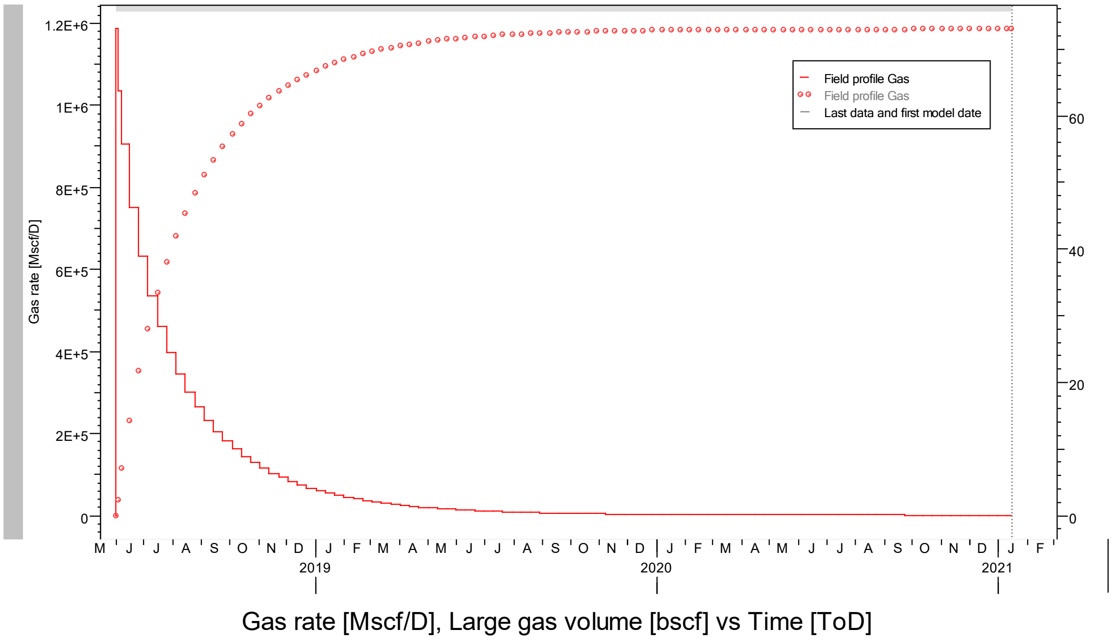

Figure 59: Dry Gas Multi-well Well #1, Production Flow Rate & cumulative production vs. Time.

<u>Well #1</u>

Model Match

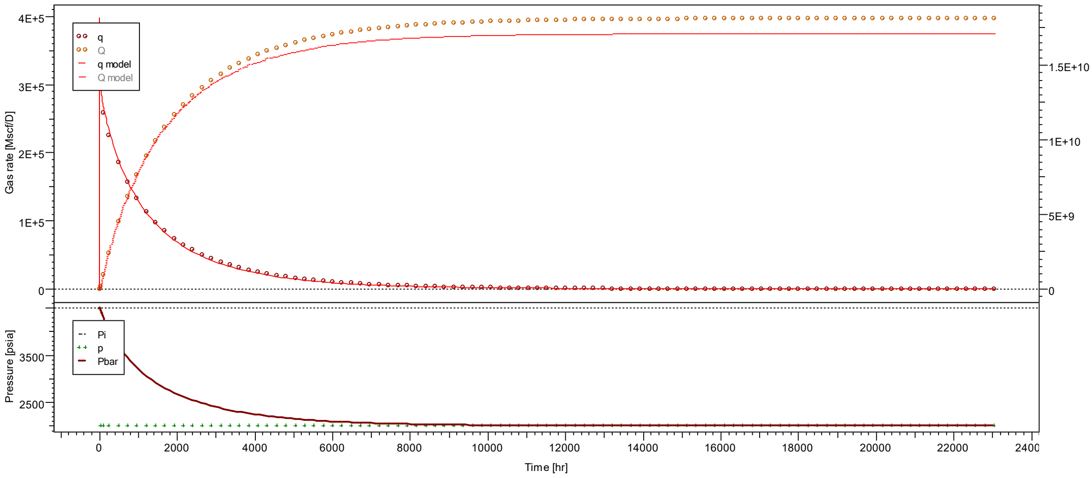

Production history plot (Gas rate [Mscf/D], Pressure [psia] vs Time [hr])

Figure 60: Dry Gas Multi-well Well #1 History Match. Rate, Cumulative production, flowing pressure and model reservoir average pressure vs. Time.

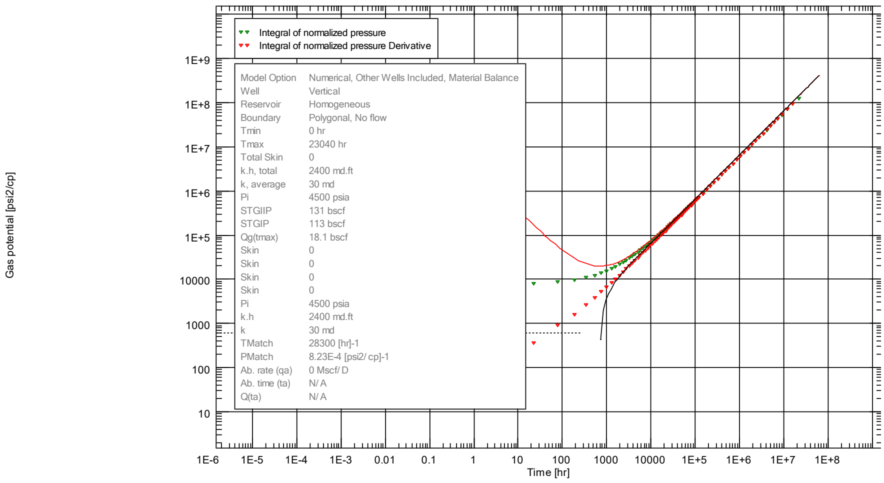

Loglog plot: Int[(m(pi)-m(p))*q_ref/q]/te and d[Int[(m(pi)-m(p))*q_ref/q]/te]/dln(te) [psi2/cp] vs te/2 [hr]

Figure 61: Dry Gas Multi-well Well #1 Log-Log Plot Match.

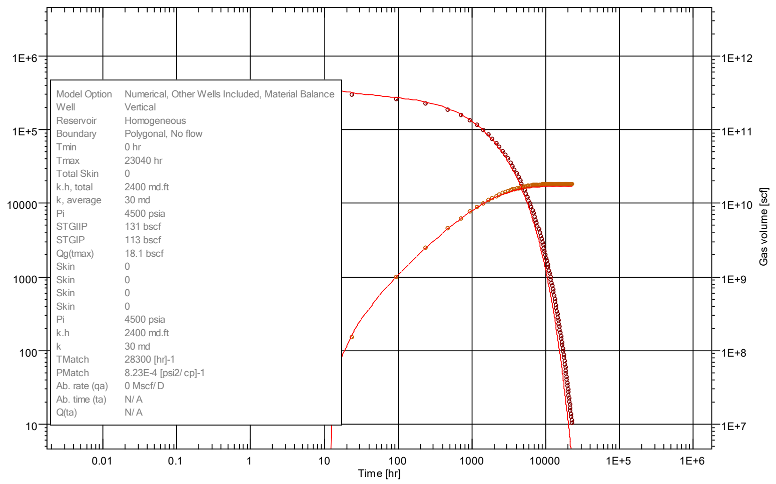

Fetkovich plot: q [Mscf/D], Q [scf] vs dt [hr]

Figure 62: Dry Gas Multi-well Well #1 Model Fetkovich Plot Match.

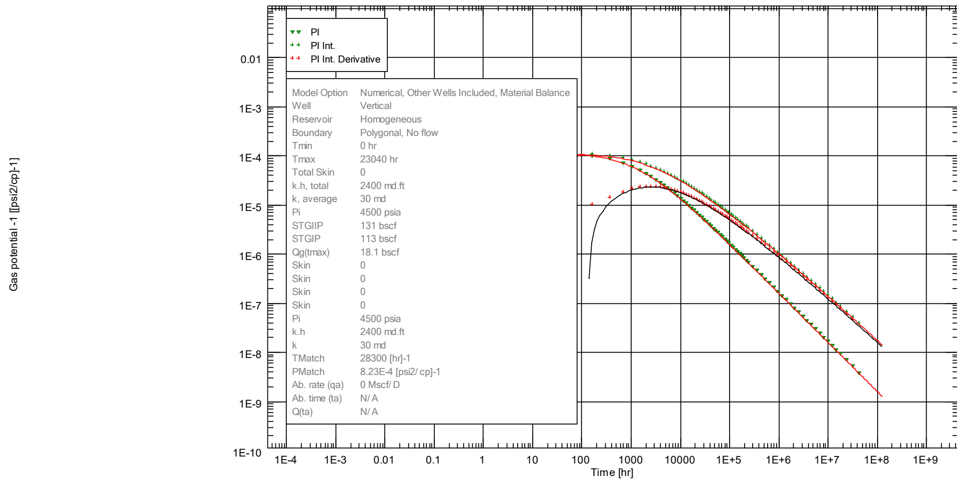

Blasingame plot: q/q_ref/(m(pi)-m(p)), Int[q/q_ref/(m(pi)-m(p))]/te and d[Int[q/q_ref/(m(pi)-m(p))]/te]/dlnte [[psi2/cp]-1] vs te [hr]

Figure 63: Dry Gas Multi-well Well #1 Model Blasingame Plot Match.

Fetkovich Type-curves

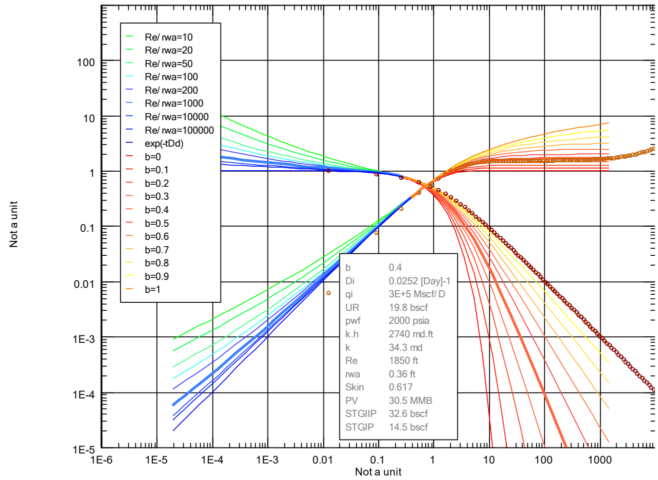

Fetkovich type curve plot: qDd and QDd vs tDd

Figure 64: Dry Gas Multi-well Well #1 Fetkovich Type-curves Match.

From Fetkovich Type-curves match, we can have an estimation of the Gas in place in the drainage area covered by well #1

G1 ~ 32.6 BSCF

Blasingame Type-curves

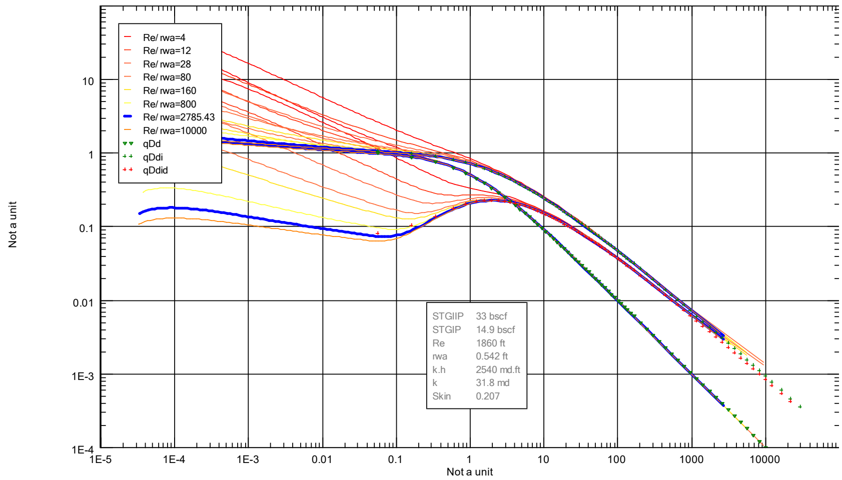

Blasingame type curve plot: qDd, qDdi and qDdid vs tDd

Figure 65: Dry Gas Multi-well Well #1 Blasingame Type-curves Match.

From Blasingame Type-curves match we obtain G1 ~33 BSCF

4.4.3. Flowing Material Balance

The FMB approaches are implemented for each well individually where the results obtained represents the Gas originally in place in the drainage area covered by each well. To have the total initial gas in place we sum the results of the 4 well for the same approach as in table 24.

The same procedure developed for the single well is performed for the multiwall model, each well individually and the results are obtained in the figures below.

Gas Flowing Material Balance

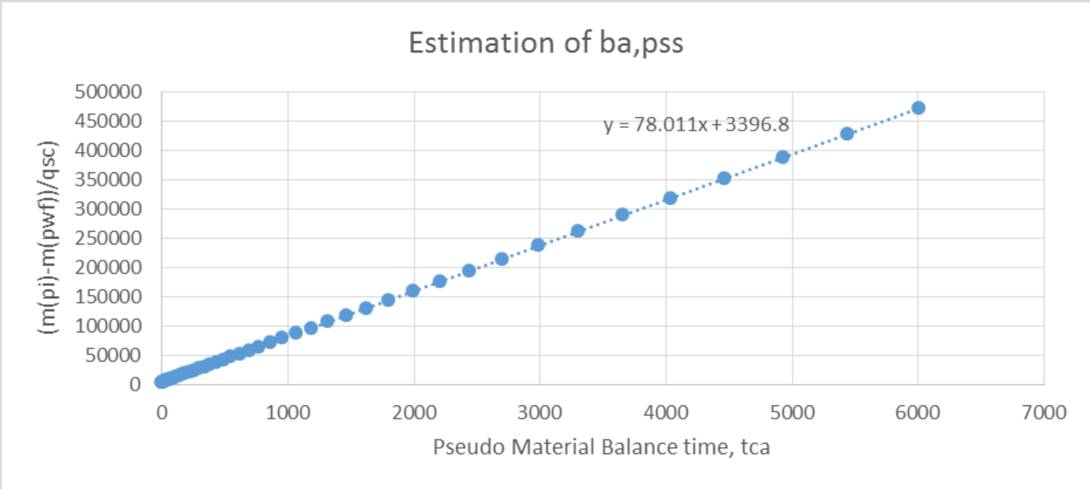

Figure 66: Dry Gas Multi-well Well #1 FMB, b_{pss} is obtained as the Y-intercept of the straight line

Table 22: Dry Gas Multi-well Well #1, reservoir permeability using FMB approach.

$b_{a,pss}$	3397	
kh	2499	md.ft
k	31	md

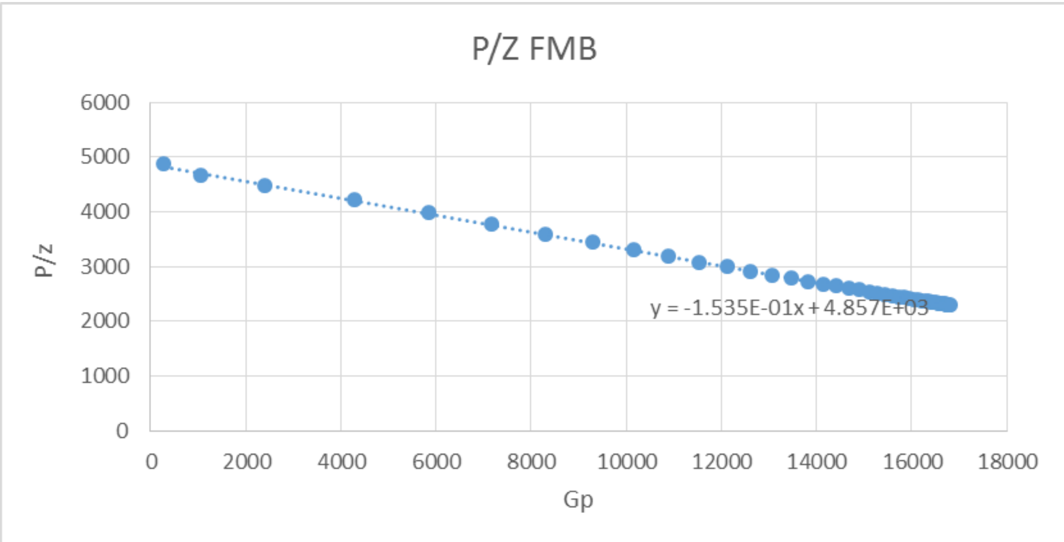

Figure 67: Dry Gas Multi-well Well #1, Gas Flowing Material Balance, P/z Plot.

G1 ~ 30.2 BSCF

Agarwal – Gardner Method

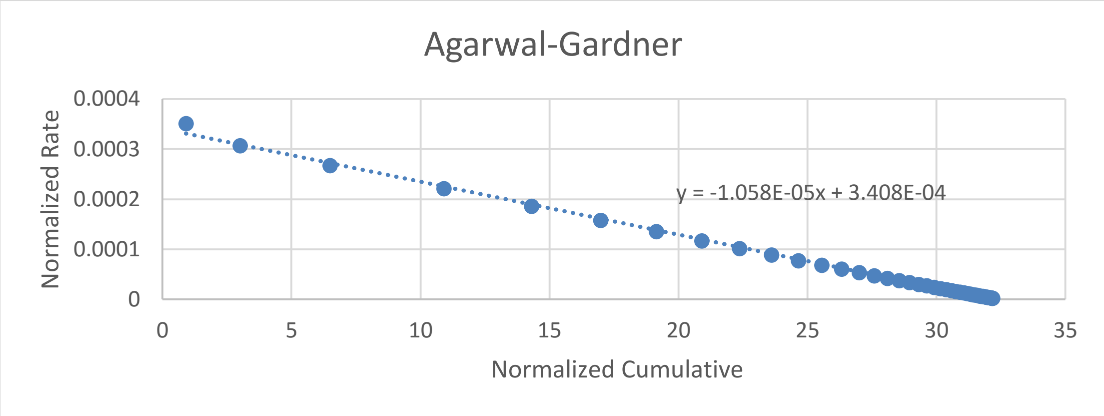

Figure 68: Dry Gas Multi-well Well #1, Agarwal Gardner Approach.

G1 ~ 32.3 BSCF

The New Material Balance Function

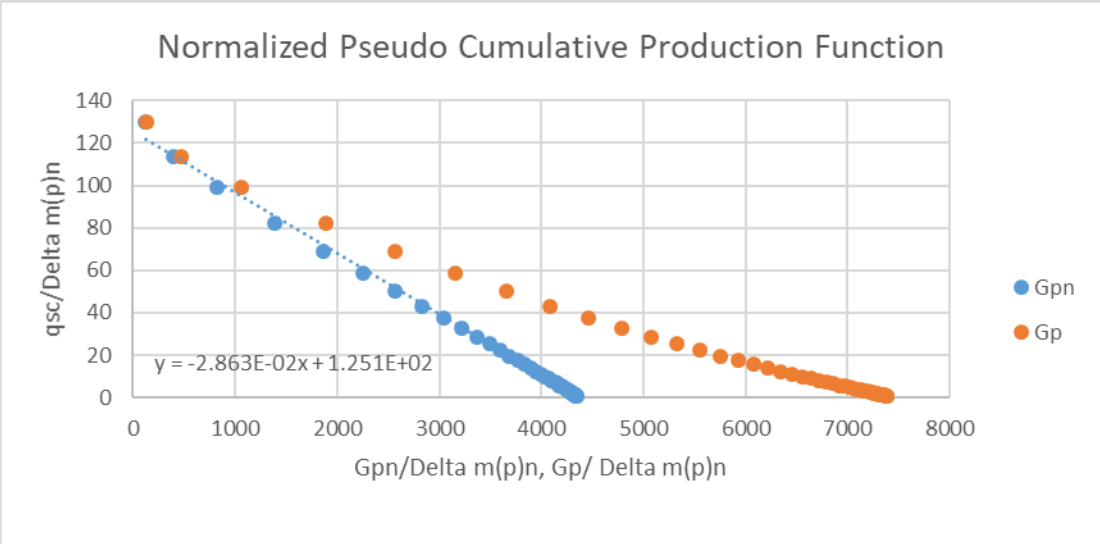

Figure 69: Dry Gas Multi-well Well #1 Using The New Pseudo Material Balance Function.

G1 ~ 34.8 BSCF

For Well #2, #3, #4. See Appendix C.

Table 23: Dry Gas Multi-well OGIP comparison between the different approaches.

Approach	Numerical Simulation Model	Rate Transient Analysis			Flowing Material Balance		
		Model	Fetkovich Type Curves	Blasingame Type Curves	Gas FMB	Agarwal-Gardner	New Material Balance Function
Well #1	-	-	32.6	33	30.2	32.3	34.8
Well #2	-	-	32.1	32.8	30.5	32.5	34.9
Well #3	-	-	32.7	32.4	30.5	32.6	34.9
Well #4	-	-	32.7	32.5	30.8	32.8	35.1
G (BSCF)	131	131	130.1	130.7	122	130	139.7

Chapter 5 Conclusions

Production Analysis methods used in this study (RTA & FMB) demonstrated comparable results of hydrocarbon initially in place and also reservoir characteristics (Permeability).

Dead Oil Single well

Rate Transient Model matching required fine exponentially increasing time steps to match the transient period and the analytical model underestimated the Oil Originally in place with only 3% comparing the value obtained from the numerical simulation model. For the permeability, the production data matched the model represented approximately the same permeability used in developing the synthetic data by Eclipse. Both models assumed no skin around the wellbore.

The results obtained by both Fetkovich Type-curves were approximately the same as the numerical simulation model with 1% underestimation of both the oil in place and the permeability. Blasingame Type-curves perfectly matched the OOIP value but overestimated the permeability with ~ 10%.

For Flowing Material Balance, the approaches used showed that replacing the oil compressibility in the material balance equation for oil used by (Mattar & Anderson, Dynamic Material Balance(Oil or Gas-In-Place Without Shut-In), 2005) with total compressibility would give better results as using oil compressibility underestimated the oil originally in-place with~ 10% error. However, using total compressibility would underestimate OOIP by only 2 %.

Dead Oil Multi-well

Although all values obtained by the different approaches were underestimating the OOIP in the multi-well model as the values obtained from the production data analysis of each well were representing the drainage area covered by each well, the underestimation did not exceed 3% of the OOIP (except for FMB using Oil compressibility that overestimated the OOIP) which confirms the validation of the approaches used in estimating the OOIP.

Flowing Material Balance for Dead Oil overestimated the permeability obtained by the analysis of the production data assuming no skin around the wellbore.

This confirms that obtaining PVT representing the production data would generally improve the quality of estimation for oil PVT were considered constant over the production profile and a small change in the data used would highly affect the results on both OOIP and permeability.

Dry Gas Single Well

The Production Analysis approaches used in our study confirm its validation for not only estimating the OGIP but also for reservoir characteristics evaluation (Permeability). The different approaches for Dry Gas Single Model demonstrated a high quality of estimating the OGIP with ±3% comparing with the numerical simulation model (131 BSCF, 50 mD).

RTA analytical model match overestimated the OGIP by ~ 4 BSCF. Permeability estimation was 48 mD. Fetkovich and Blasingame Type-curves perfectly matched the OGIP value as both gave G as 131 BSCF. Blasingame type-curves match gave a permeability of 50 mD. However, Fetkovich type-curves match with a permeability of 47 mD.

Flowing Material Balance approaches used in this study strongly confirmed its validation as the new method of estimating OGIP using production data. The newly introduced iterative method gave comparable results from the second iterative step.

For Gas FMB and Agarwal – Gardner approaches, both required to iterate the assumed value of G in two steps to reach the representing value of G for the single well model. However, the results did not confirm what demonstrated in study of (Ismadi, Kabir, & Hasan, 2012) based on comparing the two approaches. They showed that Agarwal – Gardner approach should give more accurate results than the Gas FMB approach as evaluating the average pressure in the first approach (Agarwal – Gardner) depends on the conventional MBE. However in the later (Gas FMB), the evaluation uses the fluid flow equation after estimating the pseudo-steady state constant b_{pss}. In our study, we observed that Gas FMB perfectly gave the OGIP value estimated by the numerical simulation model and Agarwal – Gardner method overestimated the value. Nevertheless, the difference is less than 1 % of the numerical simulation model.

On the other hand, using the new material balance function introduced by (Mohammed & Enty, 2013) and was confirmed later by (Molokwu & Onyekonwu, 2016) highly overestimated the OGIP value.

The reason of this unexpected overestimation could be due to the quality of the PVT data generated for this approach. The calculation of the normalized pseudo cumulative function depends on the viscosity compressibility ratio values at the representing cumulative production values. This is developed by fitting a polynomial equation that showed a considerable error that could be clearly seen in Figure 29 as the first value of the viscosity compressibility should be equal to 1. This error because of the consecutive usage of polynomial equations of for generating compressibility and viscosity values from the PVT data imported from Ecrin.

Dry Gas Multi-Well

The match of the numerical model of RTA on Topaze, Fetkovich type-curve and Blasingame type-curves gave the value of Gas in place in the drainage areas covered by the wells and the summation of these values gave a strong agreement with the OGIP value estimated by the numerical simulation model.

For Flowing Material Balance approaches, the contrary of what was experienced in the single well model happened. The Agarwal – Gardner approach showed its validation for estimating OGIP over the FMB approach using material balance time. Although the normalized pseudo cumulative function showed its equivalence with the material balance time function or it is even better as it is not sensitive to the time step and the gas properties change is considered as a function of the cumulative production, not as a function of time, the application of the new material balance approach using the normalized pseudo cumulative function still overestimated the OGIP and again this is a result of the PVT data.

To sum up, Production Data Analysis approaches could give reliable results for the estimation of the initial hydrocarbon in place and the reservoir characteristics. Flowing Material Balance is a valid approach for estimating the Original Hydrocarbon in Place. PVT data surveillance during production is crucial for production analysis in general and for FMB in specific.

Bibliography and References

Agarwal, R. G., Gardner, D. C., Kleinsteiber, S. W., & Fussell, D. D. (1998). Analyzing Well Production Data Using Combined Type Curve and Decline Curve Analysis Concepts. .

Ahmed, T. (2010). *Reservoir engineering handbook, Fourth edition.* Elsvier.

Arps , J. J. (1945). Analysis of Decline Curves. . Society of Petroleum Engineers.

Aziz , K., & Settari , A. (1979). Petroleum Reservoir Simulation . In *Petroleum Reservoir Simulation .* Amesterdam: Elsevier Applied Science Publisher .

Callard, J. G., & Schenewerk, P. A. (1995). Reservoir Performance History Matching Using Rate/Cumulative Type-Curves. Society of Petroleum Engineers.

Choudhury, Z., & Gomes, E. (2000). Material Balance Study of Gas Reservoirs by Flowing Well Method: A Case Study of Bakhrabad Gas Field. Society of Petroleum Engineers.

Dake, L. (n.d.). Fundamentals of Reservoir Engineering. The Netherlands: Shell Internationale Petroleum Maatschappij B. V.The Hague.

Damoah, L. O., Mohammed, S., & Enty, G. S. (2015). Utilizing early time boundary-dominated flow data to make an initial estimate of gas-in-place: An aid to computing material balance pseudotime. Society of Petroleum Engineers .

DIATI, P. (2018). *Reservoir Engineering Lectures.* Turin.

Elgmati , A. R. (2015). Analysis of production and pressure data to characterize the performance of oil and gas reservoir. Society of Petroleum Engineers .

Fekete.com. (n.d.). *Agarwal-Gardner Theory*. Retrieved June 3, 2018, from http://www.fekete.com/SAN/WebHelp/FeketeHarmony/Harmony_WebHelp/Content/HTML_Files/Reference_Material/Analysis_Method_Theory/Agarwal-Gardner_Theory.htm

Fekete.com. (n.d.). *Blasingame Theory*. Retrieved June 5, 2018, from http://www.fekete.com/SAN/WebHelp/FeketeHarmony/Harmony_WebHelp/Content/HTML_Files/Reference_Material/Analysis_Method_Theory/Blasingame_Theory.htm

Fekete.com. (n.d.). *Fetkovich Theory*. Retrieved June 2, 2018, from http://www.fekete.com/SAN/WebHelp/FeketeHarmony/Harmony_WebHelp/Content/HTML_Files/Reference_Material/Analysis_Method_Theory/Fetkovich_Theory.htm

Fekete.com. (n.d.). *Flowing Material Balance Theory*. Retrieved June 30, 2018, from http://fekete.com/SAN/TheoryAndEquations/HarmonyTheoryEquations/Content/HTML_Files/Reference_Material/Analysis_Method_Theory/FMB_Theory.htm

Fekete.com. (n.d.). *Material Balance Time Theory*. Retrieved May 30, 2018, from http://www.fekete.com/SAN/WebHelp/FeketeHarmony/Harmony_WebHelp/Content/HTML_Files/Reference_Material/General_Concepts/Material_Balance_Time_Theory.htm

Fekete.com. (n.d.). *Traditional Decline Theory*. Retrieved June 25, 2018, from http://www.fekete.com/SAN/WebHelp/FeketeHarmony/Harmony_WebHelp/Content/HTML_Files/Reference_Material/Analysis_Method_Theory/Traditional_Decline_Theory.htm

Fetkovich, M. J. (1980). Decline curve analysis using type curves. Society of Petroleum Engineers.

Guzman, J. D., Arevalo, J. A., & Espinola, O. (2014). Reserves evaluation of dry gas reservoirs through flowing pressure material balance method. Society of Petroleum Engineers .

Harold Vance Department of Petroleum Engineering. (n.d.). Introduction to Petroleum Engineering. Texas A&M University.

Institute of Petroleum Engineering, . (n.d.). *Reservoir Simulation Book.* United Kingdom: Heriot-Watt University.

Ismadi, D., Kabir, C. S., & Hasan, R. (2012). The use of combined static- and dynamic-material-balance methods with real-time surveillance data in volumetric gas reservoirs. Society of Petroleum Engineers.

Istayeva, U., & King, G. (2014). Application of the extended dynamic material balance method to a super-giant carbonate oilfield. Society of Petroleum Engineers.

Ltd., S. (2014). *Eclipse Reference Manual Version 2014.1.* Schlumberger Ltd.

Mattar , L., & Anderson, D. (2005). Dynamic Material Balance(Oil or Gas-In-Place Without Shut-In). Petroleum Society of Canada.

Mattar , L., & McNeil, R. (1998). The "Flowing" Gas Maerial Balance . Petroleum Society of Canada .

McNeil, R. (1995). The "Flowing" Material Balance Procedure. Petroleum Society of Canda.

Meunier, D. F., Kabir, C. S., & Wittmann, M. J. (1987). Gas Well Test Analysis: Use of Normalized Pseudovariables. Society of Petroleum Engineers.

Mohammed, S., & Enty, G. S. (2013). Analysis of Gas Production Data Using Flowing Material Balance Method. Society of Petroleum Engineers .

Molokwu, V. C., & Onyekonwu, M. O. (2016). A Nonlinear Flowing Material Balance for Analysis of Gas Well Production Data. Society of Petroleum Engineers.

Morad , K., & Clarkson, C. R. (2006). Application of Flowing P/z* Material Balance for Dry Coalbed-Methane Reservoirs . Society of Petroleum Engineers .

Nnaemeka, E. (2011). *Petroleum Reservoir Engineering Practice .* USA .

Ojo, K. P., & Osisanya, S. O. (2006). Material Balance Revisited. Sociey of Petroleum Engineers.

Ojo, K. P., Tiab, D., & Osisanya, S. O. (2006). Dynamic Material Balance Equation and Solution Technique Using Production and PVT Data. Society of Petroleum Engineers .

Oliver, H., Didier , V., Ole, S. F., & et al. (2013). The theory and practice of pressure transient, Production analysis, Well performance analysis, Production logging and the use of permanent downhole gauge data. KAPPA V.4.20.2015.

Palacio, J. C., & Blasingame, T. A. (1993). Decline-Curve Analysis With Type Curves - Analysis of Gas Well Production Data. Society of Petroleum Engineers .

Ukauku, I., Johnson, A., Olatunji, B., Korubo, W., Olugbenga, D., Nwashinemere, U., & Iledare, W. (2017). Flowing material balance and rate transient analysis modeling with augmented non-continuous permanent downhole gauge data. Society of Petroleum Engineers .

Van Everdingen, A. F., & Hurst, W. (1949). The Application of the Laplace Transformation to Flow Problems in Reservoirs. Society of Petroleum Engineers .

Appendix A

Fluid Flow Equations in Porous medium for different flow regimes (DIATI, 2018)

In this part we develop the derivation of the fluid flow equations that would be further used in the FMB approaches.

We start from the solution to the diffusivity equation. The diffusivity equation is a differential equation obtained by combining continuity equation that governs the conservation of mass, flaw law and state equations. It's a Partial differential equation that describes the change of the pressure in space in time in the reservoir.

Assuming Monophasic flow of a slightly compressible fluid (Liquid) through a homogeneous and Isotropic porous medium, pressure gradients are small and Darcy's law applies we reach:

$$\nabla^2 p = \frac{\mu\phi c_t}{k}\frac{\partial p}{\partial t} = \frac{1}{\eta}\frac{\partial p}{\partial t}$$ **Equation A-1**

Where η is defined as Diffusivity constant

$$\eta = \frac{k}{\mu\phi c_t}$$ **Equation A-2**

Developing the equation for radial flow we reach:

- **Steady State Flow**

$$\frac{\partial^2 p}{\partial r^2} + \frac{1}{r}\frac{\partial p}{\partial r} = 0$$ **Equation A-3**

Defining the initial and boundary conditions: $\begin{cases} \frac{\partial p}{\partial t} = 0 \quad \forall r, \forall t \\ p = p_i = const. \quad r = r_e \end{cases}$

Solving the diffusivity equation we get MUSKAT Equation where

$$q = \frac{2\,\pi k h}{\mu}\frac{p_i - p_w}{\ln\frac{r_e}{r_w}}$$ **Equation A-4**

which also can be written as:

$$p_{wf} = p_i - \frac{q\,\mu}{2\,\pi k h}\ln\frac{r_e}{r_w}$$ **Equation A-5**

Introducing the skin factor we reach

$$p_{wf} = p_i - \frac{q\,\mu}{2\,\pi k h}\ln\left(\frac{r_e}{r_w} + S\right)$$ **Equation A-6**

Knowing that this in the SI units we can get this equation in Oil-field units as:

$$p_{wf} = p_i - \frac{141.27\,q\,B\mu}{kh}\ln\left(\frac{r_e}{r_w} + S\right)$$ **Equation A-7**

Where,

p (psi)
q (STB/d)
μ (cP)
K (mD)
h (ft)
r_e, r_w (ft)
B (bbl/STB) , S (-)

- **Transient Flow**

$$\frac{\partial^2 p}{\partial r^2} + \frac{1}{r}\frac{\partial p}{\partial r} = \frac{\mu\phi c_t}{k}\frac{\partial p}{\partial t}$$ **Equation A-8**

Initial and boundary conditions: $\begin{cases} t = o, p = p_i \quad \forall r \\ t > 0 \begin{cases} p = p_i \quad r = r_e \quad Constant\ Terminal\ Rate \\ \frac{\partial p}{\partial r} = constant \quad r = r_w \end{cases} \end{cases}$

Solving the diffusivity equation we reach

$$p(r_w, t) = p_i - \frac{q\ \mu}{2\ \pi kh}\ P\left(\frac{r}{r_w}, t_D\right)$$ **Equation A-9**

Before we proceed, we would like to define what is called dimensionless variables. Dimensionless Variables have been used in well testing to solve the unsteady-state flow equation and to simply the diffusivity equation and its solution. Hence, reduce the number of unknowns by combining the reservoir parameters (Such as permeability, Porosity). (Ahmed, 2010)

- Dimensionless Pressure Variable P_D:

$$P_D = \frac{2\ \pi\ k\ h}{q\ \mu}\Delta p$$ **Equation A-10**

In the oil field units:

$$P_D = \frac{kh}{141.27\ q\ B\ \mu}\Delta p = \frac{0.007082\ kh}{q\ B\ \mu}\Delta p$$ **Equation A-11**

- Dimensionless Time Variable t_D:

$$t_D = \frac{t}{t_c} = \frac{kt}{\mu\phi c_t r_w^2}$$ **Equation A-12**

Where t_c is the characteristic time:

$$(t)_c = \frac{\mu\phi c_t r_w^2}{k} \quad \textbf{Equation A-13}$$

In the oil field units:

$$t_D = \frac{t}{(t)_c} = \frac{0.0002637\ kt}{\mu\phi c_t r_w^2} \quad \textbf{Equation A-14}$$

- ❖ Dimensionless Outer Boundary Radius Variable r_{eD}:

$$r_{eD} = \frac{r_e}{r_w} \quad \textbf{Equation A-15}$$

- ❖ Dimensionless Radius Variable r_D:

$$r_{eD} = \frac{r_e}{r_w} \quad \textbf{Equation A-16}$$

Back to the solution of the diffusivity equation, the solution of the term $P\left(\frac{r}{r_w}, t_D\right)$ was found in literature as:

$$P\left(\frac{r}{r_w}, t_D\right) = -\frac{1}{2} E_i\left(-\frac{r^2}{4\,\eta t}\right) \quad \textbf{Equation A-17}$$

Where, $$E_i\left(-\frac{r^2}{4\,\eta t}\right) = \ln\left(\frac{4}{e^\gamma} t_D\right) = \ln(2.25\ t_D) = \ln\left(2.25\frac{\mu\phi c_t r_w^2}{kt}\right) \quad \textbf{Equation A-18}$$

Where $\gamma = 0.57721$ is defined as Euler's Constant

Therefore, $$p\ (r_w, t) = p_i - \frac{q\ \mu}{2\ \pi kh}\left(-\frac{1}{2}\ln\left(2.25\frac{\mu\phi c_t r_w^2}{kt}\right)\right) \quad \textbf{Equation A-19}$$

$$p\ (r_w, t) = p_i - \frac{q\ \mu}{4\ \pi kh}\ln\left(2.25\frac{kt}{\mu\phi c_t r_w^2}\right) = p_i - \frac{q\ \mu}{4\ \pi kh}\ln(2.25 t_D) \quad \textbf{Equation A-20}$$

Introducing the skin factor

$$p\ (r_w, t) = p_i - \frac{q\ \mu}{4\ \pi kh}\ln\left(2.25\frac{kt}{\mu\phi c_t r_w^2} + 2S\right) \quad \textbf{Equation A-21}$$

$$p\ (r_w, t) = p_i - \frac{q\ \mu}{4\ \pi kh}\ln(2.25 t_D + 2S\ ) \quad \textbf{Equation A-22}$$

In the Oil-Field Units

$$p\ (r_w, t) = p_i - \frac{70.64\ q\ B\ \mu}{kh} \ln\left(2.25 \frac{kt}{\mu\phi c_t r_w^2} + 2S\right) \qquad \textbf{Equation A-23}$$

$$p\ (r_w, t) = p_i - \frac{70.64\ q\ B\ \mu}{kh} \ln(2.25 t_D + 2S\ ) \qquad \textbf{Equation A-24}$$

- **Pseudo-Steady State Flow**

$$\frac{\partial^2 p}{\partial r^2} + \frac{1}{r}\frac{\partial p}{\partial r} = \frac{\mu\phi c_t}{k}\frac{\partial p}{\partial t} \qquad \textbf{Equation A-25}$$

Initial and boundary conditions: $\begin{cases} t = o, p = p_i \quad\quad r = r_e \\ t\ > 0 \begin{cases} \frac{dp}{dt} = const \quad\quad \forall\, r \\ \frac{\partial p}{\partial r} = 0 \quad\quad r = r_e \end{cases} \end{cases}$

A Pseudo-Steady State condition is reached when all boundaries of the reservoir is touched and the reservoir is acting as enclosed system where the pressure starts to drop with the same rate at each point in the reservoir.

From the flow equation of the transient flow, we can define the time to reach the pseudo-steady state (Stabilization time) as:

$$t_s = \frac{1}{2.25}\frac{\mu\phi c_t r_e^2}{k} \qquad \textbf{Equation A-26}$$

However, the reservoir boundaries rarely take a regular shape and therefore the well is probably asymmetrically located in a bounded, irregularly shaped drainage area which makes the flow equations we have developed in a porous medium are no longer valid because of the additional pressure drop of due to the reflection of the pressure disturbances on the boundaries.

Applying the superposition in space and assuming a linear boundary we get:

$$p\ (r_w, t) = p_i - \frac{q\ \mu}{2\ \pi kh}\left(\frac{1}{2}\ln(2.25 t_D)\ + P\left(\frac{d}{r_w}, t_D\right)\right) \qquad \textbf{Equation A-27}$$

As d is the distance between the well and the boundary at which the pressure disturbance will reflect. Therefore,

$$P\ \left(\frac{d}{r_w}, t_D\right) = \ -\frac{1}{2}E_i\left(-\frac{d^2}{4\ \eta t}\right) \qquad \textbf{Equation A-28}$$

However, the well could be affected by the reflections of infinite number of boundaries each according to the distance from the well and therefore:

$$p\,(r_w,t) = p_i - \frac{q\,\mu}{4\,\pi kh}\left[\ln\,2.25t_D - \sum_{j=1}^{\infty} E_i\left(-\frac{d_j^2}{4\,\eta t}\right)\right] \qquad \textbf{Equation A-29}$$

To solve this newly introduced term we introduce another dimensionless variable. Dimensionless time Variable with respect to the drainage are t_{DA}:

$$t_{DA} = \frac{kt}{\mu\phi c_t A} = t_D\frac{r_w^2}{A} \qquad \textbf{Equation A-30}$$

In addition (Matthews, Brons, Hazeborek) introduced a function called MBH or F function that depends on $\begin{cases} Time \\ Shape\ of\ the\ Drainage\ area \\ Well\ Location \end{cases}$ that will be used to solve this term where:

$$F = 4\,\pi\,t_{DA} + \sum_{j=1}^{\infty} E_i\left(-\frac{d_j^2}{4\,\eta t}\right) \qquad \textbf{Equation A-31}$$

This gives us the general flow equation that is also used in late transient flow to address the influence of the boundaries of the drainage as:

$$p\,(r_w,t) = p_i - \frac{q\,\mu}{4\,\pi kh}\,[\ln\,2.25t_D + 4\,\pi\,t_{DA} - F\,] \qquad \textbf{Equation A-32}$$

When Pseudo-Steady State (PSS) it's found that F function stabilizes and becomes linear

$$F = \ln C_A t_{DA} \qquad \textbf{Equation A-33}$$

Where C_A is defined as Dietz Shape Factor that depends on the shape of the drainage are and on the well location within it.

$$p\,(r_w,t) = p_i - \frac{q\,\mu}{4\,\pi kh}\,[\ln\,2.25t_D + 4\,\pi\,t_{DA} - F\,] \qquad \textbf{Equation A-34}$$

$$p\,(r_w,t) = p_i - \frac{q\,\mu}{4\,\pi kh}\,[\ln\,2.25t_D + 4\,\pi\,t_{DA} - \ln C_A t_{DA}\,] \qquad \textbf{Equation A-35}$$

$$p\,(r_w,t) = p_i - \frac{q\,\mu}{4\,\pi kh}\left[\ln\,2.25\,\frac{A}{C_A r_w^2} + 4\,\pi\,t_{DA}\,\right] \qquad \textbf{Equation A-36}$$

In the meanwhile, if the reservoir conditions reached PSS this means that depletion started to occur. Depletion energy is completely driven by the compressibility of the fluid in the pores of the reservoir roc and from the definition of the compressibility:

$$c = \frac{1}{V}\frac{\Delta V}{\Delta P} \qquad \textbf{Equation A-37}$$

We reach: $$p_i - \bar{p} = \frac{qt}{cAh\phi}$$ **Equation A-38**

Knowing that $$\frac{q\,\mu}{4\,\pi kh}\,(4\,\pi\,t_{DA}) = \frac{q\,\mu}{4\,\pi kh}\,4\,\pi\,\frac{kt}{\mu\phi c_t A} = \frac{qt}{c_t Ah\phi}$$ **Equation A-39**

Therefore, $$p\,(r_w, t) = p_i - \frac{q\,\mu}{4\,\pi kh}\left[\ln\,2.25\,\frac{A}{C_A r_w^2} + 4\,\pi\,t_{DA}\right]$$ **Equation A-40**

$$p\,(r_w, t) = p_i - \frac{qt}{cAh\phi} - \frac{q\,\mu}{4\,\pi kh}\left[\ln\,2.25\,\frac{A}{C_A r_w^2}\right]$$ **Equation A-41**

$$p\,(r_w, t) = \bar{p} - \frac{q\,\mu}{4\,\pi kh}\left[\ln\,2.25\,\frac{A}{C_A r_w^2}\right]$$ **Equation A-42**

This equation represents the fluid flow equation in a porous medium in PSS conditions.

$\bar{p}$ The average reservoir pressure which is really important for the material balance calculations, can be obtained, using the FMB, combining this equation with the depletion equation

$$p_i - \bar{p} = \frac{qt}{cAh\phi}$$ **Equation A-43**

For a well symmetrically centered in a circular drainage area C_A is found equal to 31.6. By substituting and also by putting $A = \pi r_e^2$ we reach:

$$p\,(r_w, t) = \bar{p} - \frac{q\,\mu}{4\,\pi kh}\left[\ln\,2.25\,\frac{\pi r_e^2}{31.6\,r_w^2}\right]$$ **Equation A-44**

$$p\,(r_w, t) = \bar{p} - \frac{q\,\mu}{2\,\pi kh}\left[\frac{1}{2}\ln 0.2236\frac{r_e^2}{r_w^2}\right]$$ **Equation A-45**

$$p\,(r_w, t) = \bar{p} - \frac{q\,\mu}{2\,\pi kh}\left[\ln 0.476\frac{r_e}{r_w}\right]$$ **Equation A-46**

$$p\,(r_w, t) = \bar{p} - \frac{q\,\mu}{2\,\pi kh}\left[\ln\frac{r_e}{r_w} - \frac{3}{4}\right]$$ **Equation A-47**

This is the liquid flow equation in a porous medium in a PSS conditions for an asymmetrically centered well in a circular drainage area.

Liquid Flow Equations:

1) General equation: This equation is used in late transient conditions.

$$p_{wf} = p_i - \frac{q_o\,\mu_o}{4\,\pi kh}\,[\ln\ 2.25 t_D + 4\,\pi\,t_{DA} - F + 2S\,] \qquad \textbf{Equation A-48}$$

2) Early Transient conditions (where no boundary is felt) and in RTA is called Infinite Acting Radial Flow

$$p_{wf} = \ p_i - \frac{q_o\,\mu_o}{4\,\pi kh}\ln(2.25 t_D + 2S\,) \qquad \textbf{Equation A-49}$$

3) Pseudo-Steady State Conditions:

$$p_{wf} = \ \bar{p} - \frac{q_o\,\mu_o}{4\,\pi kh}\left[\ln\ 2.25\,\frac{A}{C_A r_w^2}\right] \qquad \textbf{Equation A-50}$$

Gas Flow Equations:

Instead of derivation all equations again for the gas, we use the dimensionless terms.

Recall the dimensionless pressure variable Equation A-10:

$$\Delta p = \ \frac{q\,\mu}{2\,\pi\,k\,h}\,P_D = p_i - p(r_w, t) \qquad \textbf{Equation A-51}$$

Therefore we could express the dimensionless pressure variable according to the flow regime

- ❖ General Equation (Always Valid)

$$P_D = \ \frac{1}{2}\,[\ln\ 2.25 t_D + 4\,\pi\,t_{DA} - F] \qquad \textbf{Equation A-52}$$

- ❖ Early Transient Conditions

$$P_D = \frac{1}{2}\,\ln(2.25 t_D\,) \qquad \textbf{Equation A-53}$$

- ❖ Pseudo-Steady State Conditions

$$P_D = \frac{1}{2}\left[\ln\ 2.25\,\frac{A}{C_A r_w^2} + 4\,\pi\,t_{DA}\right] \qquad \textbf{Equation A-54}$$

- ❖ Pseudo Steady State conditions (Well symmetrically centered in a circular drainage area)

$$P_D = \ 2\pi t_{DA} + \left[\ln\,\frac{r_e}{r_w} - \frac{3}{4}\right] \qquad \textbf{Equation A-55}$$

This found in literature expressed as:

$$P_D = \frac{2\, t_D}{r_{eD}^2} + \ln(r_{eD}) - \frac{3}{4} \quad \textbf{Equation A-56}$$

Using these equations gives the same equations with only two changes:

- The Pseudo Pressure Function instead of the Pressure to account for the change of compressibility factor Z and viscosity of the gas with the change of pressure.

  In literature, the pseudo-pressure function could be found expressed as:

$$m(p) = 2\int_{p_o}^{p} \frac{p}{Z\mu} dp \quad \textbf{Equation A-57}$$

- The proportionality in the dimensionless parameters equation
  For Liquid Flow equation we found in Equation A-10

$$\Delta p = \frac{q\, \mu}{2\, \pi\, k\, h}\, P_D$$

However, for gas flow equations with introducing the pseudo pressure function to have the rigorous solution of the diffusivity equation, it is found that:

$$\Delta m(p) = \frac{q_g\, T}{\pi\, k\, h} \left(\frac{P_{sc}}{T_{sc}}\right) P_D \quad \textbf{Equation A-58}$$

1) General equation: This equation is used in late transient conditions.

$$m(p_{wf}) = m(p_i) - \frac{q_g\, T}{2\pi\, k\, h}\left(\frac{P_{sc}}{T_{sc}}\right) [\ln\ 2.25 t_D + 4\, \pi\, t_{DA} - F + 2S\,] \quad \textbf{Equation A-59}$$

2) Early Transient conditions (where no boundary is felt) and in RTA is called Infinite Acting Radial Flow

$$m(p_{wf}\,) = m(p_i) - \frac{q_g\, T}{2\pi\, k\, h}\left(\frac{P_{sc}}{T_{sc}}\right) \ln(2.25 t_D + 2S\,) \quad \textbf{Equation A-60}$$

3) Pseudo-Steady State Conditions:

$$m(p_{wf}) = m(\bar{p}) - \frac{q_g\, T}{2\pi\, k\, h}\left(\frac{P_{sc}}{T_{sc}}\right) \left[\ln\ 2.25\, \frac{A}{C_A r_w^2}\right] \quad \textbf{Equation A-61}$$

Appendix B

Well #2

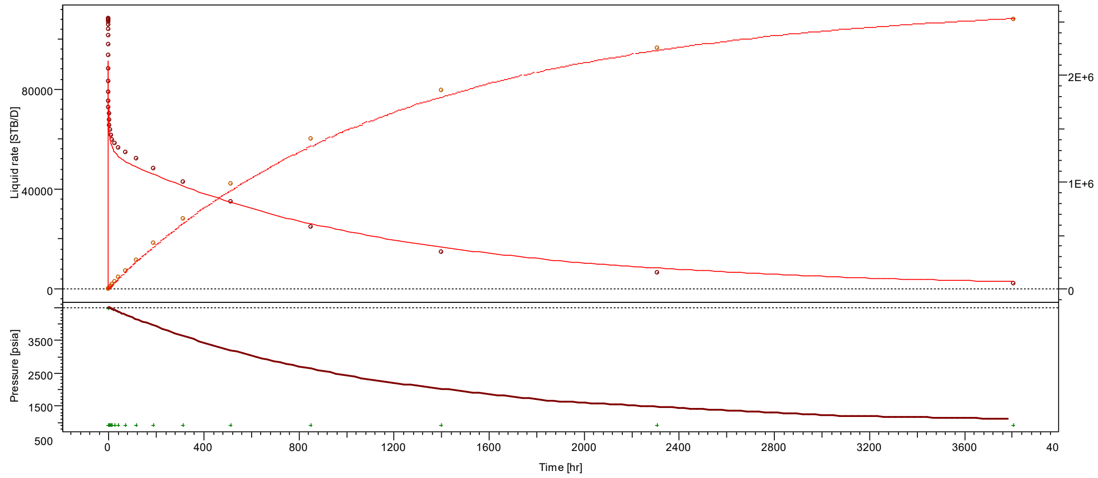

Production history plot (Liquid rate [STB/D], Pressure [psia] vs Time [hr])

Figure 70: Dead Oil Multi-well Well #2 History Match. Rate, Cumulative production, flowing pressure and model reservoir average pressure vs. Time.

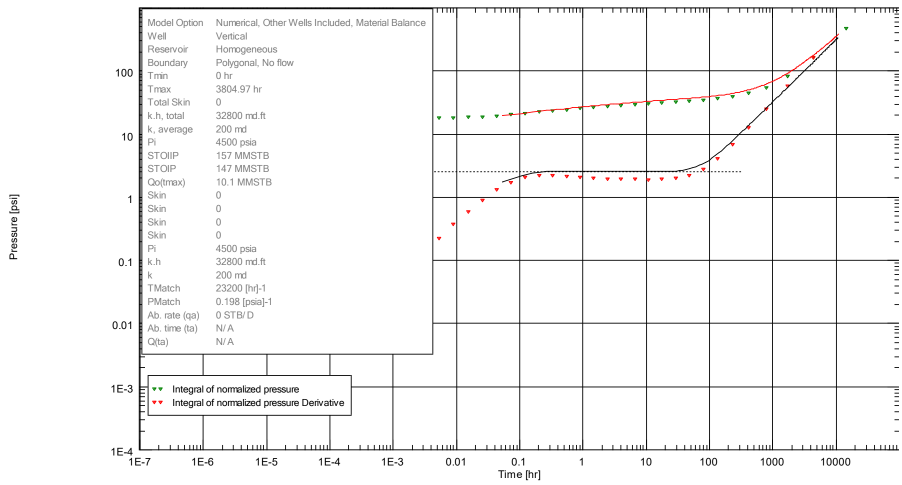

Loglog plot: Int[(pi-p)*q_ref/q]/te and d[Int[(pi-p)*q_ref/q]/te]/dln(te) [psi] vs te/2 [hr]

Figure 71: Dead Oil Multi-well Well #2 Log-Log Plot Match.

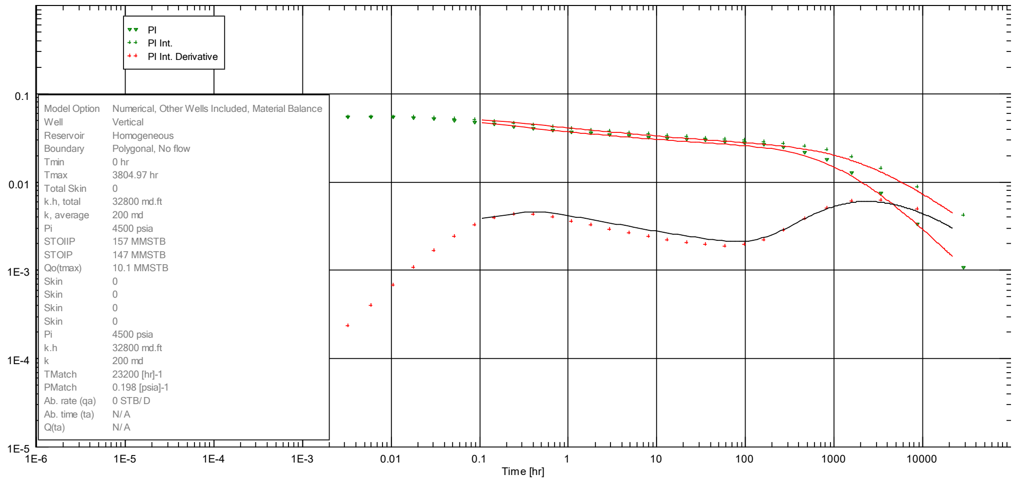

Blasingame plot: q/q_ref/(pi-p), Int[q/q_ref/(pi-p)]/te and d[Int[q/q_ref/(pi-p)]/te]/dInte [[psi]-1] vs te [hr]

Figure 72: Dead Oil Multi-well Well #2 Model Blasingame Plot Match.

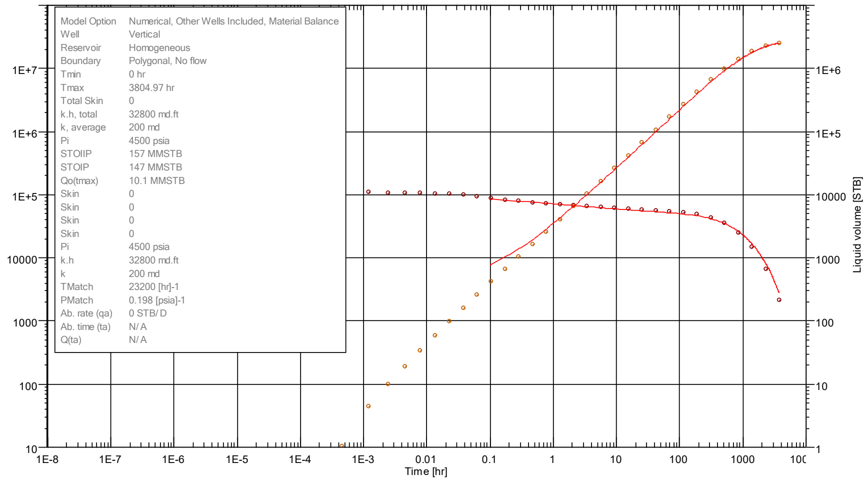

Fetkovich plot: q [STB/D], Q [STB] vs dt [hr]

Figure 73: Dead Oil Multi-well Well #2 Model Fetkovich Plot Match.

Fetkovich Type-curves Match

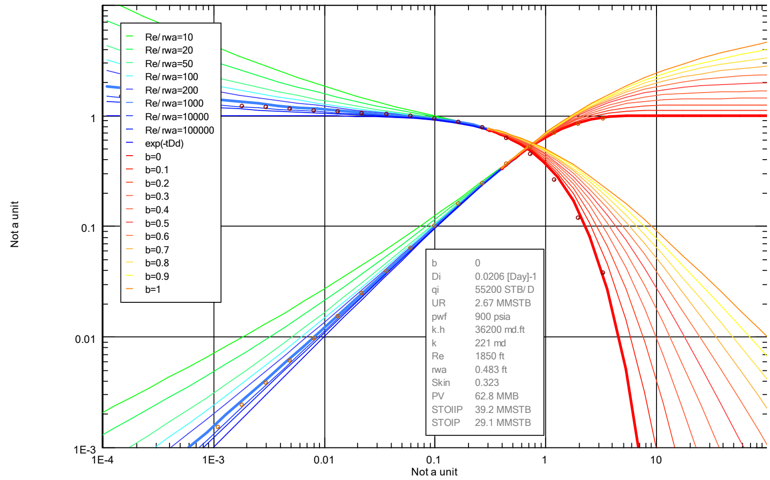

Fetkovich type curve plot: qDd and QDd vs tDd

Figure 74: Dead Oil Multi-well Well #2 Fetkovich Type-curves Match.

From Fetkovich Type-curves match we obtain the OOIP in the drainage area of each well. For well #2 we obtain ~ 39.2 MMSTB

Blasingame Type-curves

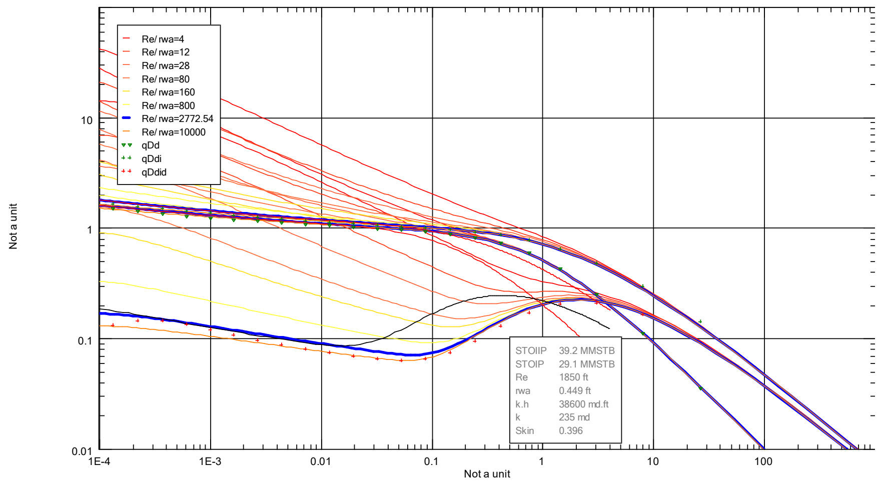

Blasingame type curve plot: qDd, qDdi and qDdid vs tDd

Figure 75: Dead Oil Multi-well Well #2 Blasingame Type-curves Match.

The match of the Blasingame type-curve give an estimation of the OOIP stored in the drainage area covered by each well. For Well #2 it gives ~ 39.2 MMSTB

Flowing Material Balance

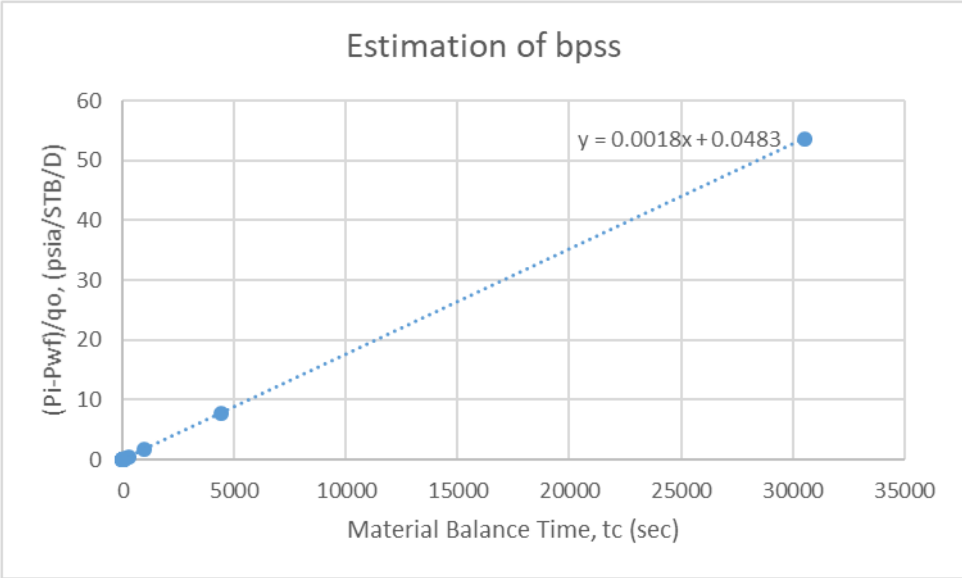

Figure 76: Dead Oil Multi-well Well #2 FMB, bpss is obtained as the Y-intercept of the straight line.

Table 24: Dead Oil Multi-well Well #2, reservoir permeability using FMB approach.

b_{pss}	0.0483	psia/STB/D
Kh	44123.43	mD.ft
k	269.0	mD

The permeability estimated by the flowing material balance is over estimated and this might be because of the neglecting of the skin effect.

From b_{Pss} we get P_{avg} to plot $\frac{Pi-\bar{P}}{q}$ vs $\frac{Np}{c}$ to get the Original Oil in place as $\frac{1}{slope}$. The first values representing the transient period where they do not follow the straight line.

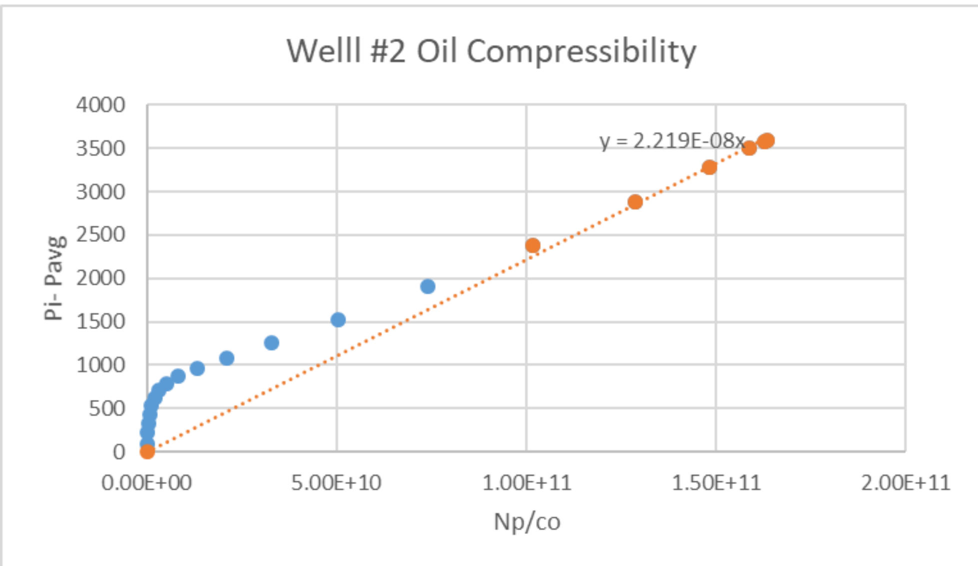

Figure 77: Dead Oil Multi-well Well #2 Flowing Material Balance using Oil Compressibility

N2= 45.07 MMSTB

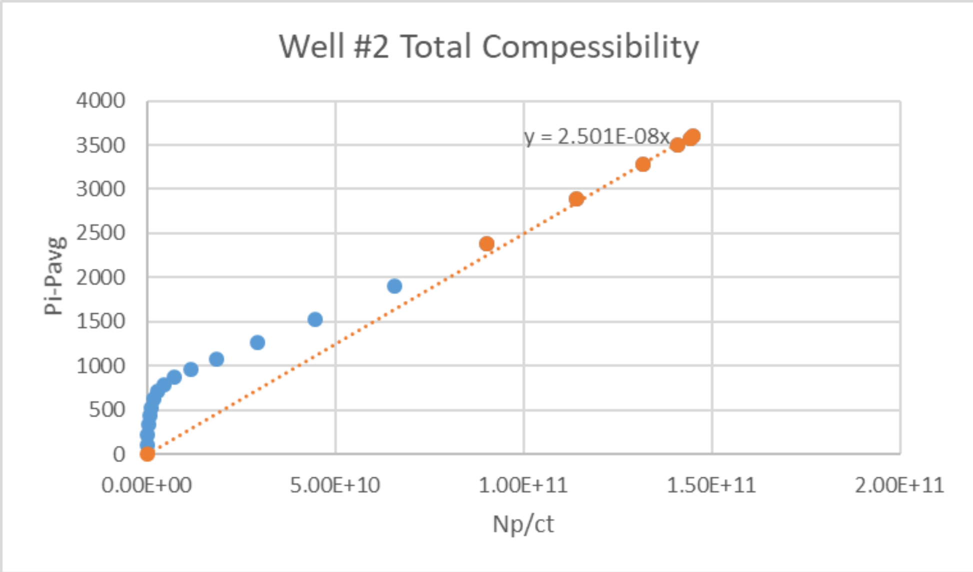

Figure 78: Dead Oil Multi-well Well #2 Flowing Material Balance using Total Compressibility

N2= 40.0 MMSTB

The early data representing the transient period do not follow the straight line of the Pseudo Steady Sate.

Well #3

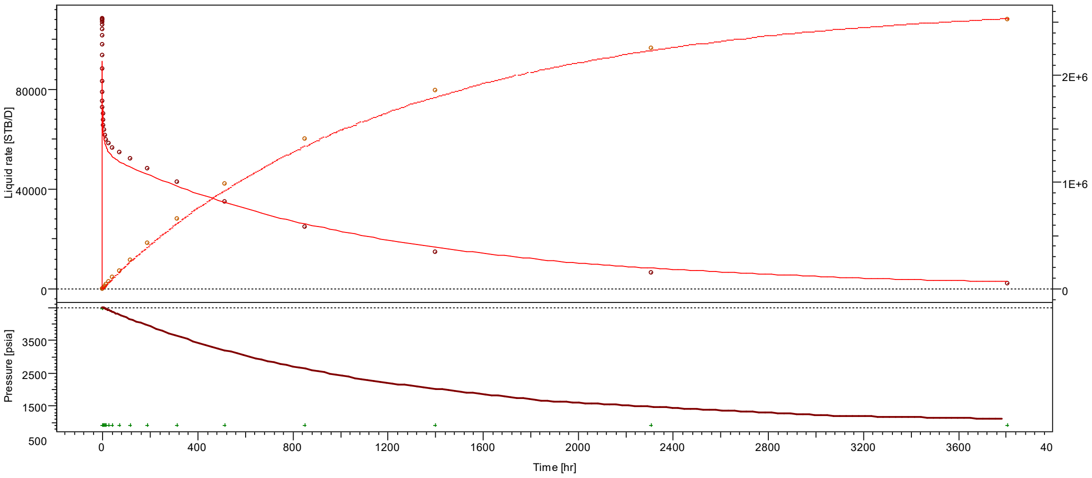

Production history plot (Liquid rate [STB/D], Pressure [psia] vs Time [hr])

Figure 79: Dead Oil Multi-well Well #3 History Match. Rate, Cumulative production, flowing pressure and model reservoir average pressure vs. Time.

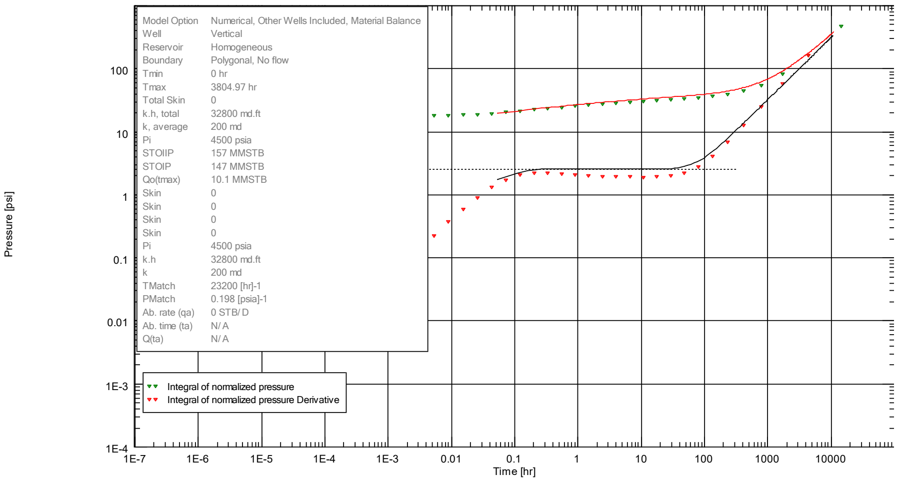

Loglog plot: Int[(pi-p)*q_ref/q]/te and d[Int[(pi-p)*q_ref/q]/te]/dln(te) [psi] vs te/2 [hr]

Figure 80: Dead Oil Multi-well Well #3 Log-Log Plot Match.

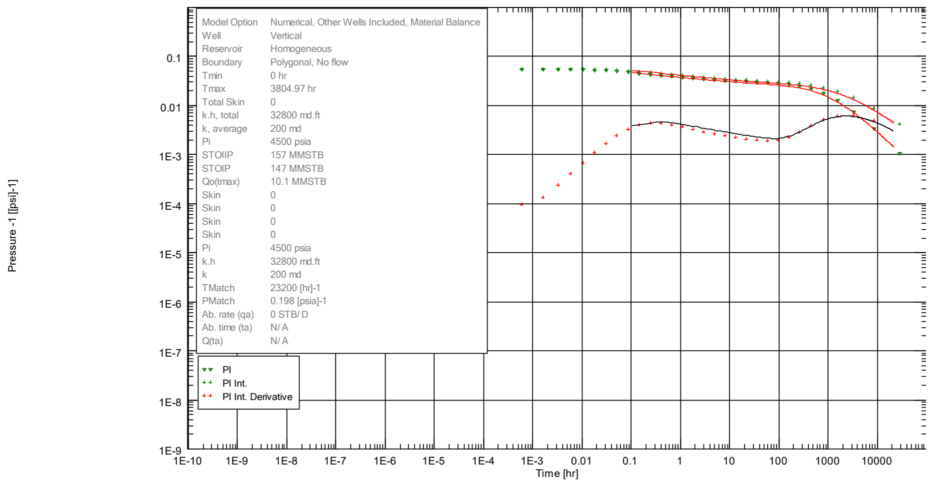

Blasingame plot: q/q_ref/(pi-p), Int[q/q_ref/(pi-p)]/te and d[Int[q/q_ref/(pi-p)]/te]/dInte [[psi]-1] vs te [hr]

Figure 81: Dead Oil Multi-well Well #3 Model Blasingame Plot Match.

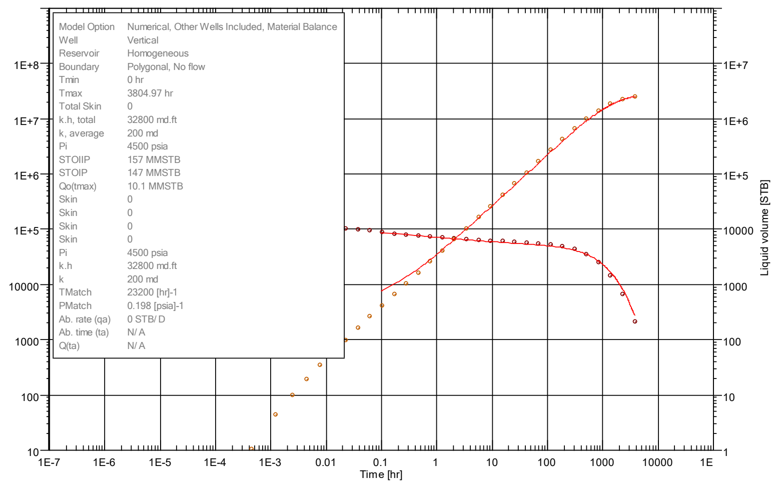

Fetkovich plot: q [STB/D], Q [STB] vs dt [hr]

Figure 82: Dead Oil Multi-well Well #3 Model Fetkovich Plot Match.

Fetkovich Type-curves Match

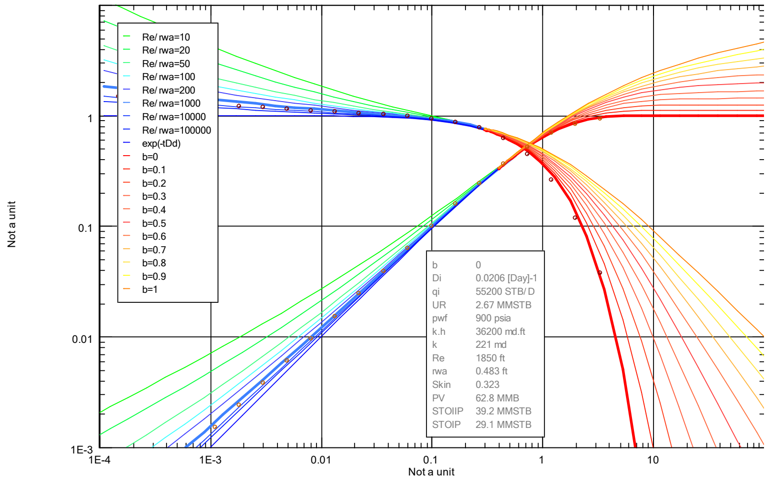

Fetkovich type curve plot: qDd and QDd vs tDd

Figure 83: Dead Oil Multi-well Well #3 Fetkovich Type-curves Match.

From Fetkovich Type-curves match we obtain the OOIP in the drainage area of each well. For well #3 we obtain ~ 39.2 MMSTB

Blasingame Type-curves

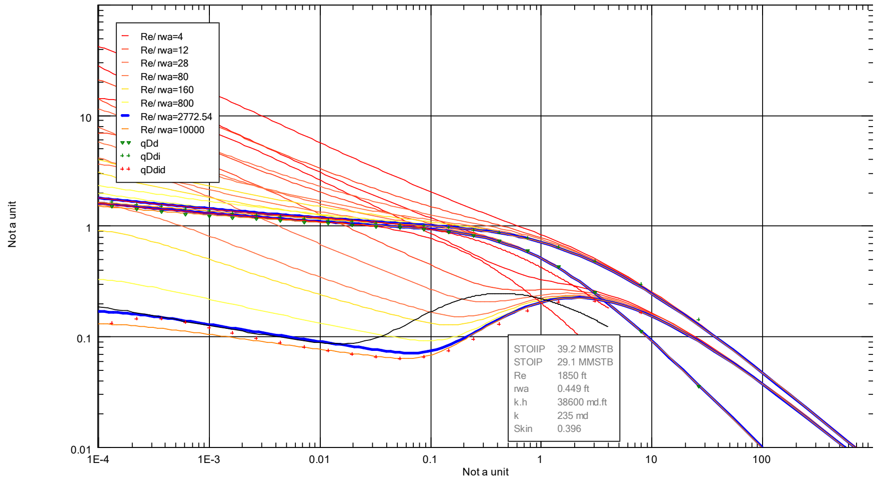

Blasingame type curve plot: qDd, qDdi and qDdid vs tDd

Figure 84: Dead Oil Multi-well Well #3 Blasingame Type-curves Match.

The match of the Blasingame type-curve give an estimation of the OOIP stored in the drainage area covered by each well. For Well #3 it gives ~ 39.2 MMSTB

Flowing Material Balance

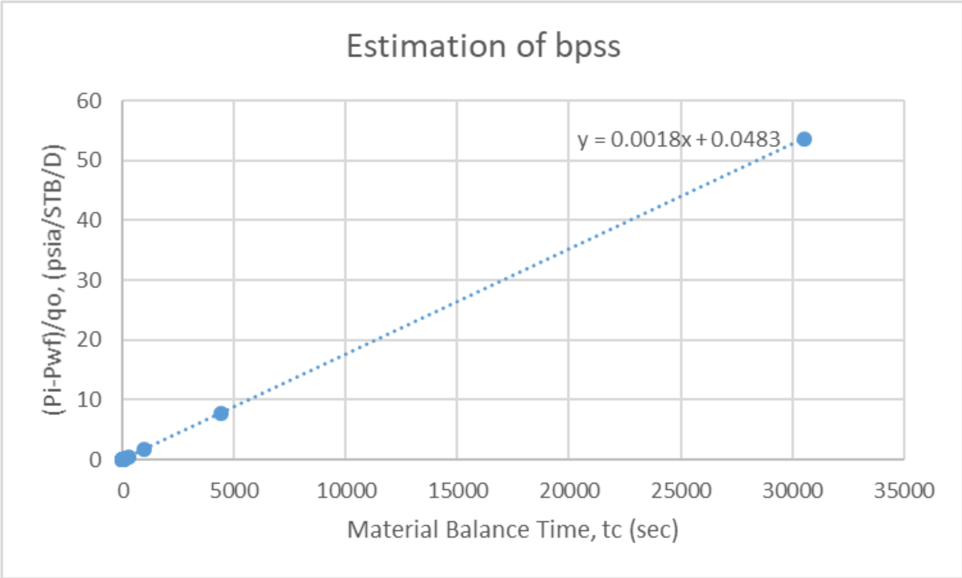

Figure 85: Dead Oil Multi-well Well #3 Well FMB, b_{pss} is obtained as the Y-intercept of the straight line

Table 25: Dead Oil Multi-well Well #3, reservoir permeability using FMB approach.

b_{pss}	0.0483	psia/STB/D
Kh	44123.43	mD.ft
k	269.0	mD

The permeability estimated by the flowing material balance is over estimated and this might be because of the neglecting of the skin effect.

From b_{Pss} we get P_{avg} to plot $\frac{Pi-\bar{P}}{q}$ vs $\frac{Np}{c}$ to get the Original Oil in place as $\frac{1}{slope}$. The first values representing the transient period where they do not follow the straight line.

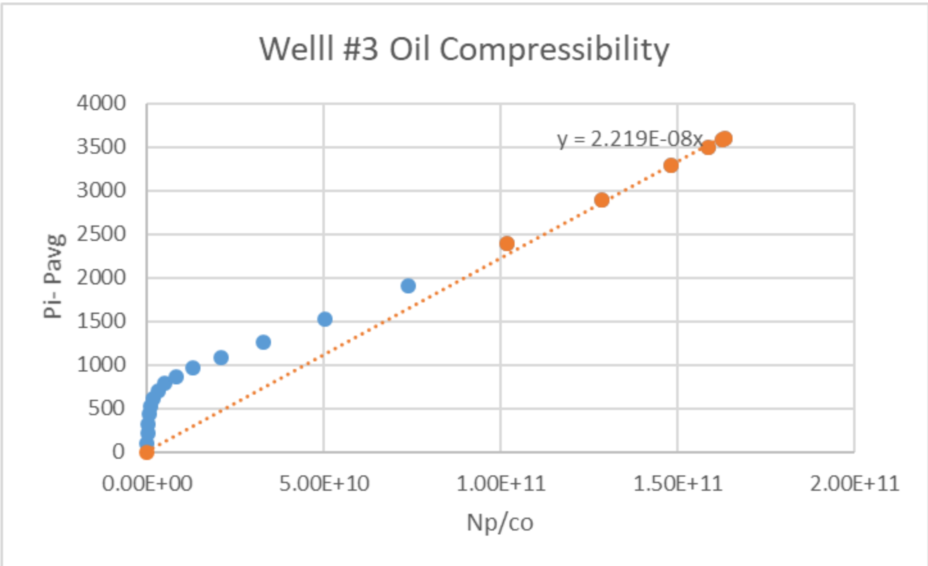

Figure 86: Dead Oil Multi-well Well #3 Flowing Material Balance using Oil Compressibility

N3= 45.0 MMSTB

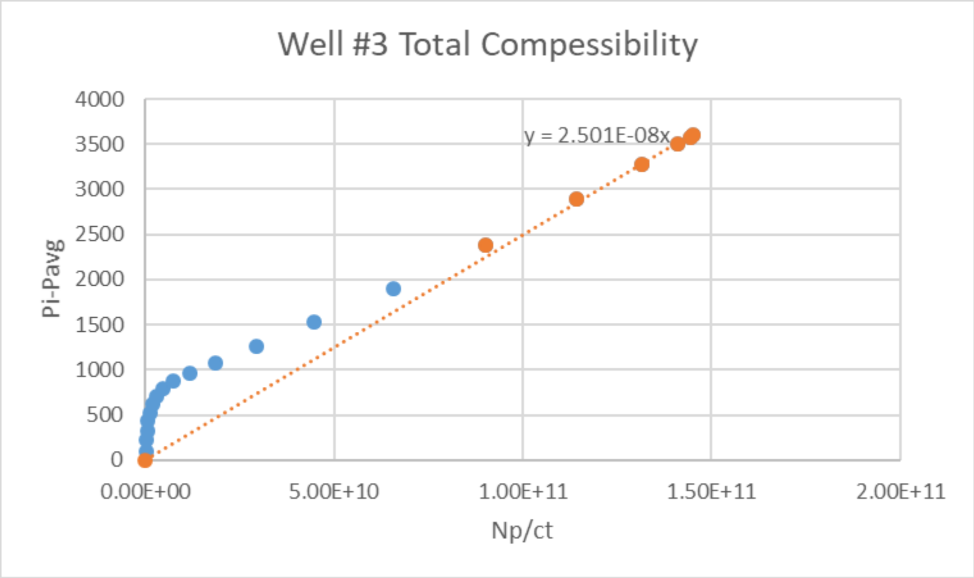

Figure 87: Dead Oil Multi-well Well #3 Flowing Material Balance using Total Compressibility.

N3 = 40.0 MMSTB

The early data representing the transient period do not follow the straight line of the Pseudo Steady Sate.

Well #4

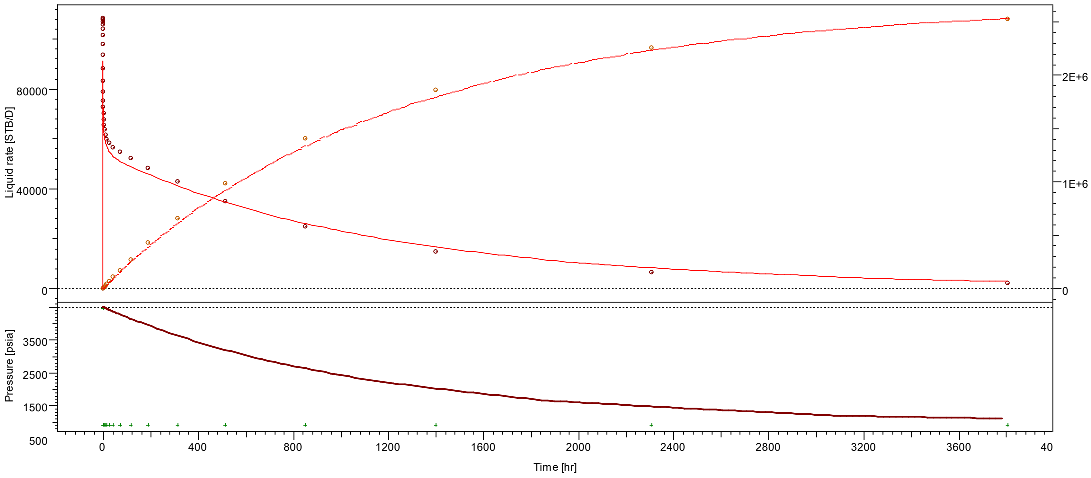

Production history plot (Liquid rate [STB/D], Pressure [psia] vs Time [hr])

Figure 88: Dead Oil Multi-well Well #4 History Match. Rate, Cumulative production, flowing pressure and model reservoir average pressure vs. Time.

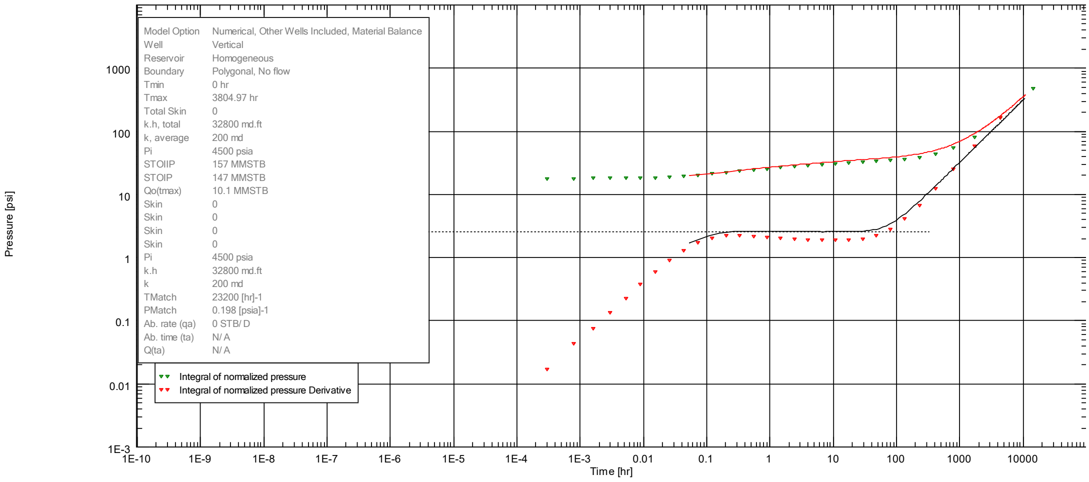

Loglog plot: Int[(pi-p)*q_ref/q]/te and d[Int[(pi-p)*q_ref/q]/te]/dln(te) [psi] vs te/2 [hr]

Figure 89: Dead Oil Multi-well Well #4 Log-Log Plot Match.

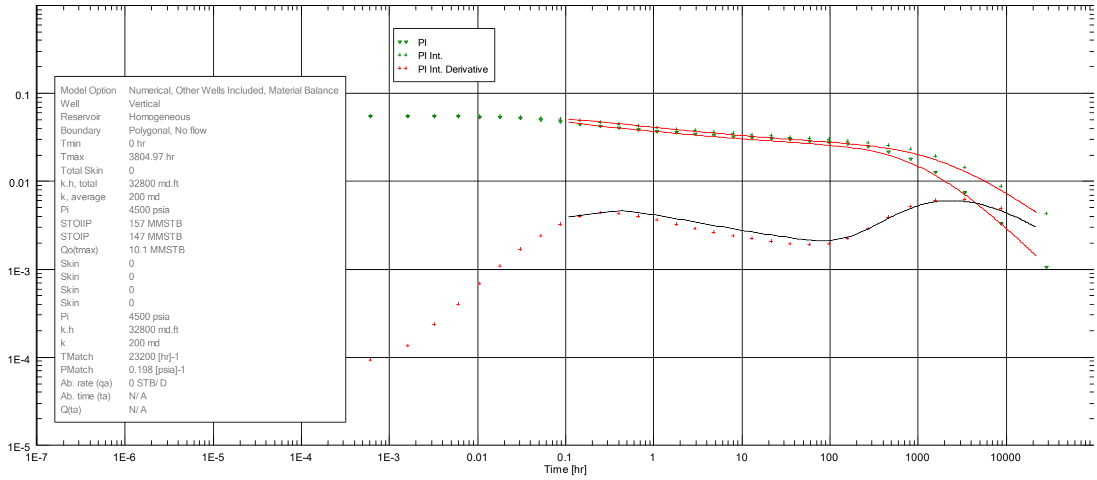

Blasingame plot: q/q_ref/(pi-p), Int[q/q_ref/(pi-p)]/te and d[Int[q/q_ref/(pi-p)]/te]/dInte [[psi]-1] vs te [hr]

Figure 90: Dead Oil Multi-well Well #4 Model Blasingame Plot Match.

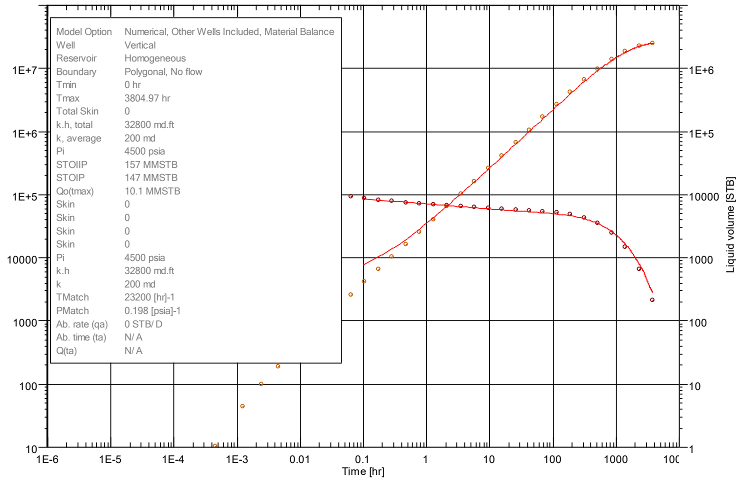

Fetkovich plot: q [STB/D], Q [STB] vs dt [hr]

Figure 91: Dead Oil Multi-well Well #4 Well Model Fetkovich Plot Match.

Fetkovich Type-curves Match

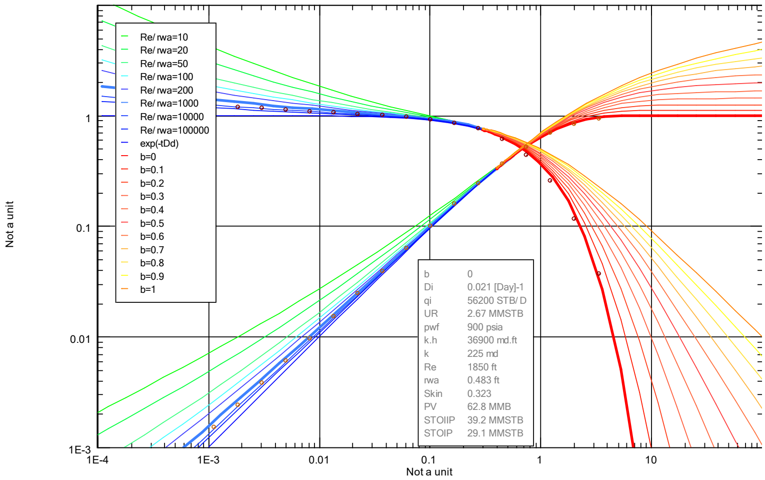

Fetkovich type curve plot: qDd and QDd vs tDd

Figure 92: Dead Oil Multi-well Well #4 Fetkovich Type-curves Match.

From Fetkovich Type-curves match we obtain the OOIP in the drainage area of each well. For well #3 we obtain ~ 39.2 MMSTB

Blasingame Type-curves

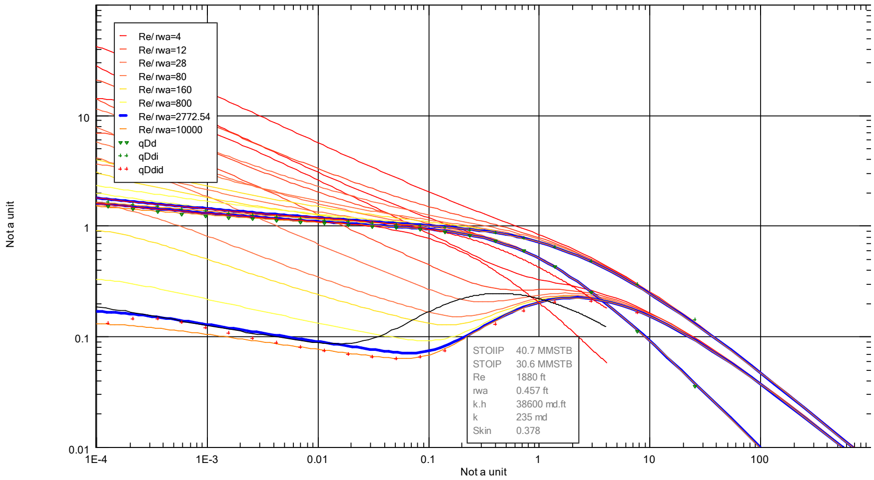

Blasingame type curve plot: qDd, qDdi and qDdid vs tDd

Figure 93: Dead Oil Multi-well Well #4 Blasingame Type-curves Match.

The match of the Blasingame type-curve give an estimation of the OOIP stored in the drainage area covered by each well. For Well #3 it gives ~ 40.7 MMSTB

Flowing Material Balance

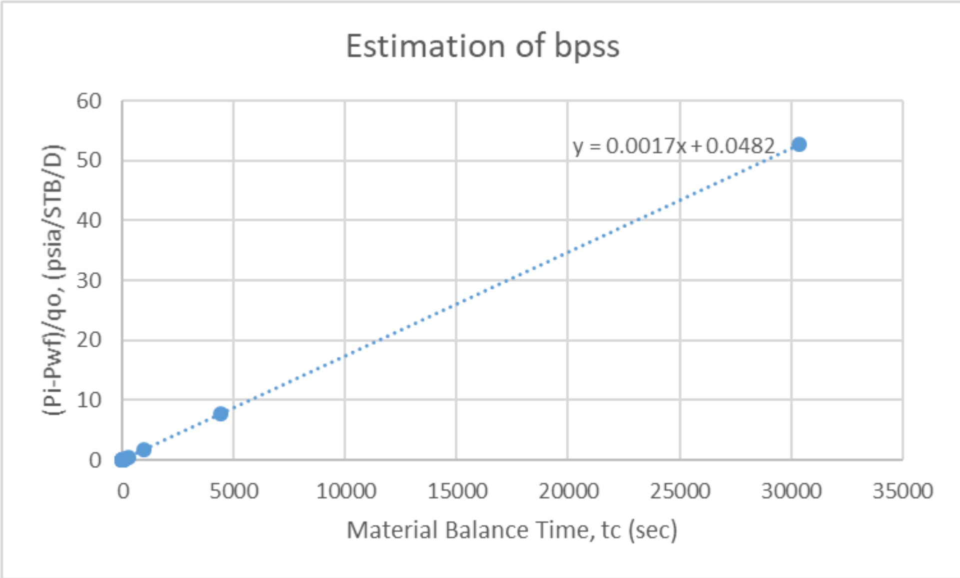

Figure 94: Dead Oil Multi-well Well #4 FMB, b_{pss} is obtained as the Y-intercept of the straight line.

Table 26: Dead Oil Multi-well Well #4, reservoir permeability using FMB approach.

b_{pss}	0.0482	psia/STB/D
Kh	44214.98	mD.ft
k	269.6	mD

The permeability estimated by the flowing material balance is over estimated and this might be because of the neglecting of the skin effect.

From b_{Pss} we get P_{avg} to plot $\frac{Pi-\bar{P}}{q}$ vs $\frac{Np}{c}$ to get the Original Oil in place as $\frac{1}{slope}$. The first values representing the transient period where they do not follow the straight line.

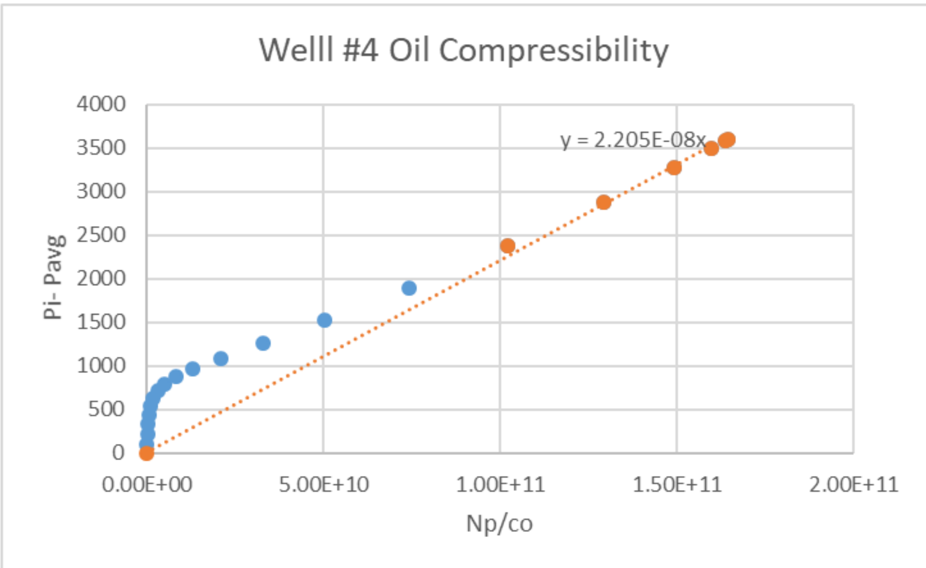

Figure 95: Dead Oil Multi-well Well #4 Flowing Material Balance using Oil Compressibility.

N4= 45.35 MMSTB

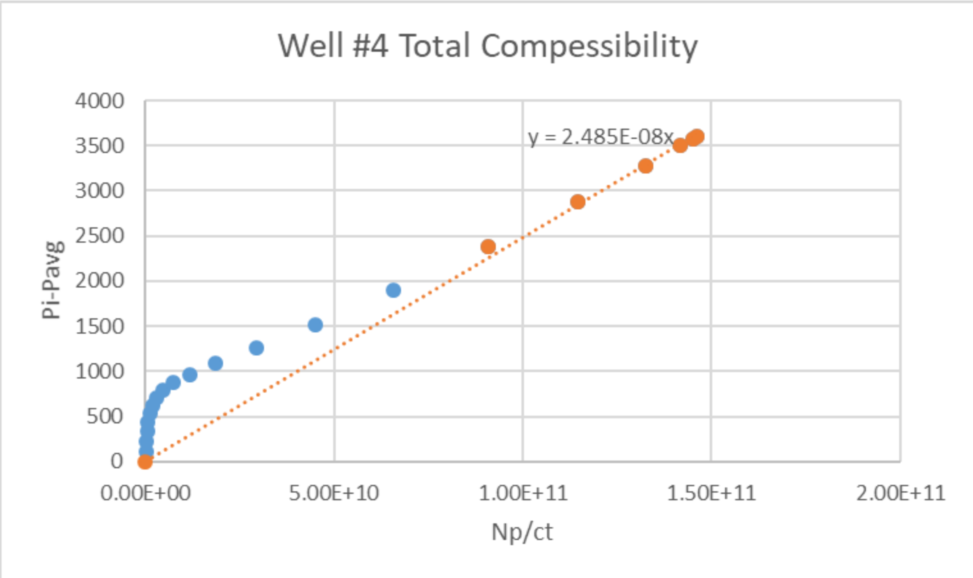

Figure 96: Dead Oil Multi-well Well #4 Flowing Material Balance using Total Compressibility.

N4 = 40.2 MMSTB

The early data representing the transient period do not follow the straight line of the Pseudo Steady Sate.

Appendix C

Dry Gas Multi-Well Results

<u>Well #2</u>

Model Match

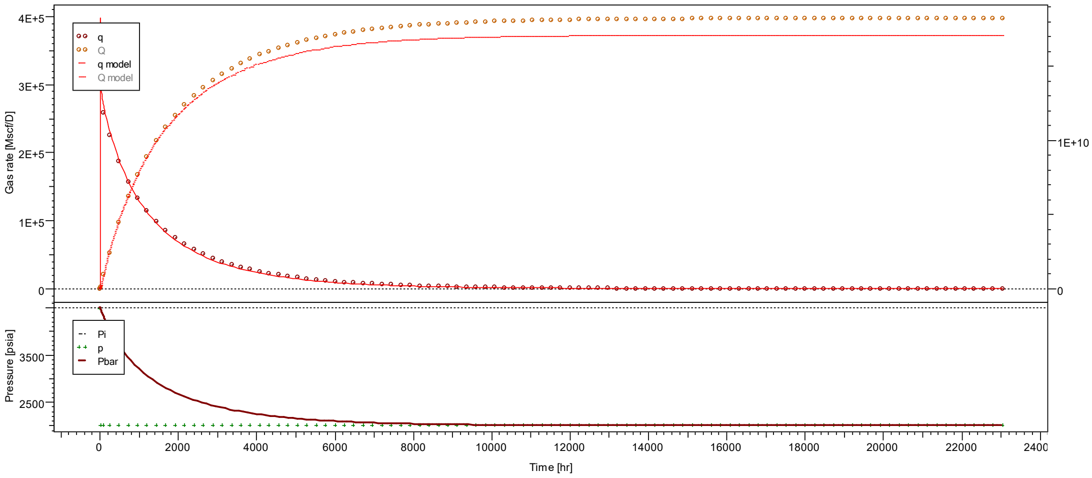

Production history plot (Gas rate [Mscf/D], Pressure [psia] vs Time [hr])

Figure 97: Dry Gas Multi-well Well #2 History Match. Rate, Cumulative production, flowing pressure and model reservoir average pressure vs. Time.

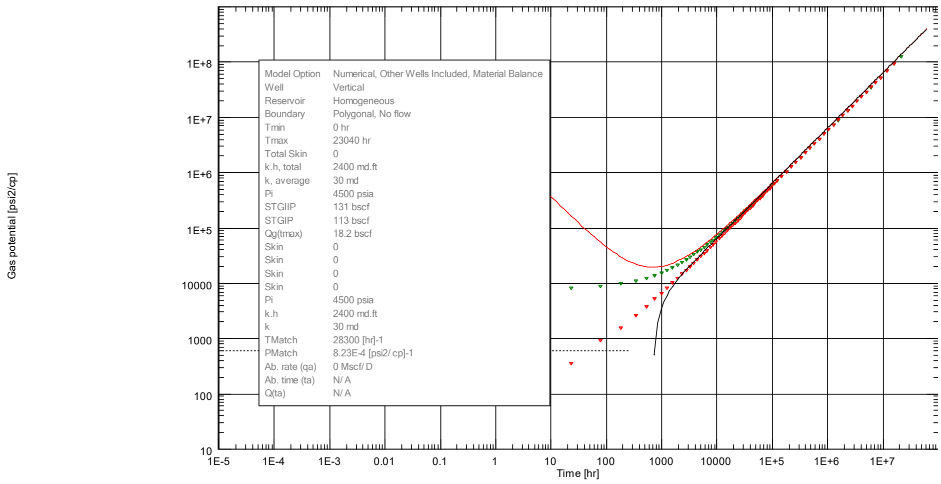

Loglog plot: Int[(m(pi)-m(p))*q_ref/q]/te and d[Int[(m(pi)-m(p))*q_ref/q]/te]/dln(te) [psi2/cp] vs te/2 [hr]

Figure 98: Dry Gas Multi-well Well #2 Log-Log Plot Match.

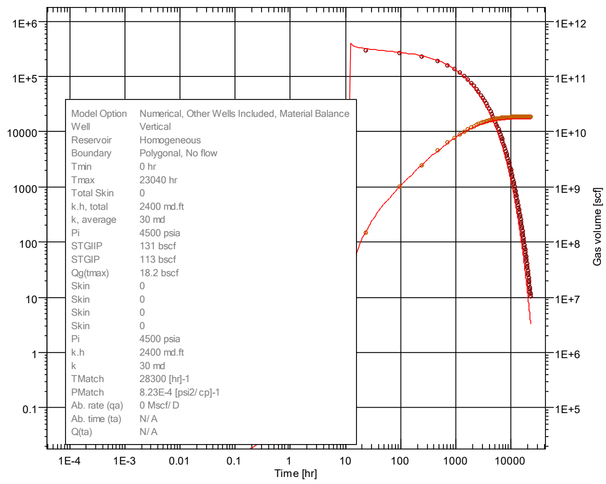

Fetkovich plot: q [Mscf/D], Q [scf] vs dt [hr]

Figure 99: Dry Gas Multi-well Well #2 Model Fetkovich Plot Match.

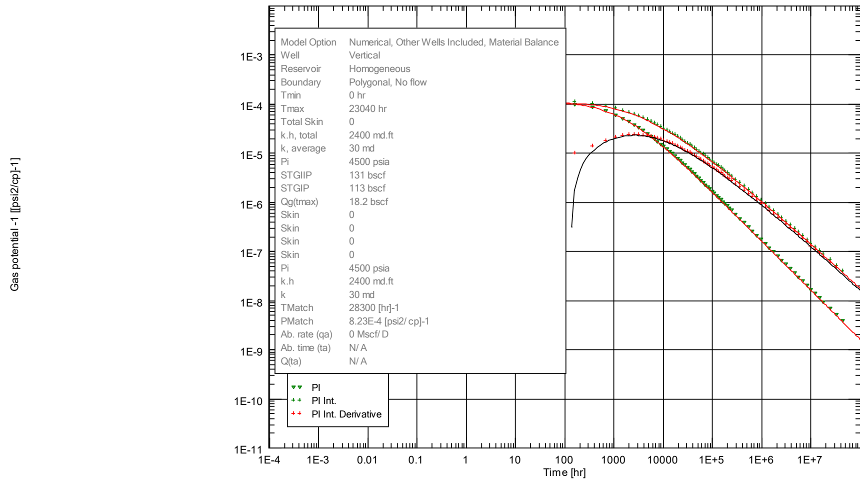

Blasingame plot: q/q_ref/(m(pi)-m(p)), Int[q/q_ref/(m(pi)-m(p))]/te and d[Int[q/q_ref/(m(pi)-m(p))]/te]/dlnte [[psi2/cp]-1] vs te [hr]

Figure 100: Dry Gas Multi-well Well #2 Model Blasingame Plot Match.

Fetkovich Type-curves

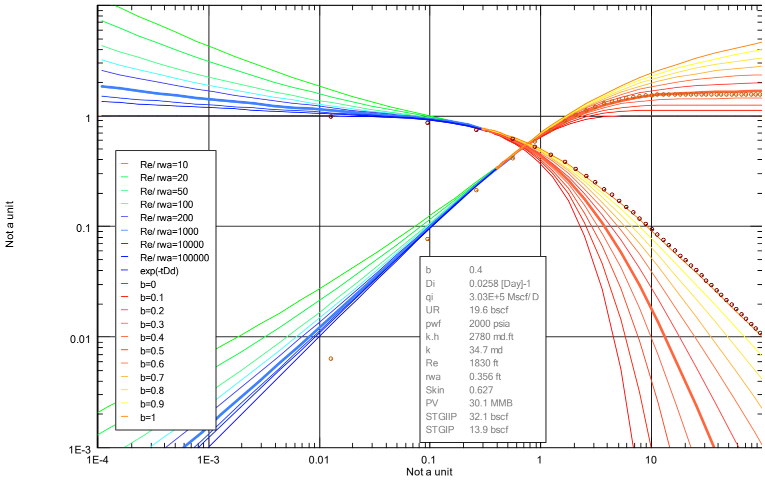

Fetkovich type curve plot: qDd and QDd vs tDd

Figure 101: Dry Gas Multi-well Well #2 Fetkovich Type-curves Match.

G2 ~ 32.1 BSCF

Blasingame Type-curves

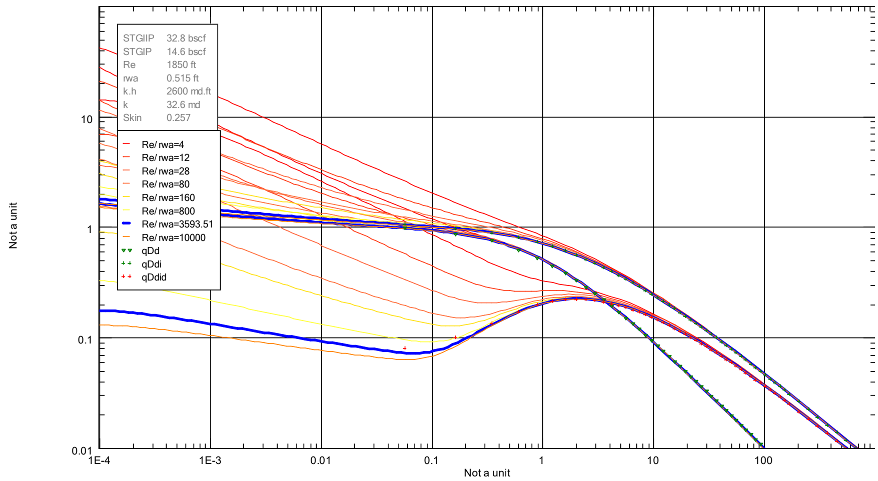

Blasingame type curve plot: qDd, qDdi and qDdid vs tDd

Figure 102: Dry Gas Multi-well Well #2 Blasingame Type-curves Match.

From Blasingame Type-curves match we obtain G2 ~32.8 BSCF

Flowing Material Balance

Gas Flowing Material Balance

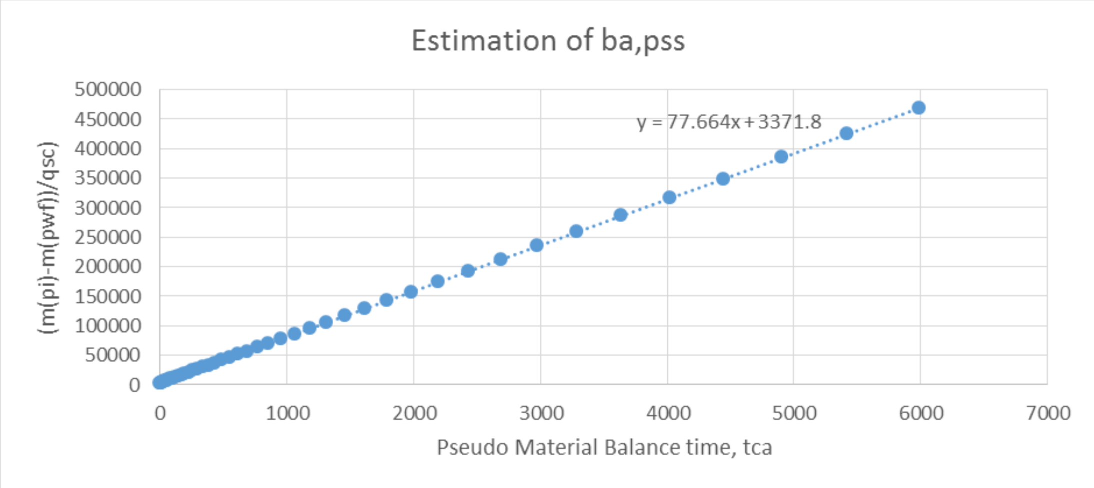

Figure 103: Dry Gas Multi-well Well #2 FMB, bpss is obtained as the Y-intercept of the straight line

Table 27: Dry Gas Multi-well Well #2, reservoir permeability using FMB approach.

B`$_{a,pss}$	3372	
kh	2518	md.ft
k	31	md

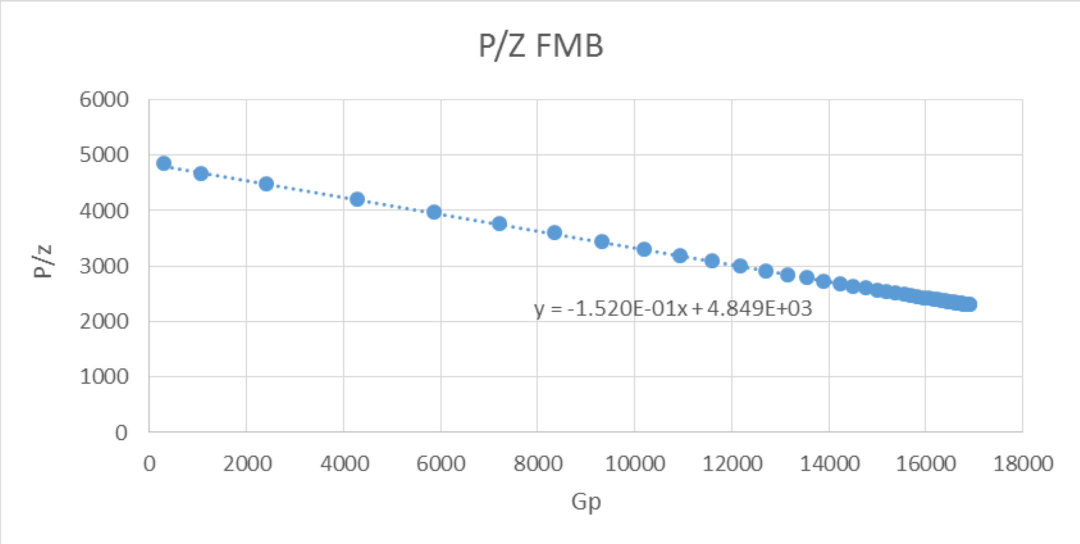

Figure 104: Dry Gas Multi-well Well #2, Gas Flowing Material Balance, P/z Plot.

G2 ~ 30.5 BSCF

Agarwal Gardener

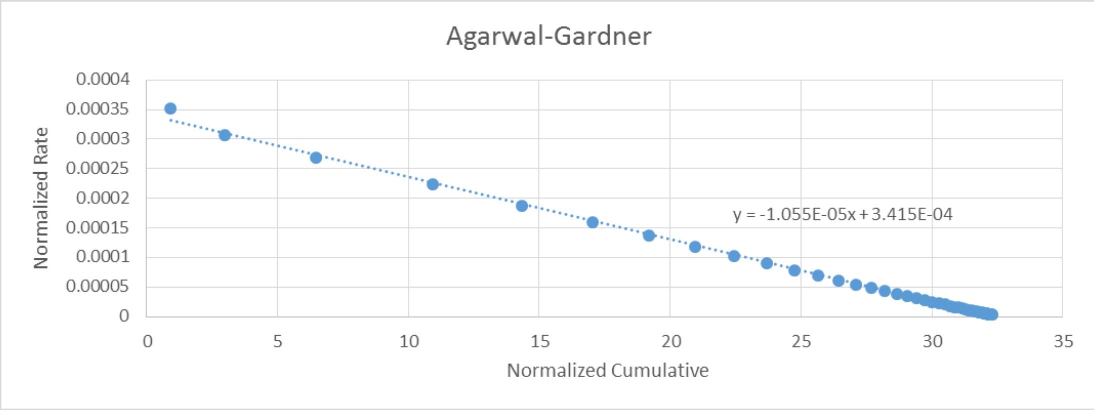

Figure 105: Dry Gas Multi-well Well #2, Agarwal Gardner Approach.

G2 ~ 32.5 BSCF

New Material Balance Time

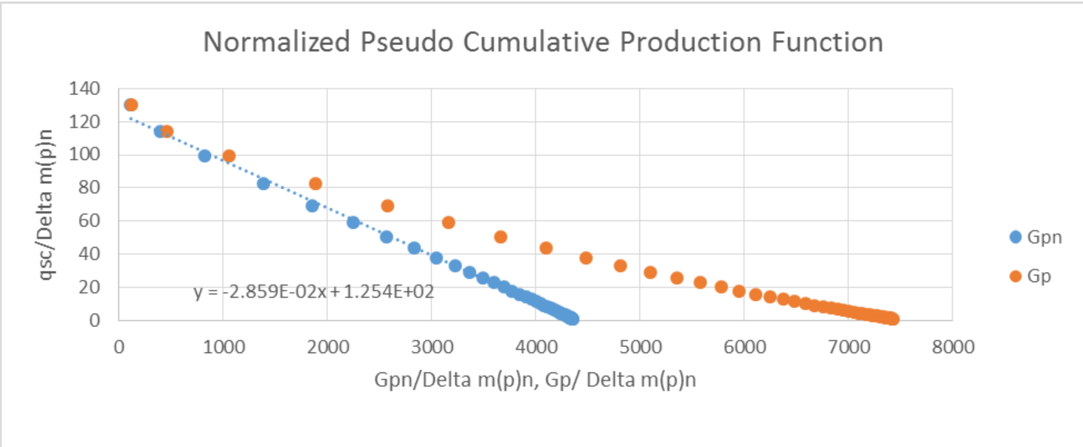

Figure 106: Dry Gas Multi-well Well #2 Using The New Pseudo Material Balance Function.

G2 ~ 34.9 BSCF

Well #3

Model Match

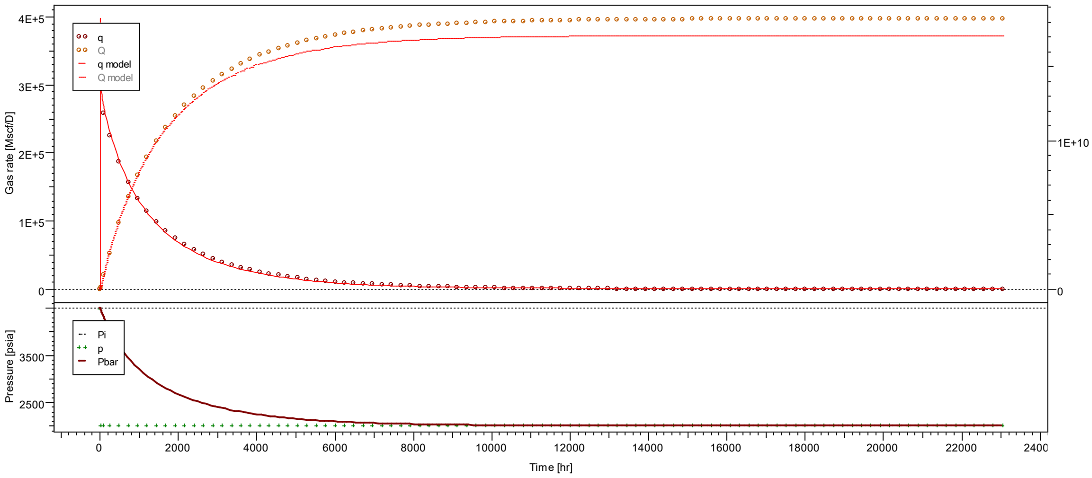

Production history plot (Gas rate [Mscf/D], Pressure [psia] vs Time [hr])

Figure 107: Dry Gas Multi-well Well #3 History Match. Rate, Cumulative production, flowing pressure and model reservoir average pressure vs. Time.

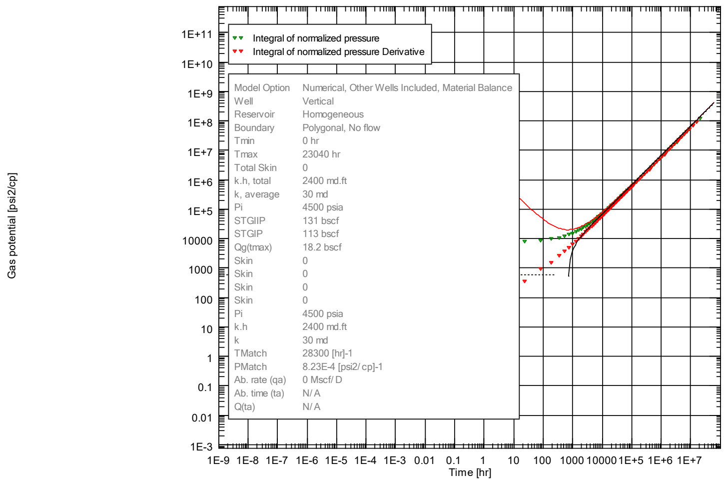

Loglog plot: Int[(m(pi)-m(p))*q_ref/q]/te and d[Int[(m(pi)-m(p))*q_ref/q]/te]/dln(te) [psi2/cp] vs te/2 [hr]

Figure 108: Dry Gas Multi-well Well #3 Log-Log Plot Match.

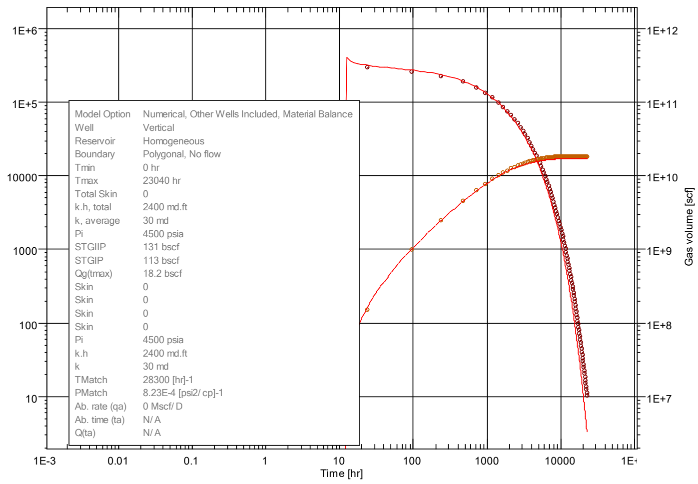

Fetkovich plot: q [Mscf/D], Q [scf] vs dt [hr]

Figure 109: Dry Gas Multi-well Well #3 Model Fetkovich Plot Match.

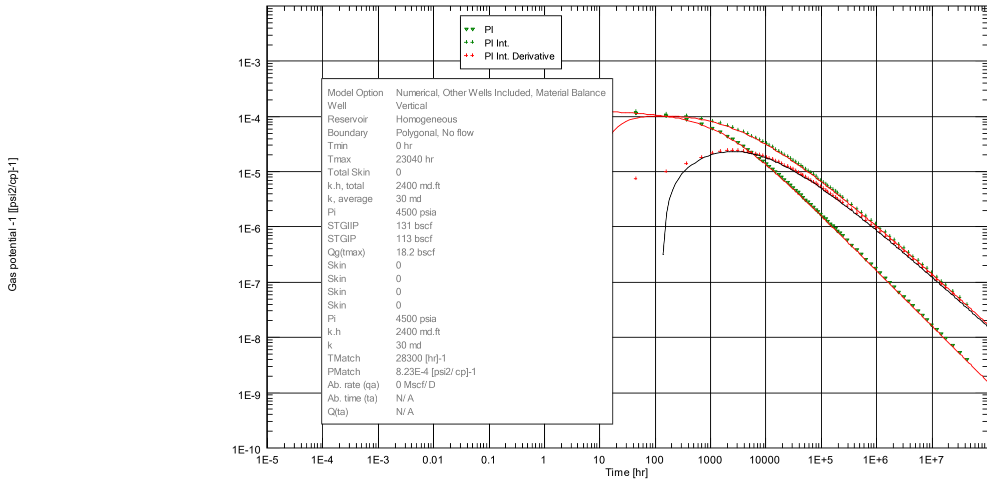

Blasingame plot: q/q_ref/(m(pi)-m(p)), Int[q/q_ref/(m(pi)-m(p))]/te and d[Int[q/q_ref/(m(pi)-m(p))]/te]/dlnte [[psi2/cp]-1] vs te [hr]

Figure 110: Dry Gas Multi-well Well #3 Model Blasingame Plot Match.

Fetkovich Type-curves

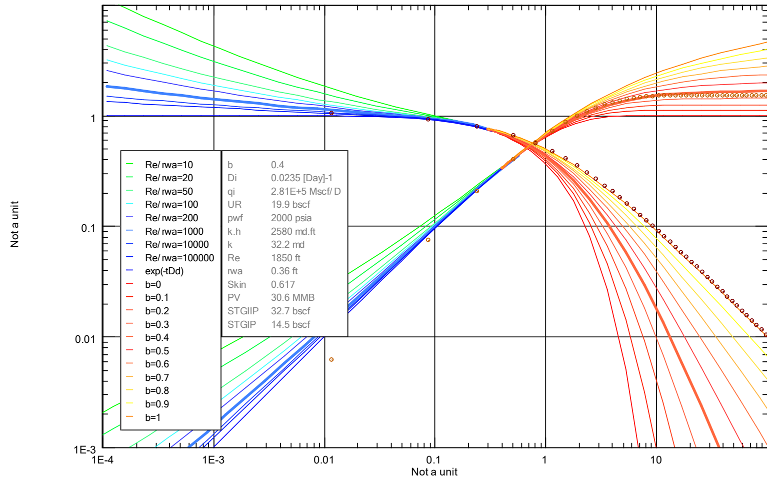

Fetkovich type curve plot: qDd and QDd vs tDd

Figure 111: Dry Gas Multi-well Well #3 Fetkovich Type-curves Match.

G3 ~ 32.7 BSCF

Blasingame Type-curves

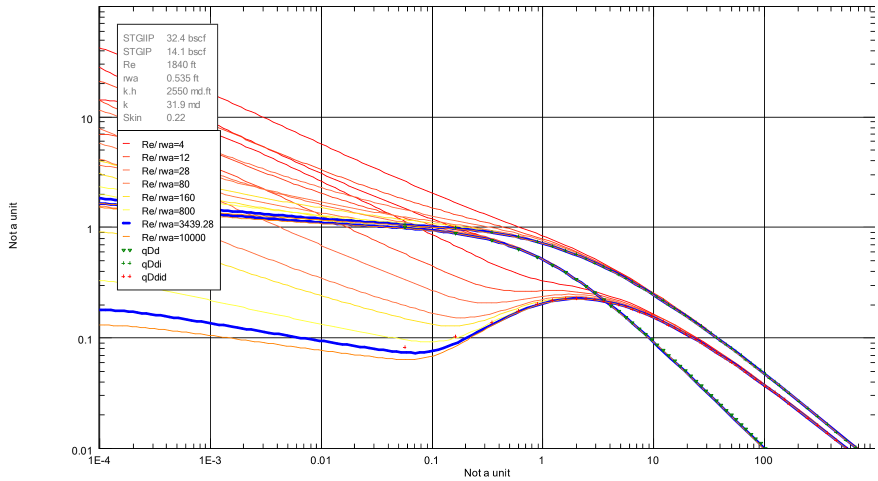

Blasingame type curve plot: qDd, qDdi and qDdid vs tDd

Figure 112: Dry Gas Multi-well Well #3 Blasingame Type-curves Match.

From Blasingame Type-curves match we obtain G3 ~32.4 BSCF

Flowing Material Balance

Gas Flowing Material Balance

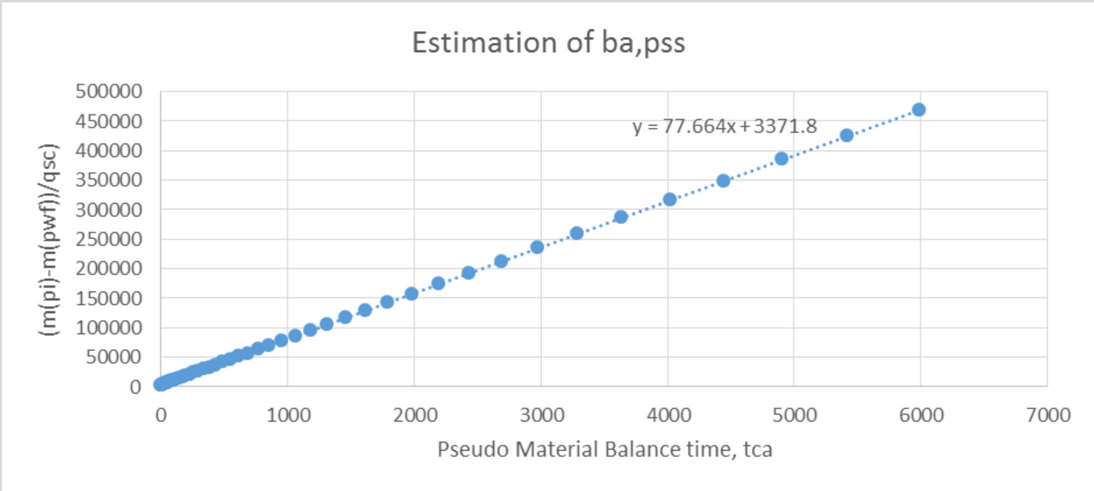

Figure 113: Dry Gas Multi-well Well #3 FMB, b_{pss} is obtained as the Y-intercept of the straight line

Table 28: Dry Gas Multi-well Well #3, reservoir permeability using FMB approach.

$b_{a,pss}$	3372	
kh	2518	md.ft
k	31	md

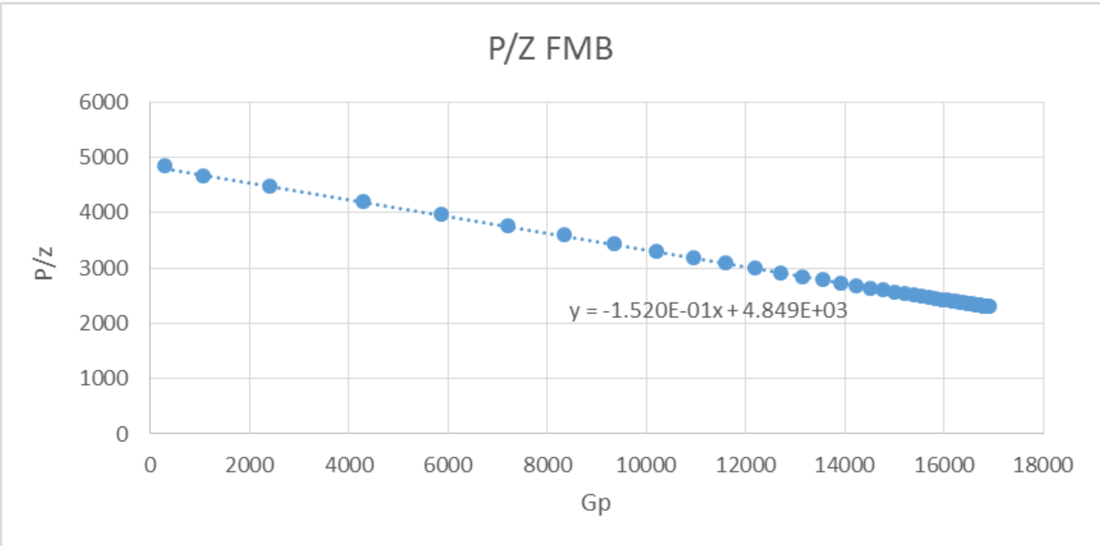

Figure 114: Dry Gas Multi-well Well #3, Gas Flowing Material Balance, P/z Plot.

G3 ~ 30.5 BSCF

Agarwal Gardener

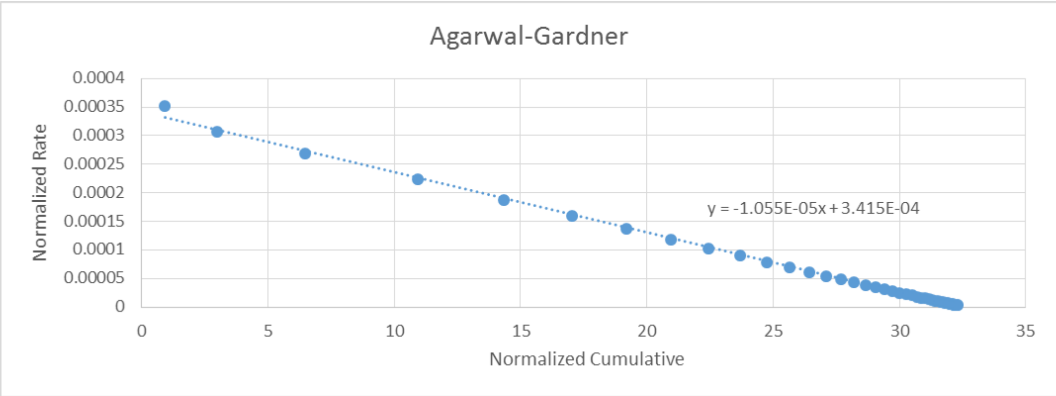

Figure 115: Dry Gas Multi-well Well #3, Agarwal Gardner Approach.

G3 ~ 32.6 BSCF

New Material Balance Time

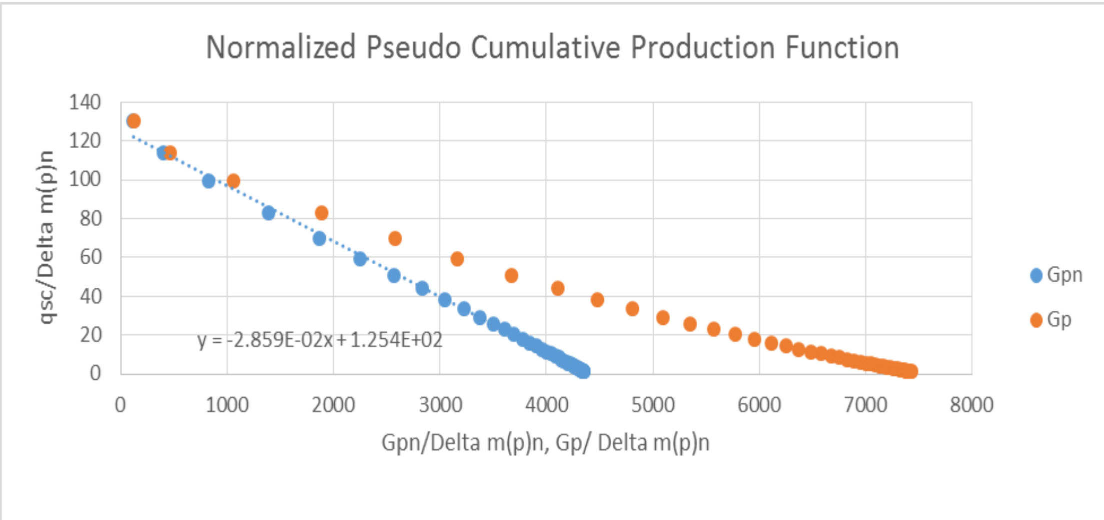

Figure 116: Dry Gas Multi-well Well #3 Using The New Pseudo Material Balance Function.

G2 ~ 34.9 BSCF

Well #4

Model Match

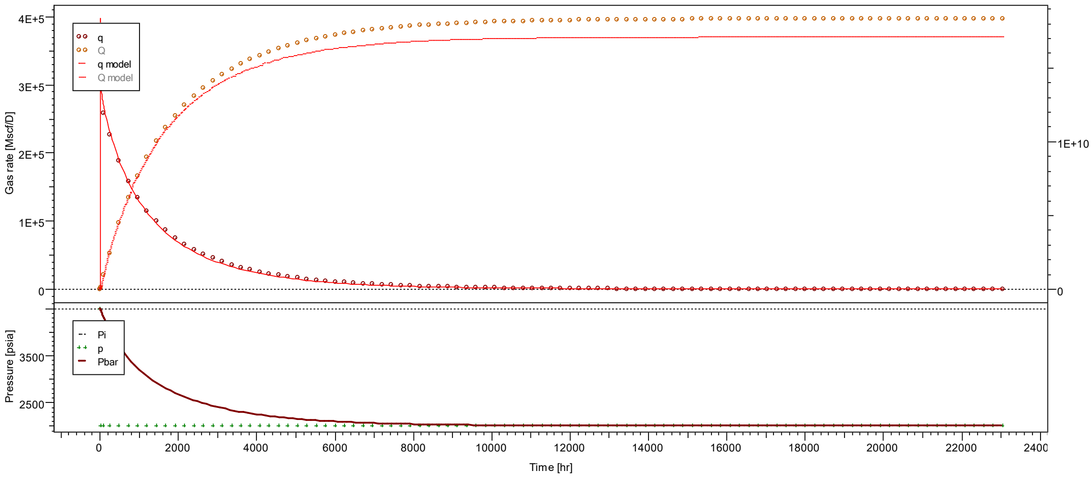

Production history plot (Gas rate [Mscf/D], Pressure [psia] vs Time [hr])

Figure 117: Dry Gas Multi-well Well #4 History Match. Rate, Cumulative production, flowing pressure and model reservoir average pressure vs. Time.

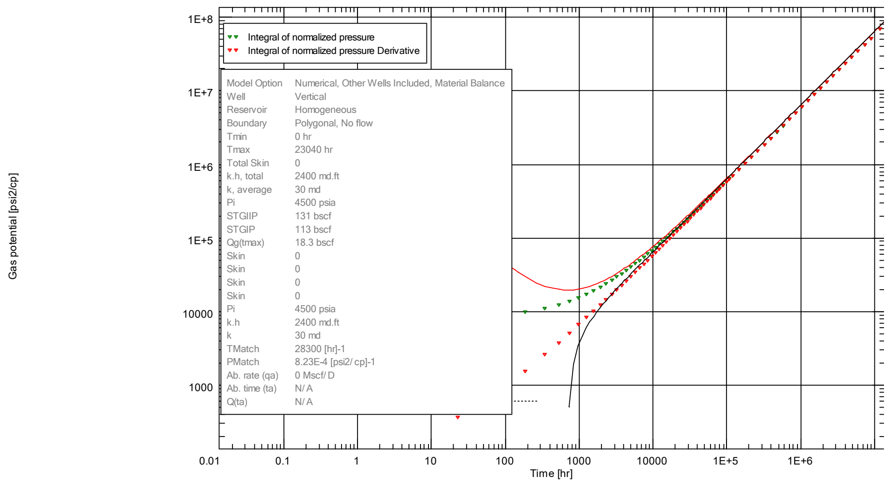

Loglog plot: Int[(m(pi)-m(p))*q_ref/q]/te and d[Int[(m(pi)-m(p))*q_ref/q]/te]/dln(te) [psi2/cp] vs te/2 [hr]

Figure 118: Dry Gas Multi-well Well #4 Log-Log Plot Match.

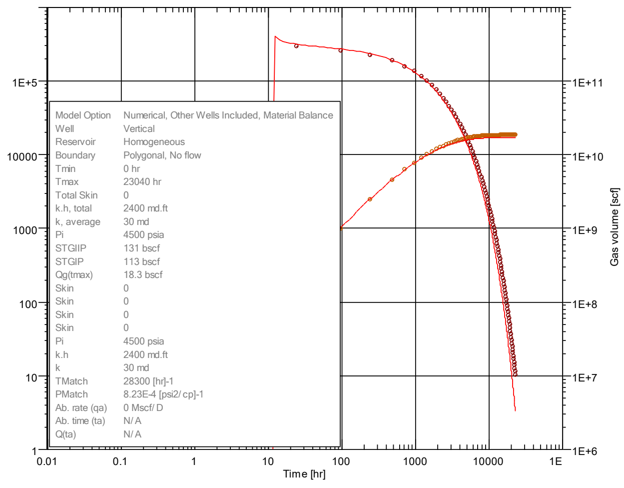

Fetkovich plot: q [Mscf/D], Q [scf] vs dt [hr]

Figure 119: Dry Gas Multi-well Well #4 Model Fetkovich Plot Match.

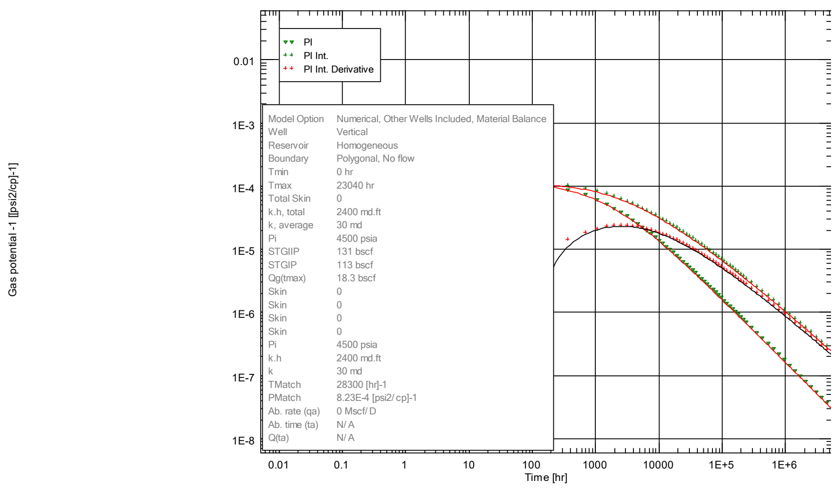

Blasingame plot: q/q_ref/(m(pi)-m(p)), Int[q/q_ref/(m(pi)-m(p))]/te and d[Int[q/q_ref/(m(pi)-m(p))]/te]/dlnte [[psi2/cp]-1] vs te [hr]

Figure 120: Dry Gas Multi-well Well #4 Model Blasingame Plot Match.

Fetkovich Type-curves

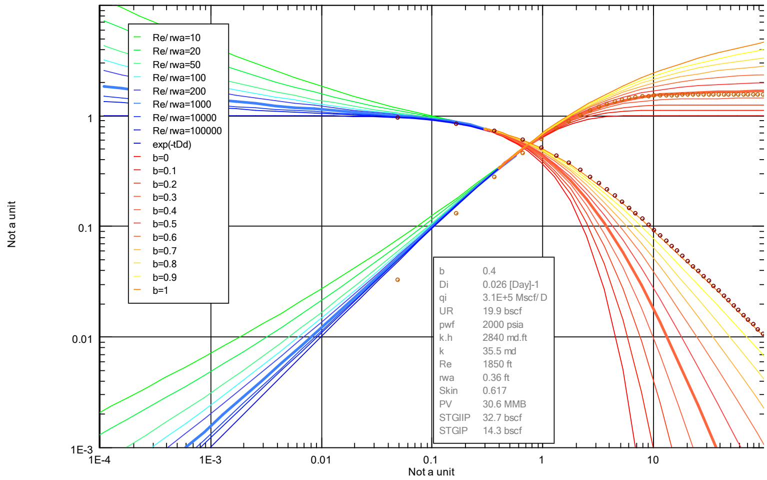

Fetkovich type curve plot: qDd and QDd vs tDd

Figure 121: Dry Gas Multi-well Well #4 Fetkovich Type-curves Match.

G4 ~ 32.7 BSCF

Blasingame Type-curves

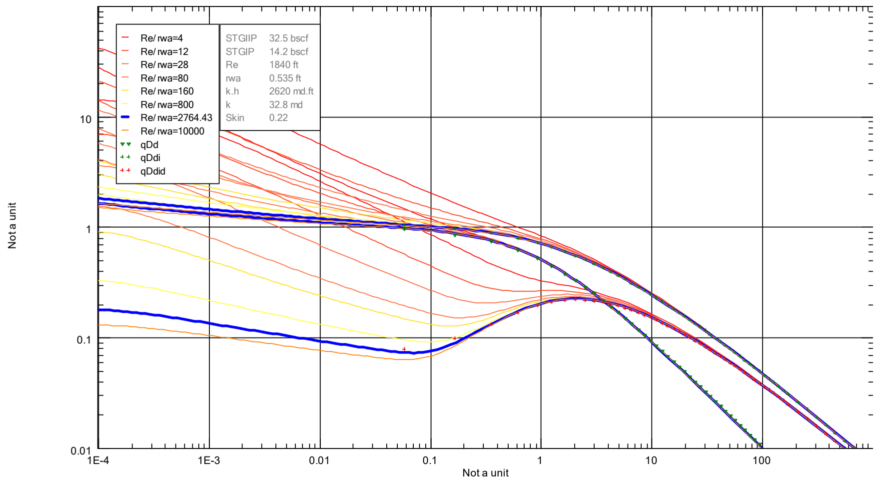

Blasingame type curve plot: qDd, qDdi and qDdid vs tDd

Figure 122: Dry Gas Multi-well Well #4 Blasingame Type-curves Match.

From Blasingame Type-curves match we obtain G4 ~32.5 BSCF

Flowing Material Balance

Gas Flowing Material Balance

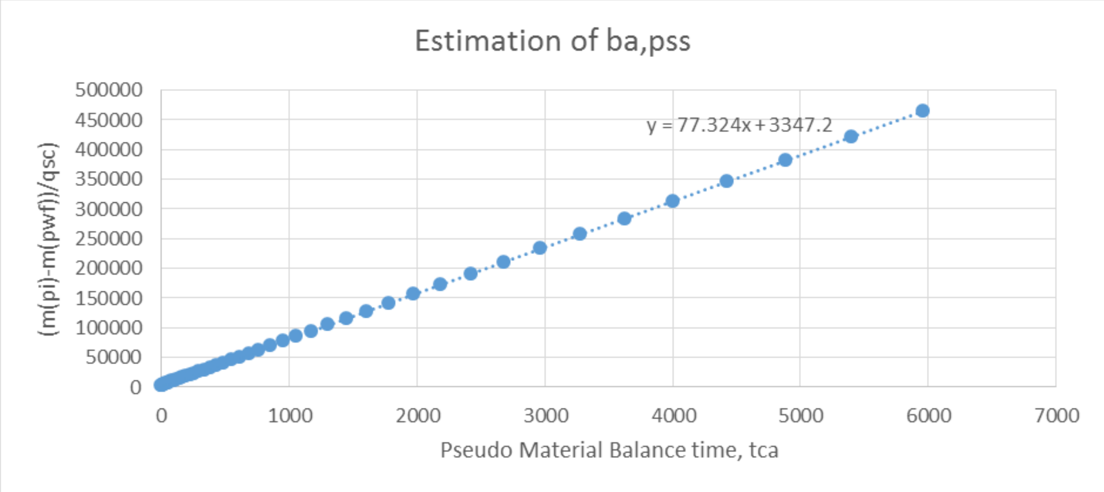

Figure 123: Dry Gas Multi-well Well #4 FMB, b_{pss} is obtained as the Y-intercept of the straight line

Table 29: Dry Gas Multi-well Well #4, reservoir permeability using FMB approach.

$b_{a,pss}$	3347	
kh	2537	md.ft
k	32	md

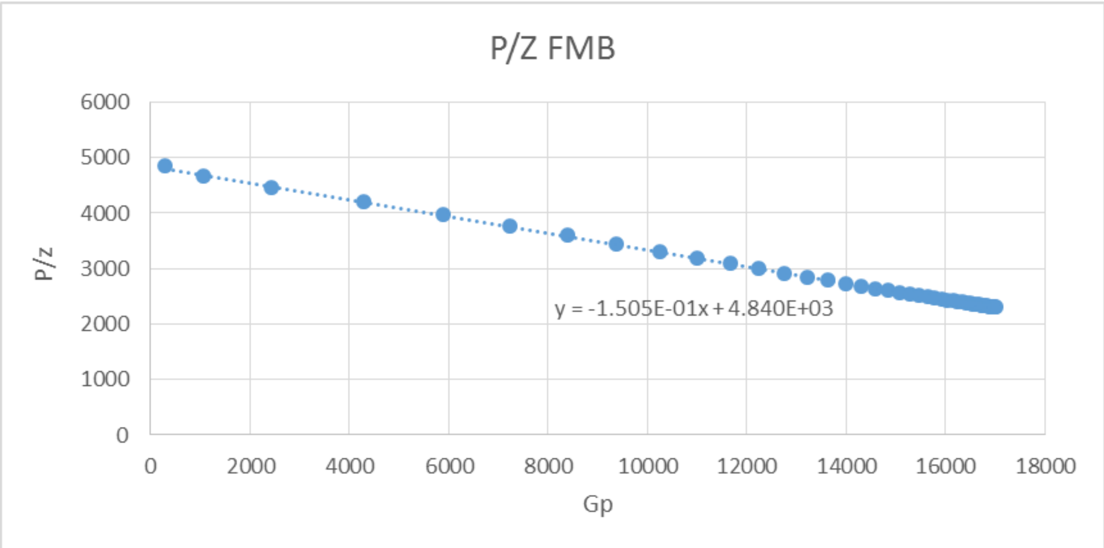

Figure 124: Dry Gas Multi-well Well #4, Gas Flowing Material Balance, P/z Plot.

G4 ~ 30.8 BSCF

Agarwal Gardener

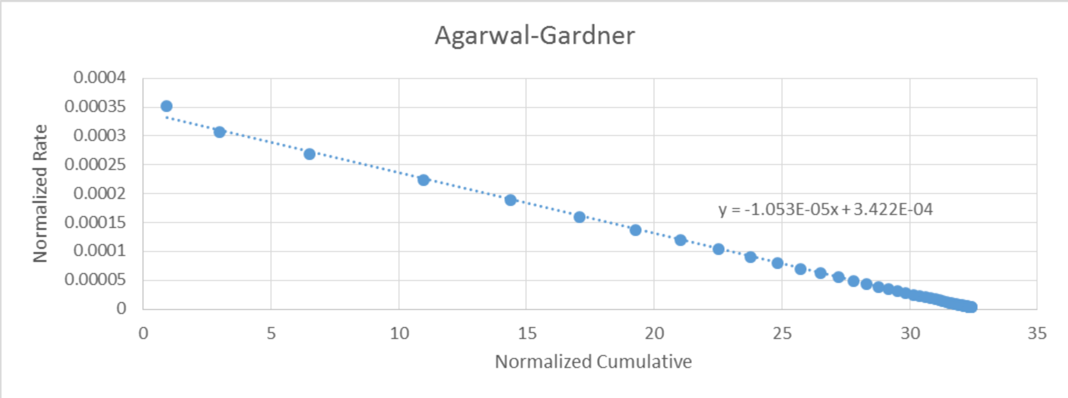

Figure 125: Dry Gas Multi-well Well #4, Agarwal Gardner Approach.

G4 ~ 32.8 BSCF

New Material Balance Time

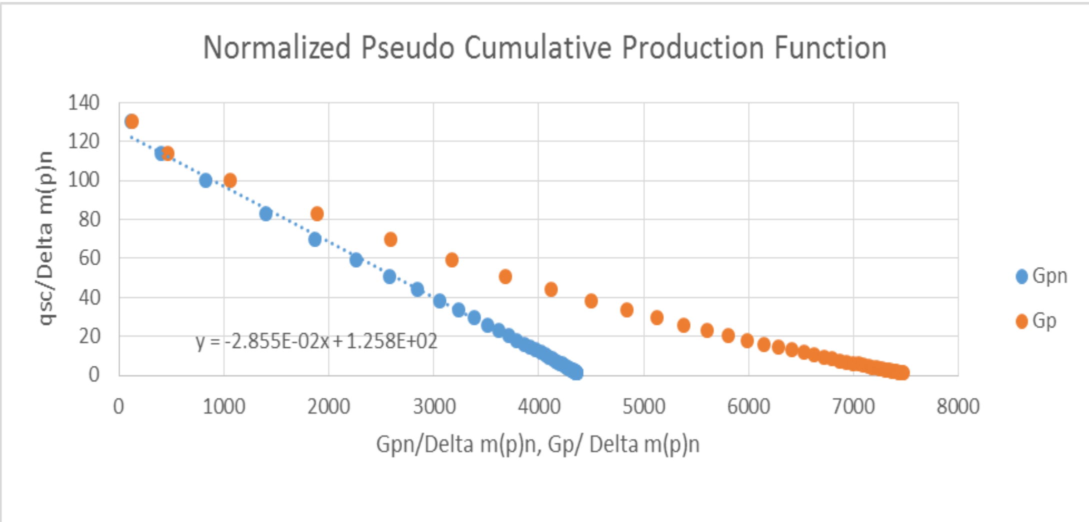

Figure 126: Dry Gas Multi-well Well #4 Using The New Pseudo Material Balance Function.

G4~ 35.1 BSCF